“Probiotic Lipases: Applications to Polymer Degradation, Biofuel Synthesis and Greener Nanobiotechnology”

THESIS

Submitted in partial fulfillment of

the requirements for the degree of

Doctor of Philosophy

By

Mohammed Imran Khan

ID. No: 2013PHXF0401H

Under the supervision of

Dr. Jayati Ray Dutta

Co-supervisor

Dr. Ramakrishnan Ganesan

BIRLA INSTITUTE OF TECHNOLOGY AND SCIENCE, PILANI

Hyderabad campus, Telangana, INDIA

2019

BIRLA INSTITUTE OF TECHNOLOGY AND SCIENCE, PILANI
HYDERABAD CAMPUS

CERTIFICATE

This is to certify that the thesis entitled **"Probiotic Lipases: Applications to Polymer Degradation, Biofuel Synthesis and Greener Nanobiotechnology"** was submitted by Mohammed Imran Khan, ID. No. 2013PHXF0401H for the award of Ph. D. degree of the Institute embodies original work done by him under my supervision.

Signature in full of the supervisor : _____

Name in capital block letters : **Dr. Jayati Ray Dutta**

Designation : **Associate Professor**

Department of Biological Sciences

Date :

Signature in full of the co-supervisor : _____

Name in capital block letters : **Dr. Ramakrishnan Ganesan**

Designation : **Associate Professor**

Department of Chemistry

Date :

ACKNOWLEDGEMENT

First of all, I would like to thank the Almighty for giving me the opportunity to do this research work with good health and prosperity.

My heart-felt gratitude to, Director (BITS-Pilani, Hyderabad Campus), for permitting me to carry out my research work in the Biological Sciences Department.

I wish to express my sincere gratitude and heartfelt thanks to my supervisor ***Dr. Jayati Ray Dutta***, Department of Biological Sciences and co-supervisor, ***Dr. Ramakrishnan Ganesan,*** Department of Chemistry for their excellent guidance, constant encouragement, enormous patience and good advice with a smiling face throughout my research work. I would like to acknowledge them for the moral support at every instance, without which, this work would not have been completed.

I am grateful to ***Prof. K.N. Mohan***, Head of Department of Biological Sciences for giving me an opportunity to carry out my research work in the laboratory.

I would like to extend my gratitude to my Doctoral Advisory Committee members, ***Prof. Anupam Bhattacharya,*** Department of Chemistry and ***Dr. Debashree Bandyopadhyay,*** Department of Biological Sciences, for their valuable suggestions.

I wish to express my thanks and take immense pleasure in acknowledging all the faculty of Department of Biological Sciences, BITS, Pilani-Hyderabad Campus for their support and encouragement to carry out this research work.

I express my thanks to laboratory technicians, Department of Biological Sciences for all their help in one way or the other.

Lastly, but most importantly I would like to acknowledge my mother Sabera Begum, sisters for their amazing support and my reason to smile even on difficult days. I heart fully acknowledge my friend Quoseena Mir for her support, I would never have been able to achieve this dream without her constant encouragement.

Abstract

Lipases play a very important role as natural biocatalysts of several biochemical reactions. There has been an increased demand for microbial lipases due to inability of plant and animal lipases to meet the global requirement. The current focus of the study was intended to explore a probiotic lipase obtained from *Lactobacillus sp.* for various applications such as polymer degradation, cell growth studies on degraded polymer film, biofuel production, nanoparticle synthesis, their characterization and nanobiotechnological applications. This probiotic lipase was isolated from *Lactobacillus plantarum, Lactococcus brevis* strains and their co-cultures. The production parameters were optimized by both classical, statistical methods previously established in our lab, followed by cloning and expression to further improve the yield.

In the present study, three different lipases derived from *Lactobacillus brevis, Lactobacillus plantarum* and their co-culture have been utilized to explore their efficiency towards Poly-ε-caprolactone [PCL] degradation via enzyme pouring method. The effect of parameters like enzyme loading and degradation time had been studied to understand the efficiency of the enzymes used. Various characterization techniques such as thermogravimetric analysis (TGA), differential thermal analysis (DTA), scanning electron microscopy (SEM) and Fourier transform infrared spectroscopy (FTIR) have been employed to study the enzymatic degradation and its possible mechanistic insight. The enzymatic degradation was found to be significantly influenced by the concentration, time of exposure and the type of the enzyme. Among the three enzymes screened in this study, the lipase from *Lactobacillus plantarum* was found to possess the maximum PCL degradation activity at a nominal loading of 5 mg/mL. Thermogravimetric analysis results showed that with increasing exposure time of enzyme, the thermal stability of the

PCL films decreased due to its degradation. The DTA analyses revealed that the enzyme preferentially degraded the amorphous regions at first, as evidenced by the increase in percentage crystallinity of the polymer. While the SEM analysis had shown the cracked polymer surface after enzymatic degradation whereas, the FTIR analyses confirmed the hydrolytic action of the enzymes on the ester bonds of the PCL films. The study revealed the potential of genetically engineered probiotic *Lactobacillus* class of lipases towards polymer degradation with enhanced efficiency.

Enzyme embedded polymer degradation was reported to be an attractive alternative approach to the conventional surface pouring method for efficient degradation of polymers using fungal derived enzyme *Candida antarctica* Lipase B (CALB). Despite the enormous potential, this approach is still in its infancy. This thesis employs, probiotic lipase obtained from *Lactobacillus plantarum* has been employed for the first time to study the enzyme embedded polymer degradation approach using poly(ε-caprolactone) (PCL) as the semicrystalline polymer candidate. PCL films embedded with 2 to 8 wt% of lipase are studied under static conditions for their enzymatic degradation up to 8 days of incubation. Thermogravimetric analyses (TGA) have shown a clear trend in decreasing thermal stability of the polymer with increasing lipase content and number of incubation days. Differential thermal analyses (DTA) have revealed that the percentage crystallinity of the left-over PCL films increases with the progress in enzymatic degradation due to the efficient action of lipase over the amorphous regions of the films. Thus, the higher lipase loading in the PCL matrix and more number of incubation days have resulted in higher percentage crystallinity in the left-over PCL films, which has further been corroborated by X-ray diffraction (XRD) analyses. In a similar line, higher percentage mass loss of the PCL films has been observed with increased enzyme loading and number of incubation days. Field emission scanning electron microscopy (FE-SEM) has been

employed to follow the surface and cross-sectional morphologies of the polymer films, which has revealed micron-scale pores on the surface as well as bulk polymer matrix with the progress in enzymatic polymer degradation. Additionally, FE-SEM studies have revealed the efficient enzyme-catalyzed hydrolysis of the polymer matrix in a three-dimensional fashion, unique to this approach. In addition to the first time utility of a probiotic lipase for embedded polymer degradation approach, the present work provides insights on the PCL degradation under static and ambient temperature conditions with no-replenishment of enzymes.

Owing to the eco-friendly nature of probiotic lipases, there lies a huge interest in exploring them as capping agents for various nanoparticle synthesis to achieve stability and biocompatibility. Lipase extracted from the probiotic *Lactobacillus plantarum* is utilized for the first time to study its efficacy in capping gold nanoparticles (GNPs) at room temperature synthesis using gold chloride solution ($HAuCl_{4)}$. The synthesized lipase-capped GNPs were characterized using UV-visible spectroscopy, FT-IR, High Resolution - Transmission Electron Microscope (HR-TEM), Dynamic Light Scattering (DLS) and zeta potential measurements. Importantly, selected area electron diffraction (SAED) studies with HR-TEM have revealed the effect of lipase capping in tuning the polycrystallinity of the GNPs. The lipase-capped GNPs were also explored for their catalytic efficiency towards an environmentally and industrially important conversion of 4-nitrophenol to 4-aminophenol. Exploiting the amine functional groups in the protein, the recoverability and reusability of the GNPs have been demonstrated through immobilization over amine-functionalized Fe_3O_4 nanoparticles.

Gold nanoparticles (GNPs) are key diagnostic and therapeutic agents in biomedical sciences. Several studies have been carried out in different therapeutic areas such as in cancer treatment, antibacterial topical and imaging agents. There is a necessity

to evaluate the gold nanoparticles cytotoxicity at all fronts. Since blood is the first point of contact in any therapy, it is required to have a thorough *in vitro* investigation of gold nanoparticles interacting with blood to avoid any adverse effects. For this study, blood was collected from healthy volunteers. Platelets, plasma were separated using double centrifugation method from the blood and all the samples were treated with lipase capped gold nanoparticles, except control. Plasma fibrinogen, platelet aggrometry, blood clotting kinetic tests was performed. We found out that nanoparticles with certain physicochemical properties (e.g., size, charge, hydrophobicity) synthesized have no undesirable effects on the blood coagulation system. Our study revealed that lipase capped GNPs synthesized were hemocompatible. There was a significant increase in the fibrinogen levels in blood due to the exposure of the lipase capped nanoparticles which is consistent with other studies.

There was no significant platelet aggregation, change in blood clotting time, kinetics and clot strength upon exposure to nanoparticles indicating the non-toxicity of lipase capped GNPs towards blood coagulation system, which is critical before carrying out any *in vivo* applications.

Further, we studied the lipase enzyme isolated from *Lactobacillus plantarum* for stabilization of silver nanoparticles and explored the antimicrobial activity of the silver nanoparticles. The microbial resistance to different drugs due to excessive usage of antibiotics in various domains has become a serious environmental threat in the recent years. This gave the impetus to the researchers to find alternatives that do not lead to multi-drug resistant microbes. In this backdrop, silver nanoparticles (Ag NPs) have become a popular choice due to their potential broad spectrum antimicrobial attributes. Recent literature caution that about 400 metric tons of Ag NPs are synthesized annually all over the world that could cause environmental hazards when used at higher

concentrations than the toxicity limit. However, most of the literature reports use higher concentrations of Ag NPs and exposure to such concentrations may lead to environmental and health hazards. In this study, a series of Ag NPs have been synthesized using a lipase derived from a probiotic source Lactobacillus plantarum as the stabilizing agent. The Ag NPs synthesized through different combinations of lipase and $AgNO_3$ are characterized using various techniques such as UV-visible spectroscopy, FT-IR, XRF (X-Ray Fluorescence), Dynamic Light Scattering (DLS) and HR-TEM. The lipase capped Ag NPs have been studied for their antimicrobial activity against representative microbes such as *Pseudomonas putida*, *Staphylococcus aureus* and *Aspergillus niger*. Our initial results reveal that the lipase capped Ag NPs possess high potential towards broad spectrum antimicrobial applications at concentrations much lower than the toxicity limit of the standard model, zebra fish.

The application of free and sodium alginate immobilized lipase from *L. plantarum, L. brevis* was then studied for biodiesel production. Biodiesel synthesis has gained substantial attention of late, due to its biodegradability and non-polluting nature. Recent past, enzyme mediated transesterification of cooking oil for biodiesel production is highly focused. Enzymatic transesterification yields high purity biodiesel and enables easy separation from the by product, glycerol. But the cost of raw material remains a barrier for its industrial implementation. In order to make the synthesis process cost effective, we also explored the use of probiotic lipase isolated from *Lactobacillus plantarum, L. brevis* for generation of biodiesel from waste cooking oil as a raw material. We studied various parameters affecting the biodiesel synthesis such as molar ratio of oil to methanol, reaction temperature, stirring intensity and concentration of enzyme added. The results obtained for all the biodiesel samples were significant and the maximum average value was 81%, 59 %, 67%, 54% using immobilized lipase, free lipase at, 45 ^{o}C,

160 rpm, with 1:6 fresh olive oil to methanol ratios for immobilized lipases using *Lactobacillus plantarum, Lactobacillus brevis* respectively, whereas for used olive oil the maximum average value obtained was 65%, 58.5%, 55%, 41% using immobilized lipase, free lipase at, 45 ^{o}C, 160 rpm, with 1:6 fresh olive oil to methanol ratios for immobilized lipases using *Lactobacillus plantarum, Lactobacillus brevis* respectively. The bioconversion of oil was found to be at par with other reports available in literature. These results also indicated that the obtained biodiesel can be used as fuel in diesel engine since the viscosity and density properties fall within the limits set by American Society for Testing Materials (ASTM) D 6751.

CONTENTS **Page No.**

Certificate i

Acknowledgement ii

Abstract iv

Table of contents x

List of Tables xiv

List of Figures xv

Abbreviations xviii

CHAPTER-1: Introduction and Review of literature 1

1.1 Introduction 2

1.2 Sources of lipase 4

1.3 Enzyme production 5

1.4 Review of literature 6

1.4.1 Applications of Lipases in Polymer degradation 6

1.4.2 Applications of Lipases in detergent industries 9

1.4.3 Applications of Lipases in production of biodiesel 10

1.4.4 Applications of Lipases in ester synthesis 10

1.4.5 Applications of Lipases as biosensors 11

1.4.6 Applications of Lipases in cosmetics 11

1.4.7 Applications of Lipases in medical treatment 12

1.4.8 Applications of Lipases in oil degradation 13

1.4.9 Enzyme mediated nanoparticle synthesis 13

1.5 Gaps in existing research 16

1.6 Scope and objective of the work 18

CHAPTER-2: *Lactobacillus sps.* Lipase mediated poly (ε-caprolactone) degradation 19

2.1 Introduction 20

2.2 Material and Methods: 22

2.2.1 Materials 22

2.2.2 Sources 22

2.2.3 Preparation of Lipase 22

2.2.4 Determination of Lipase activity 22

2.2.5 Characterization 22

2.3 Preparation of PCL film 23

2.4 Lipase mediated PCL degradation 25

2.5 Results & Discussion 25

2.6 Conclusion 32

CHAPTER-3 : Embedded Enzymatic Degradation of PCL Polymer 34

3.1 Introduction 35

3.2 Material and Methods: 37

3.2.1 Materials 37

3.2.2 Sources 37

3.2.3 Preparation of Lipase 37

3.2.4 Determination of Lipase activity 38

3.2.5 Characterization 38

3.2.6 Lipase mediated PCL degradation 38

3.3 Results & Discussion 39

3.4 Conclusion 52

CHAPTER-4 : Towards single crystalline, highly monodisperse and catalytically active gold nanoparticles capped with probiotic *Lactobacillus sps.* derived lipase 54

4.1 Introduction 55

4.2 Experimental 57

4.3 Results and Discussion 58

4.4 Conclusion 70

CHAPTER-5: In vitro hemocompatability evaluation of gold nanoparticles capped with *Lactobacillus sps.* derived lipase 72

5.1 Introduction 73

5.2. Materials and methods 74

5.2.1 Whole Blood Collection and Platelets isolation 74

5.2.2 Synthesis and Characterization of Gold nanoparticles (GNPs) 75

5.2.3 Platelet aggregation studies 76

5.2.4 Plasma fibrinogen tests 76

5.2.5 Blood clotting tests 77

5.3 Results and discussion 77

5.4 Conclusion 84

CHAPTER-6: Extracellular probiotic lipase capped silver nanoparticles as highly efficient broad spectrum antimicrobial agents 85

6.1 Introduction 86

6.2 Materials and Methods 88

6.2.1 Materials 88

6.2.2 Preparation of lipase immobilized silver nanoparticle using sodium borohydride 89

6.2.3 Physical Characterization of lipase capped silver nanoparticle 89

6.2.4 Characterization of antimicrobial activity of the silver nanoparticle on *P. putida* 89

6.2.5 Characterization of antimicrobial activity of the silver nanoparticle on *S. aureus* 90

6.2.6 Characterization of antimicrobial activity of the silver nanoparticle on *A. niger* 90

6.3 Results & Discussion 91

6.4 Conclusion 102

CHAPTER-7: Biodiesel Synthesis from Waste Cooking Oil Employing Immobilized Lipase from Probiotic *Lactobacillus sps.* 104

7.1 Introduction 105

7.2 Materials and Methods 106

7.2.1 Materials 106

7.2.2 Methods 107

7.2.2.1 Preparation of immobilized enzyme using sodium alginate 107

7.2.2.3 Transesterification of waste cooking oil 107

7.3. Results 108

7.3.1 Effect of molar ratio of oil to methanol 108

7.3.2 Effect of the amount of catalyst used 110

7.3.3 Effect of reaction temperature 112

7.3.4 Effect of mixing intensity of the reactants 114

7.3.5 Viscosity and density properties of the biodiesel obtained 116

7.4 Discussion 117

7.5 Conclusions 119

CHAPTER-8: Summary and Conclusions 121

8.1 Summary 122

8.2 Conclusions 122

8.3 Major contributions of the work 126

8.4 Future scope of work 127

References 128

Biography of Student 163

Biography of Supervisor 167

Biography of Co-Supervisor 168

List of Tables

Table No.	Title	Page No
Table 1	The occurrence of lipases in different microorganisms	4
Table 2	Variation in percentage crystallinity analyzed from the DTA data	28
Table 3	Variation in percentage crystallinity obtained from DTA measurements with varying enzyme loading against number of incubation days	42
Table 4	GPC analyses of 8% lipase embedded PCL films before (control) and after 2 to 8 days of enzymatic degradation	52
Table 5	Rate constants for 4-NP to 4-AP conversion using GNPs capped with varying amount of lipase	69
Table 6	Particle size analysis using DLS for the lipase-capped and citrate-capped GNPs	79
Table 7	Comparison of MIC values of Ag NPs against different microbes reported in the literature	101
Table 8	Parameters used for biodiesel production	110
Table 9	Viscosity and density of biodiesel produced from waste cooking oil employing free lipase from *L plantarum*	116
Table 10	Viscosity, density properties of biodiesel produced from waste cooking oil employing immobilized lipase from *L plantarum*	117

List of Figures

Figure number	Title	Page
Figure 1.	Pictorial representation of various applications of enzymes	3
Figure 2.1	Relative weight loss comparison after 10 day treatment of PCL film with different concentrations of *L. plantarum, L. brevis* and co-cultured lipases	24
Figure 2.2	TGA plot of the PCL film treated with *L. plantarum* lipase over different time periods	26
Figure 2.3	TGA plot of the PCL film treated with *L. brevis* lipase over different time periods	27
Figure 2.4	TGA plot of the PCL film treated with co-culture lipase over different time periods	27
Figure 2.5	DTA plot of the PCL film degraded by *L. plantarum* lipase over different time periods	29
Figure 2.6	DTA plot of the PCL film degraded by *L. brevis* lipase over different time periods	30
Figure 2.7	DTA plot of the PCL film degraded by co-cultured lipase over different time periods	30
Figure 2.8	FT-IR spectra of control and PCL films treated with *L. plantarum* and co-cultured lipases	31
Figure 2.9	SEM images of (a) control and (b) *L. plantarum* treated PCL film	32
Figure 3.1	TGA mass loss analyses of 2, 4, 6, 8% enzyme embedded PCL film and the control	41
Figure 3.2	DTA images of 2, 4, 6, 8% enzyme embedded PCL film and control	43
Figure 3.3	XRD patterns of pristine PCL film, 8% lipase embedded PCL film (control), and 8% lipase embedded PCL film after 8 days of incubation	44
Figure 3.4	Figure 3.4. (a) Lipase release kinetics, and (b) polymer mass loss analyses of 2, 4, 6, and 8% lipase embedded PCL films after 2, 4, 6, and 8 days of incubation	46
Figure 3.5	FE-SEM images of the enzyme embedded before subjecting to degradation	48
Figure 3.6	FE-SEM images of lipase-embedded PCL samples after subjecting to 2 days of enzymatic degradation	49
Figure 3.7	FE-SEM images of lipase-embedded PCL samples after subjecting to 4 days of enzymatic degradation	49
Figure 3.8	FE-SEM images of lipase-embedded PCL samples after subjecting to 6 days of enzymatic degradation	50
Figure 3.9	FE-SEM images of lipase-embedded PCL samples after subjecting to 8 days of enzymatic degradation	51

Figure 4.1	Pictorial representation of the synthesis of GNPs and their anchoring over amine-functionalized Fe3O4 nanoparticles for magnetic recoverability	58
Figure 4.2	UV-Vis absorption spectra of GNPs capped with varying amount of lipase	59
Figure 4.3	FT-IR spectra of pristine (uncapped) GNPs, pristine lipase and lipase-capped GNPs	60
Figure 4.4	Size measurement of pristine lipase and GNPs with varying amount of lipase-capping	62
Figure 4.5.	Zeta potential measurement over pristine lipase and lipase-capped GNPs as a function of pH	63
Figure 4.6.	Zeta potential measurements over pristine Fe_3O_4, APTES-functionalized Fe_3O_4 and GNPs anchored over Fe_3O_4 as a function of pH	64
Figure 4.7	Composite HR-TEM images of (a) 0.5 mg/mL, (b) 1 mg/mL, (c) 2 mg/mL, (d) 6 mg/mL and (e) 10 mg/mL lipase-capped GNPs. Inset shows the particle size distribution. HR-TEM image of GNPs anchored over Fe_3O_4 nanoparticles is given in (f). The dotted circle shows the Moiré patterns arising from Fe_3O_4 support	65
Figure 4.8	SAED patterns of (a) 0.5 mg/mL, (b) 1 mg/mL, (c) 2 mg/mL, (d) 6 mg/mL and (e) 10 mg/mL lipase-capped GNPs. Merged SAED image of 1 mg/mL lipase-capped GNPs and the same anchored onto Fe_3O_4 nanoparticles for comparison (f)	66
Figure 4.9	Catalytic reduction of 4-NP over GNPs capped with varying amount of lipase	67
Figure 4.10	Turn over frequency of GNPs for the catalysis	68
Figure 4.11	Pseudo-first order kinetics of catalytic reduction of 4-NP over GNPs capped with varying amount of lipase to Fe_3O_4 nanoparticles	69
Figure 4.12	Catalytic reduction of 4-NP over GNPs capped with varying amount of lipase to Fe_3O_4 nanoparticles	70
Figure 5.1	Study of Hemocompatibility of lipase capped GNPs on human blood	78
Figure 5.2	UV-VIS Spectra of lipase capped GNPs	78
Figure 5.3	HR-TEM images of lipase capped GNPs	79
Figure 5.4	Plasma Fibrinogen test (A) 1 nM lipase capped GNPs treatment of whole blood (B) 5 nM lipase capped GNPs treatment of whole blood	80
Figure 5.5	Estimation of Clot Strength (A) 1 nM lipase capped GNPs treatment of whole blood (B)5 nM lipase capped GNPs treatment of whole blood	81

Figure 5.6	Estimation of Clot time test (A) 1 nM lipase capped GNPs treatment of whole blood (B) 5 nM lipase capped GNPs treatment of whole blood	81
Figure 5.7	Estimation of Clot formation (A) 1 nM lipase capped GNPs treatment of whole blood (B) 5 nM lipase capped GNPs treatment of whole blood	82
Figure 5.8	Estimation of Platelet aggregation in presence of lipase capped GNPs	83
Figure 6.1	UV-Vis absorption spectra of Ag NPs synthesized from (a) 0.2mM, (b) 0.6 mM and (c) 1.0 mM $AgNO_3$ solutions with varying amount of lipase. (d) Energy dispersive X-ray fluorescence (ED-XRF) spectra of Ag NPs synthesized from the above mentioned $AgNO_3$ solutions with 100 µg/mL of lipase capping	92
Figure 6.2	FT-IR spectra of pristine Ag NPs, pristine lipase and lipase-capped Ag NPs	93
Figure 6.3	DLS measurement 25, 50, 100, 200 µg of lipase capped 0.2 mM Silver Nanoparticle synthesized	95
Figure 6.4	HR TEM images of a, b) 0.2 mM AgNPs capped with 25 µg of lipase c, d) with 50 µg of lipase e, f) 100 µg of lipase g, h) 0. 6mM AgNPs capped with 100 µg of lipase i,j) 1.0 mM AgNPs capped with 100µg of lipase	96
Figure 6.5	Antimicrobial activity of Ag NPs against (a-e) *P. putida*, (f-j) *S. aureus* and (k-o) *A. niger* tested against positive control of Ampicillin and Amphotericin B (in case of *A. niger*), untreated control and negative controls of Lipase treated culture and sodium borohydride (SB)	99
Figure 7.1a	Effect of molar ratio of alcohol to oil on transesterification of fresh olive oil by free and immobilized lipase	109
Figure 7.1b	Effect of molar ratio of alcohol to oil on transesterification of waste olive oil by free and immobilized lipase	109
Figure 7.2a	Effect of enzyme to methanol ratio on transesterification of fresh olive oil by free and immobilized lipase	111
Figure 7.2b	Effect of enzyme to methanol ratio on transesterification of waste olive oil by free and immobilized lipase	112
Figure 7.3a	Effect of temperature on transesterification of fresh olive oil by free and immobilized lipase	113
Figure 7.3b	Effect of temperature on transesterification of waste olive oil by free and immobilized lipase	114
Figure 7.4a	Effect of mixing intensity on transesterification of fresh olive oil by free and immobilized lipase	115
Figure 7.4b	Effect of mixing intensity on transesterification of waste olive oil by free and immobilized lipase	115

List of Abbreviations

A	Alpha
ASTM	American Society for Testing Materials
B	Beta
DNA	Deoxyribonucleic acid
EtBr	Ethidium Bromide
IR	Infrared spectroscopy
I	Inoculum
I.P	Inoculum volume
LBb	*Lactobacillus brevis*
LBp	*Lactobacillus plantarum*
Lt	Litre
µmol	Micromoles
Min	Minute
Mg	Milligrams
Ml	Milliliter
mM	Millimolar
S	Substrate
Sp	Species
Tris-Cl	Tris-chloride
Temp	Temperature
U	Units
UV	Ultraviolet
w/v	Weight/Volume
TEG	Thromboelastography
PCL	Poly-ε-caprolactone
GNPs	Gold Nanoparticles
AgNps	Silver Nanoparticles
TEM	Transmission electron microscopy
PRP	Platelet Rich Plasma
PPP	Platelet Poor Plasma
DTA	Differential Thermal Analysis
TGA	Thermogravimetric Analysis
WBC	White Blood Cells
ECM	Extra Cellular Matrix

CHAPTER 1

INTRODUCTION AND REVIEW OF LITERATURE

1.1 Introduction

Enzymes play a vital role in many systems due to their unique function. Enzymes are protein in nature along with a co-factor for maximum activity and are designed to carry out a specific task which is unique for each enzyme [1, 2]. Similar to "key-lock" fit, each enzyme fits uniquely with one substrate and catalyzes the reaction [3, 4]. Enzymes sourced from microorganisms or animal cell cultures bring about different substrate conversions in respective reactions. They have the ability to work as catalysts in moderate to wide range of pH, pressure and temperature. In addition, they possess substrate specificity under appropriate environment and thus assist in manufacturing industrially critical products without any contaminations. Because of these benefits, enzymes are exploited in a variety of applications such as paper, cosmetics, food, detergent, textile and pharmaceutical industries [5–9]. One such significant enzyme of industrial relevance is the enzyme lipase. According to International Union of Biochemistry Nomenclature (IUBN) lipases are hydrolases and hydrolyses triglycerols to free fatty acids and glycerol [10]. Nowadays rapid progression in the enzymology is primarily the result of contemporary biotechnology's accelerated evolution over the past decades. The bulk volume of industrially exploited enzymes are hydrolyzing in action, chiefly employed for the breakdown of several natural components [11]. The commercial applications of lipases is due to their multifold properties, easy extraction procedure, very less temperature and pressure conditions and potential of unlimited supply which is lacking in traditional industrial processes. [12]. Lipase catalysis of kinetic separation and asymmetric organic molecule synthesis to extract pure molecules has also been accelerated in the recent past. They are exploited to synthesize chiral molecules during the past decade due to the greater enantioselectivity [13, 14]. They are promising in the field of Green Chemistry mainly for the synthesis of chiral molecules, food additives or

many drugs under the gentle eco-friendly conditions [15]. One more area where lipases are widely exploited is bio-transformation of polymer materials. Polymer waste is extremely stable in the environment and their-biodegradability is limited. Recent reports include, the occurrence of polymer-degrading microorganisms in the environment, the isolation of new microorganisms for biodegradation, the discovery of brand-new degradation enzymes and the gene cloning for synthetic polymer-degrading enzymes [16]. One more enthralling and area of relevance for polymer degradation is "enzymatic lithography" and it is an eco-friendly approach to degrade polymer selectively and form desirable patterns that find numerous applications in biotechnology and electronics [17]. Current trends suggest the exploitation of lipases in reduction processes for the synthesis of metal nanoparticles [18–21]. However enzyme catalysis is associated with a few problems respect to their activity and stability. These limitations can be surmounted by exploiting enzyme-reaction engineering [22]. Here our aim is to provide a brief perspective on the recent trends in enzyme-based technology on materials. Representative examples from the literature are discussed to present an overview on the subject and pictorial representation of various applications of enzymes are given below.

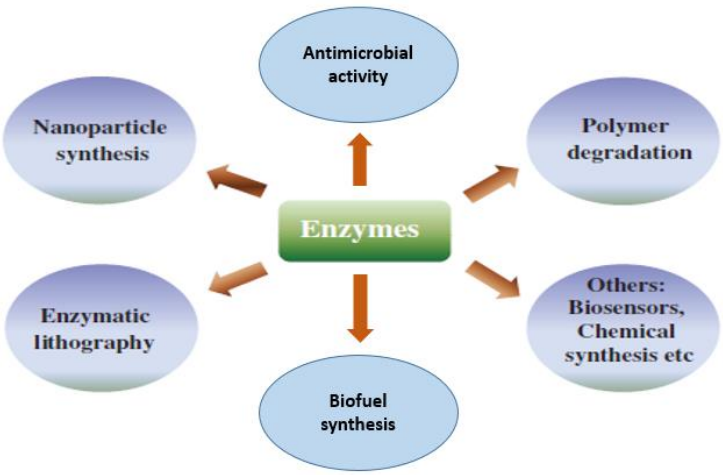

Figure. 1. Pictorial representation of various applications of enzymes.

1.2. Lipase sources and types

Lipases are usually obtained from animals, plants and microbes. Nevertheless, the attributes of the enzymes' origin determines the convenience, cost, and recovery process. In broad, lipase enzyme analogous to those of plants and animals can be obtained from microorganisms as well. There is a disposition to employ the enzymes from microbial sources for commercial purposes, since they are made abundantly by this approach [23]. The microbial enzyme industry offers rapid and robust growth of microbial sources, and thereby enables one to produce enzymes in large quantities. Microbes can be manipulated at genetic level to obtain better strains – via recombinant DNA techniques, chiefly – to better the quality of the enzyme and to obtain higher yields [24]. Lipase was first isolated & studied from bacteria like *Serattia, Pseudomonas aeruginosa* and *Pseudomonas fluorescens* in 1901 [25]. The source of lipases from bacterial, fungal and yeast sources are listed below in Table 1.

Table 1: The occurrence of lipases in different microorganisms

Organism	Author name and year	Reference number
Pseudomonas cepacian	Sugihara *et. al.,* 1992	26
Pseudomonas aeruginosa	Kukeraja *et. al.,* 2005	27
Staphylococcus sp	Ajith kumar *et. al.,* 2012	28
Achromobacter lipolyticum	Khan *et. al.,* 1967	29
Bacillus cereus	Ananth *et. al.,* 2013	30
Bacillus licheniformis VSG1	Sangeetha *et. al.,* 2010	31
Bacillus smithii BTMS 11	Ephraim *et. al.,* 2014	32
Bacillus megaterium AKG-1	Sekhon *et. al.,* 2006	33
Bacillus stearothermophilus MTCC 37	Saba *et. al.,* 2012	34
Bacillus pumilus RK-31	Kumar *et. al.,* 2012	35
Candida Antarctica ZJB09193	Liu *et. al.,* 2012	36

Candida rugosa	Pereira *et. al.,*	2001	37
Lactobacillus brevis	Chander *et. al.,*	1973	38
Lactococcus lactis	Uppada *et. al.,*	2012	39
Lactobacillus plantarum	Lopes *et. al.,*	1999	40
Enterococcus faecium MTCC 5695 *Pediococcus acidilactici*MTCC 11361	Rama Krishnan *et. al.,* 2013		41
Kluyveromyces marxianus	Deive *et. al.,*	2003	42
Lactobacillus delbrueckii subsp. Bulgaricus	El-Sawah *et. al.,*	1995	43
Lactococcus heleveticus	Rashmi *et. al.,*	2014	44
Aspergillus niger	Faloni *et. al.,*	2006	45
Aspergillus awamori	Basheer *et. al.,*	2012	46
Aspergillus fumigatus MTCC 9657	Rajan *et. al.,*	2011	47
Fusarium solani FS-1	Maia *et. al.,*	1999	48
Bacidiobolus	Okafor *et. al.,*	1990	49
Thermomyces lanuginosus	Li *et. al.,*	2009	50

1.3 Enzyme production

The enzyme industry rapidly progressed in the early 1980s and 1990s when it was established that enzymes can be obtained from the microbes. Traditionally, enzymes used to be extracted from animal and plant sources that resulted in reduced level of accessibility, swollen cost and inferior development of the enzyme industry. With the help of genetic engineering, desirable proteins are largely brought forth to satisfy the needs of enzyme industry. Therefore, to the highest degree biopharmaceuticals made nowadays are genetically modified products [51]. In recombinant synthesis, the initial step is to get the desirable DNA fragment; then the DNA is amplified and expressed in a suitable expression system. The yield, quality, production time and ease of extraction are crucial parameters for appropriate expression system for recombinant enzyme manufacturing [52]. Several enzyme expression systems have been established. These include cell cultures of bacteria, molds, mammals, yeasts, plants or insects, or via transgenic animals and plants. Various fermentation methods are employed to produce

enzymes. Microbial cultures are grown on large scale fermenters for enzyme production under optimized growth conditions [53, 54]. Solid state fermentation and submerged fermentation methods are used commonly for enzyme production, but the former one is preferred due to better maintenance of aseptic conditions and process control.

1.4 Application of lipases

1.4.1 Lipase mediated Polymer degradation

Polymer degradation research has attracted attention mainly due to the increased use of the polymeric materials in various domains like agricultural industry, packaging industry, and biomedical applications. Nevertheless, increased commercial utilization of polymers has led to the waste disposal problems. In this backdrop, polymer degradation research has attracted unspoken significant attention to address the environmental issues. Enzymatic degradation of few biopolymers is presented here from recent literature along with factors that can be decisive for degradation. Microorganisms in the environment degrade polymeric materials by the action of their secreted enzymes. In biomedical applications the used polymeric biomaterials may be degraded upon physical contact with body fluids and tissues by several enzymes via by oxidation or hydrolysis [55]. A study reported the radio-labeled polyester-urethanes (PU's) being degraded by cholesterol esterase, horseradish peroxidase and xanthine oxidase enzymes. It was found that the PU's were degraded faster by the action of cholesterol esterase; however the initiation of degradation was done by environmental oxidation. These in vitro studies suggested building of polymers with better degradation rates for in vivo implantation [56, 57]. The polymer degradation rate can be altered by changing the ratio of polymer blends. A study of Pseudomonas lipase mediated PCL degradation reports 100% weight loss for pure PCL polymer, while a blend of the same with 1% non-biodegradable polymer poly (styreneco- acrylonitrile) (SAN) degradation has yielded only 50% weight loss. The

difference in degradation pattern corresponds to the surface properties and crystal structure of the polymer blends. The enzymatic PCL degradation occurred at the amorphous surface of the polymer film. As the degradation proceeds, the content of the non-degradable component of the polymer blend increases at the surface and prevents the lipase from attacking the biodegradable PCL chains, there by stopping the polymer degradation abruptly [56]. In another similar study, degradation of poly (butylene adipate-co-butylene furandicarboxylate) (PBAFs) by porcine pancreas lipase reported that polymer degradation is influenced by the non-degradable crystalline part of the polymer. The amorphous component was degraded by the enzyme leaving the crystalline non-degradable part [57]. A study showed that the enzyme polyhydroxybutyrate (PHB) depolymerase acts on polymer surface first, and then hydrolyze the amorphous part of the polymer and later the crystalline regions [58, 59]. The same was reported by Iwata et al. that enzymatic degradation is greatly influenced by the polymer subunit's crystalline nature and molecular conformation [60–62]. Reports suggest that polymer degradation by enzymes is highly dependent on reaction temperature. Degradation of cross-linked and non-crosslinked PCL polymer was done by the enzyme AK lipase in phosphate buffer saline (PBS) having pH 7.0. The enzymatic degradation gradually increased with increase in temperature till 55 ˚C and 50 ˚C for cross-linked and normal PCL, respectively. This suggests that the increased temperature increases the catalytic activity and reaches an optimum value. After attaining the optimum any further increase in temperature results in protein degradation and hydrolytic activity [63]. G. Madras et al. reported the effect of the alkyl group substitution on enzymatic and thermal degradation of poly n-(acrylates) [poly (methyl acrylate), poly (ethyl acrylate) and poly (butyl acrylate)]. Novozyme 435, lipolase and porcine pancreases were employed to degrade poly n-(acrylates) in toluene medium at various temperatures (40, 50 and 60 °C). The

enzymatic degradability order at 60 °C precedes the identical order as of thermal degradation of the respective polymers [64]. Stereo-isomers of polymer subunits also determines the degradation rate of polymer by enzymes' stereospecificity. Several reports suggested the degradation of poly (L- lactide) by different enzymes like pronase, Proteinase K or lipase [65–68]. Proteinase K breaks down the ester bonds joining the L-lactyl units preferentially compared to D-lactyl units [69–72]. Starch based co-polymers were also analyzed for their biodegradability by employing different enzymes. Pullulanase, glucoamylase and -amylase mediated degradation of polymeric blends of corn starch with poly (ethylene-vinyl alcohol) copolymer and PCL (SEVA-C and SPCL, respectively) have been examined and reported that -amylase was exhibiting superior activity to the glucoamylase [73]. A study has shown the enzymatic degradation of starch-PCL 3-D scaffold by lipase and -amylase. It was also identified that both the enzymes were able to degrade the polymer and the polymer matrix was found to be porous in nature after the enzymatic process [74]. In a relatively new approach, embedded enzymatic polymer degradation was reported by Gross et al. In this approach, an active enzyme is embedded in a polymeric matrix, which starts to degrade the whole matrix of the polymer as opposed to the conventional polymer degradation, where the degradation begins at the polymer film surface and then penetrate to the bulk. *Candida Antarctica* Lipase B (CALB) blended with the surfactant sodium bis (2-ethylhexyl) sulfosuccinate was mixed with PCL in various proportions and casted into thin films. It was found that the PCL films containing 6.5 and 1.65% of CALB at pH 7.1 resulted in complete degradation of the polymer in 1 and 18 days, respectively [75]. This demonstrates the ability to tune the degradation kinetics of a polymer simply by altering the enzyme loading in the matrix. In a later study, the same group has optimized flow conditions and relative humidity for the PCL degradation [76]. Thus, it is clear that the

polymer degradation is influenced by the surface and nature of chemical bonds existing in the polymer. Polymer blends with various components have a significant effect in the degradation capabilities of the final material. The presence of non-degradable polymer component in polymer blends will alter the polymer films' micro-structure and thereby making it more crystalline and less accessible to the enzyme leading to lesser extent of degradation. It is evident that large number of polymers will be degraded to a great extent if proper pH, temperature conditions along with an appropriate enzyme is provided. Further investigation and understanding of polymer degradation is required that are specific towards individual enzymes.

1.4.2 Lipases in detergent industry

Lipases have been actively used in many commercial detergent preparations. The first lipase used in commercial detergents was isolated from *Thermomyces lanuginosus* [77]. This detergent preparation was more efficient for cold washing which reduces the energy consumption and wear and tear of textile fibers compared to synthetic detergents. Lipase isolated from *Staphylococcus arlettae* JPBW-1 of rock salt mines possessed an ability to remove oil stains with 52% when compared to traditional detergents. Hence, it found application as an additive in laundry detergent formulations [78]. The lipase isolated from *Staphylococcus* sp. strain ESW has ability to withstand greater alkalinity s and was active in non-ionic and anionic surfactants thereby highlighting its usage in detergent formulations [79]. Similarly, rubber seed lipase was isolated and studied for its compatibility with other commercial detergents and it was found to be functional in low temperatures, alkaline pH. The rubber seed lipase was checked for activity in various detergents. It didn't lose its activity in the presence of various surfactants and detergents which in turn incorporated as an additive in the detergent formulations [80].

1.4.3 Lipase in production of biodiesel

The transesterification action of lipase has been exploited to synthesize fatty acid methyl and ethyl esters from conventional vegetable cooking oils to use as biodiesel.

The lipases isolated from *Candida antarctica* (Novozym 435) and *Photobacterium lipolyticum* lipase (M37) has been used for the production of biodiesel [81]. A comparative study was performed to evaluate the quality, quantity of biodiesel yields exploiting lipases from two different microbes. The results showed M37 to be the best suitable strain for biodiesel production. 'Ecodiesel-100' has been produced by exploiting pig pancreatic lipase, it showed biochemical properties similar to that of the conventional biodiesel [82]. A novel lipase CS274, isolated and purified from *Ralstonia sp*. showed resistance against both the oxidizing and reducing agents and it is used in the production of biodiesel from palm oil [83].

1.4.4 Lipases in ester synthesis

Lipase based ester synthesis has been in use in food industry for decades. Short chain esters have a great significance in enhancing food taste, so they are used as synthetic flavors in food industries. Lipase isolated from fungal strain *Rhizopus oryzae* NRRL 3562 l is used to synthesize Methyl ester of pine apple flavor and octyl acetate of orange flavor, these esters are added to food as pine apple and orange synthetic flavors in food and beverage industries [84]. Similarly, Ethyl valerate, a green apple flavor ester, is synthesized by enzymatic esterification of valeric acid with ethyl alcohol by immobilized *Burkhoderia cepacia* [85].

Lipase isolated from marine actinomycete, *S. variabilis* NGP 3 produced a fragrant ester which has been potentially employed in textile and brewing industries [86]. Lipase isolated from *Rhizopus* sp. has been used for different esterification and

transesterification reactions to produce citronellyl esters like citronellyl acetate and citronellyl butyrates which are used as flavor and fragrance enhancers respectively [87].

1.4.5 Lipase as biosensor

Lipase based biosensors have been developed exploiting the enzyme specific properties, few examples are discussed here, Potentiometric biosensors were developed by employing the lipase of *Candida rugosa*, to detect organophosphorus pesticides like methyl-parathion and tributyrin in soil, to estimate the pollutants and determine the fitness of the land for agriculture [88]. Fungal lipase-labelled probes can be employed in the detection of the complementary nucleic acids by specific hybridization which potentially eliminated the risk of using unstable and hazardous radio labelled polynucleotides [89]. Lipase based medical biosensor has been shown proficient in bio-sensing the blood cholesterol and triglycerides [90].

1.4.6 Lipase in cosmetics

Lipase isolated from the fungal strains *Candida cylindracea, Rhizomucor meihei, Candida antarctica* has been employed in anti-obesity creams and hair care products. As all biological processes are based upon the activity of enzymes, these biocatalysts are also essential for body care. In the skin enzymes are responsible for uncoupling complex inactive molecules and transforming them into simpler and often more active molecules. Proteases, for example, decouple or hydrolyse proteins, glycosidases promote the enrichment of the epidermis with ceramides and tyrosinase facilitates the synthesis of melanin. On the skin and the stratum corneum, enzymatic reactions modulate keratinisation processes, ensure inter-corneocyte cohesion, encourage tanning and auto-photoprotection, act on the metabolism of sebaceous glands and adipocytes, have a whitening activity on age spots, stimulate the natural defense mechanisms of the skin or protect collagen and elastin fibers. Accordingly, enzymes obviously make promising

natural active agents for specified personal care products belonging to the so-called ‘functional cosmetics’, ‘cosmeceuticals’ or ‘treatment products’. Active lipases can mainly be found in cosmetics for surficial cleansing (e.g. ‘Facial Cleanser’ by Juju Cosmetics, ‘Revue Sebum Soap’ by Kanebo Cosmetics), anti-cellulite treatment (e.g. ‘Silhouette Sculptant Exfoliating Mousse 402’ by Maria Galland, ‘Double Minceur Cible´e’ by Guinot) or overall body slimming (e.g. ‘Bath Additive with Fat Dissolving Enzymes’ by Ishizawa Laboratories), where they are responsible for the mild loosening and removal of dirt and/or small flakes of dead corneous skin (i.e. peeling) and/or assist in breaking down fat deposits, often in combination with further enzymes such as proteases. In a different approach lipases are included in cosmetic formulations for controlled in situ release of an active ingredient (e.g. hydroxy acids) from an inactive precursor (e.g. hydroxy acid ester), an application type that has become of particular interest in the field of functional perfumery for an even development of odour over time. Increasingly, however, enzymes already present in the skin instead of added enzymes are addressed by such cosmetics, as exemplified for the ‘‘on demand released’’ deodorant active polyglycerol-3 caprylate [91].

1.4.7 Lipases in medical treatment

Lipases extracted from *Yarrowia lipolytica* are used as health care supplement in case of exocrine pancreatic insufficiency [92]. Skin inflammations can be conveniently treated by Lipases in combination with hyaluronidase enzyme [94]. Serum cholesterol level are reduced by Lovastatin, this drug is chemically synthesized by treatment of its precursor with lipase derived from *Candida rugosa* [95]. Regioselectivity activity of lipase isolated from *Serratia marcescens* has been exploited for asymmetric hydrolysis of key intermediate compound 3-phenylglycidic acid ester in the synthesis of diltiazem hydrochloride [96].

1.4.8 Lipases in oil degradation

Lipase isolated *Candida antarctica, Pseudomonas cepacia, Yarrowia lipolytica, Pseudomonas aeruginosa and Carica papaya* has been shown to possess the potential for the degradation of oil spills, fats and grease from water contaminated with oil thereby assisting in biological water cleanup thus eliminating water pollution [97].

Large success of microbial lipases in food and other biotechnological systems can be attributed to the broad biochemical diversity of the microorganisms, to the genetic manipulation of the organisms and to improved techniques for enzyme production and purification. Microbial enzymes also conform more closely to the required characteristics, such as cost of using the enzyme, activity at optimal conditions, safety of the enzyme and availability at required purity and stability, than do animal and plant lipases.

Commercial production of extra-cellular enzymes is in principle very simple, involving cultivation of a microorganism and subsequent recovery of the enzyme. This requires the use of an organism which grows on an inexpensive medium and produces high yields of enzyme in a short time. Simple and inexpensive recovery of the enzyme leading to a stable product with an acceptable appearance and which can be handled safely is also important.

These objectives are fulfilled by the combined optimization of strain properties and process parameters. Optimization of strain properties, mainly by the development of suitable mutants, usually offers an inexpensive and permanent solution to the problem.

1.4.9 Enzyme mediated nanoparticle synthesis

Synthesis of metal nanoparticles using biomolecules is attractive owing to their stability in colloidal solutions, different shapes and sizes. The broad range of nanoparticle utility is mainly due to the small size and greater surface area. A variety of synthetic

approaches have been employed for metal nanoparticle synthesis [98]. However, these processes have some liabilities due to the use of harmful radiations and chemical processes. Therefore, a lot of attention has been given in the current scenario for green and sustainable synthetic approaches for nanoparticles of various sizes and shapes while preserving monodispersity. In this context, the reductive enzymes from microorganisms like bacteria and fungi have gained significant attention for the synthesis of metal nanoparticles. Recent reports suggest the use of different reductases from *Fusarium oxysporum* for the synthesis of metal nanoparticles. In one such report, the extracellular Sulfate reductase from *Fusarium oxysporum* is employed to make cadmium sulfide nanoparticles of size 5–20 nm by the reaction of aqueous $CdSO_4$ solution with the enzyme. The enzyme reacts and converts sulfate ions to sulfide ions, which lead to the formation of CdS nanoparticles [99]. The same group, in another study, has exploited extracellular alpha-NADPH-dependent nitrate reductase for the synthesis of silver nanoparticles [100]. Brayner et al., has employed common cyanobacteria like *Anabaena*, *Leptolyngbya and Clathorix* to synthesize Au, Pd, Pt and Ag nanoparticles of regulated size in colloidal solution protected with capping protein. They identified the intracellular protein responsible for the synthesis of nanoparticles to be a nitrogenase enzyme [101]. Silver has been used in the form of silver salts for the treatment of several bacterial infections from time immemorial. But antibiotics discovery has reduced the use of silver significantly. However, due to rapid development of nanotechnology and silver in the form of nanoparticles, did a successful return as a potent germicidal agent in the form of nanolotions and nanogels that helped reducing the use of antibiotics [102]. A pure form of alpha-amylase was used to make silver nanoparticles. The alpha-amylase reduced the silver ions resulting in the fabrication of stabilized 22–44 nm silver nanoparticles [103]. Extracellular nitrate-dependent reductase from several strains of *Fusarium oxysporum*

was extracted and used in the production of silver nanoparticles [104]. Similarly, nitrate-dependent reductases from *Aspergillus niger* was shown to be capable of synthesizing silver nanoparticles. These nanoparticles were bactericidal against gram-negative *Escherichia coli* and gram-positive *Staphylococcus aureus* bacteria [105, 106]. In other developments, supernatants of *Klebsiella pneumonia*, *Escherichia coli*, and *Enterobacter cloacae* (*Enterobacteriacae*) that contain nitroreductase enzymes were used to synthesize metallic nanoparticles of silver [107]. A dimeric hydrogenase enzyme extracted from *Fusarium oxysporum* was employed to synthesize platinum nanoparticles [108]. Gold nanoparticles (Au NPs) possess large potential as drug carriers and also for gene delivery in gene therapy. One more unique feature of Au NPs is thiol group interaction, creating highly controlled means of drug or gene release [109]. Due to the surface plasmon resonance in the visible light range, Au NPs are vastly used in optical biosensors. The extract from fungi *Sclerotium rolfsii* containing NADPH-dependent enzyme was used by Narayanan et al., to synthesize gold nanoparticles in less than 15 minutes. They demonstrated the controllability of size and shape of nanoparticles by altering the salt and cell extract ratios [110]. Atul kumar et al., has shown that the enzyme activity was retained while synthesizing gold nanoparticles. A pure form of alpha-amylase was used to synthesize gold nanoparticles by reduction of tetrachloroaurate. The enzyme readily stabilized nanoparticles by capping in colloidal solution [111]. In other reports, in vitro biosynthesis of gold nanoparticles capped with peptide was done with help of sulfite reductase alpha-NADPH-dependent and phytochelatin. The enzyme sulfite reductase reduced gold ions resulting in the formation of a stable gold nanoparticle colloidal solution, with size ranging from 7–20 nm capped with the protein that stabilized the NPs in solution [112]. *Rhodopseudomonas capsulata* bacteria were employed for the synthesis of gold nanoparticles of different sizes and shapes. The key factor for

controlling the size and shape of the gold nanoparticles was found to be the pH value of the reaction mixture. It was proposed that the possible mechanism liable for the reduction of Au (3+) to Au (0) that results in the fabrication of gold nanoparticles is by the secreted cofactor NADH- and $NADH_2$- dependent enzymes by the bacteria [113]. Morse et al., exploited hydrolase from marine sponge to catalyze the hydrolysis of gallium (III) nitrate that resulted in the polycondensation of gallium oxide to form nanocrystallites at low temperatures all along the length of the filaments [114]. Enzymatic synthesis of nanoparticles is highly dependent on the nature of the metal salt, enzyme and pH of the solution. The stability is brought about by the nature of capping proteins and interaction strength of proteins with metal nanoparticles. This may lead to varied morphologies and size control and monodispersity index.

1.5 Gaps in existing research

The above review states the wide range of applications of lipase enzyme which has led to the survey of a variety of potential microorganisms to be utilized for its production. Further, lipases show enhanced substrate specificity, regio and enantioselectivity, becoming the most used enzymes across the industries. Therefore, there is a need to display the important advantages of lipase over classical chemical catalysts, to characterize various applications of lipase, optimize the process for enhanced catalysis and improve enzyme-mediated process efficiency with reduced side products under mild temperature and pressure conditions.

A careful introspection of the literature reveals several gaps exists as stated below in the current technology of polymer degradation, nanoparticle synthesis and biofuel synthesis using probiotic lipases isolated from *Lactobacillus brevis and Lactobacillus plantarum*.

- The current polymer degradation is based on either harmful chemical or physical treatment methods, and also majorly on fungal lipases. Since these methods are environmental damaging and isolation of fungal lipases is cumbersome. There is a need to develop eco-friendly approaches to degrade polymer material employing lipases from beneficial probiotic bacteria. So far no efforts have been made to employ lipases isolated from probiotic sources for degrading polymer.
- There is a necessity for synthesizing nanoparticles using green methods and exploration of these nanoparticles in various fields like drug delivery, antimicrobial agents.
- So far no attempts have been made to understand the role of probiotic lipases as capping agents and their applicability never been studied for nanoparticle synthesis, stability, catalytic activity, biocompatibility and also the role of probiotic lipase capping for enhancing the antimicrobial activity of nanoparticles has never been explored, this enables us to develop future antimicrobial agents that are biocompatible and robust.
- Further there is a need to develop strategies to convert waste cooking oil to biodiesel to make carbon neutral fuel employing bacterial probiotics lipases that can be isolated easily and stable over harsher conditions.

Lactobacillus brevis and Lactobacillus plantarum were selected for this study, since lipase isolated from those strains was rarely or meagerly explored for various applications and also the lipase enzyme from these species is metabolically versatile, stable in organic solvents, alkaline in nature, eco-friendly and these strains have a high proteome efficiency, effective at performing metabolic switch.

1.6 Scope and objective of the work

Based on the gaps in the existing literature, we made an attempt to explore the probiotic lipase isolated from *Lactobacillus sps*. to study the following objectives:

- *Lactobacillus sps*. lipase mediated poly (ε-caprolactone) degradation by pouring method.
- *Lactobacillus sps.* lipase mediated embedded PCL degradation.
- To understand the effect of probiotic *Lactobacillus plantarum* derived lipase in synthesizing and capping, catalytically active gold nanoparticles.
- To evaluate *in vitro* hemocompatibility evaluation of gold nanoparticles capped with *Lactobacillus plantarum* derived lipase.
- Evaluation of antimicrobial activity of *Lactobacillus sps*. lipase capped silver-nanoparticles.
- Free and immobilized *Lactobacillus sps.* lipase mediated transesterification of waste cooking oil to biodiesel.

CHAPTER 2

LACTOBACILLUS SPS. LIPASE MEDIATED POLY (ε-CAPROLACTONE) DEGRADATION

2.1 Introduction:

Enzymes are considered to be one of the efficient biocatalysts available in nature. Enzymes of various origins such as fungi including yeast, molds and bacteria have been shown to have a great potential towards a variety of catalytic chemical transformations. Among them, lipases are considered to be one of the important classes of enzymes, which are well known for their hydrolytic action on ester functionalities. Lipases from different bacterial strains are being screened for enhanced production, as they are easy to grow at mass level and genetically modified easily. Bacterial lipases find several promising applications in catalyst industry because of their alkaline nature, thermal stability and tolerance to organic solvents [116]. Specifically, lactic acid bacteria are universally accepted as important probiotics, non-pathogenic and healthy microflora of human mucosal surfaces [117]. In addition, lipases from these bacteria are also known for their contribution to chemical synthesis, polymer degradation, dairy industry, nutrition cosmetics and pharmaceutical processing [118, 119]. Due to the varied performance of lipases from different sources towards different applications, there is a constant effort towards screening hyperactive microbial strains for producing lipases with enhanced activity.

One of the important areas where lipases can play a major role is polymer degradation [120, 121]. In the backdrop of increasing pollution caused by various non-degradable polymers such as polystyrene, polyethylene, polypropylene, there is a necessity for replacing them with biodegradable polymers [122]. The biodegradable polymers find immense usage in biomedical applications such as tissue engineering, drug delivery and resorbable sutures [123,124]. Some of the most common biodegradable polymers include polylactide, polyglycolide, polycarbonate, and polysaccharide [125, 126]. In order to determine the applicability of a candidate polymer material, it is

important to understand its biodegradation. Thus, the study of biodegradability of polymeric materials is considered to be of paramount significance. PCL is a biodegradable and biocompatible semi crystalline linear aliphatic polyester, which is used in a wide range of bio-applications [127-130]. Extensive research has been carried out on the properties of PCL that identified this polymer to be compatible for various biomedical and environmental applications. A number of studies have reported fungal and bacterial lipase mediated PCL degradation [131-133]. In one such report, three fungal lipases of *Rhizopus delemar, Candida rugose* and *Mucor miehei* were tested to select the best enzyme for PCL degradation [134] and the lipase from *Mucor miehei* was found to effectively degrade PCL. Similarly, lipases from other fungal sources (like *Fusarium moniliforme, Chaetomium globosum, Aspergillus fischeri, Aureobasidium pullulans, Aspergillus flavus, Cryptococcus laurentii)* and bacterial source (like *Pseudomonas sps.)* were shown to be capable of degrading PCL [135-140]. Though lipases from fungi have been widely studied for PCL degradation, only a meagre literature is available with bacterial lipase other than *Pseudomonas sps.*

In this chapter, we have explored PCL degradation using lipases from *Lactobacillus brevis* (molecular weight of 26 kDa), *Lactobacillus plantarum* (molecular weight of 66 kDa) and their co-culture, whose production was previously reported by our group [141]. The study in the present chapter focusses on the change in thermal stability, crystallinity, surface morphology and weight loss of PCL films with respect to its lipase mediated degradation in detail.

2.2 Material and Methods:

2.2.1 Materials:

2.2.2 Sources: *L. plantarum* (MTCC 4461) and *L. brevis* (MTCC 4460) were purchased from IMTECH, Chandigarh, India. PCL in the form of pellets with an average molecular weight (Mw) of 45,000 Da was purchased from Sigma-Aldrich.

2.2.3 Preparation of Lipase:

Lipase gene from the bacterial cultures procured was isolated and amplified using thermal cycler. A recombinant expression vector was constructed using plasmid pMALc5X and the amplified Lipase gene, after transformation was heterologously expressed in *E.coli* strain BL21 (DE3) pLysS for lipase expression (Bionova). Since the vector contains Maltose binding protein (MBP), the fusion of a target protein (lipase) to MBP permits its one-step purification using amylose resin [142].

2.2.4 Determination of Lipase activity:

The lipase assay was performed spectrophotometrically using p-nitrophenyl palmitate as substrate [143]. The p-nitro phenol was liberated from p-nitrophenyl palmitate by lipase mediated hydrolysis and the absorbance of liberated p-nitro phenol was measured at 410 nm. One unit (U) of lipase was defined as the amount of enzyme that liberates one micromole of p-nitro phenol per minute under the assay conditions [144].

2.2.5 Characterization:

Thermogravimetric and differential thermal analyses of the samples were carried out on DTG-60, Shimadzu in order to understand the thermal degradation behavior and percentage crystallinity. Thermogravimetric and differential thermal analyses of the samples were carried out on DTG-60, Shimadzu in order to understand the thermal degradation behaviour and percentage crystallinity. PCL films have a thermal

degradation point of 400 °C, Since the PCL films are degraded by enzyme, they will lose the thermal stability with the time of degradation, this thermal degradation temperature required falls down, which can be determine by heating the degraded PCL film during thermal analysis. The specimens were heated in nitrogen atmosphere from 35 °C to 600 °C with a heating rate of 10 °C/min and a nitrogen flow rate of 20 mL/min. To follow the chemical changes in the PCL polymer, Fourier transform infrared (FT-IR) spectra of the biodegraded and non-degraded samples in KBr pellets were recorded in the frequency range of 400 to 4000 cm^{-1} using Shimadzu 8400S instrument. Lipase hydrolyse the polymer by simple breaking down the ester bond exposing alcohol and carboxylic acid groups, the FTIR analyses helps us to identify the exposed functional groups, the ftir confirmed the hydrolytic action of the enzymes on the ester bonds of the PCL films as we can see alcoholic and carboxylic functional groups in the plot. Surface morphology of the enzymatically degraded and non-degraded PCL films was studied using a scanning electron microscope (Hitachi S-3400N, Japan). SEM provides us reports of the enzyme action on the polymer, whether the polymer is being degraded in to down fashion or from interior after an initial top down degradation approach.

2.3. Preparation of PCL film:

The PCL films used for the enzymatic degradation were prepared by solvent casting method [145]. Briefly, a solution was made by dissolving the PCL pellets in chloroform (1% w/v), with stirring at 37 °C for 30 minutes at 600 rpm. This solution was then poured onto culture dishes and dried overnight in order to get PCL thin films. The casted films thus obtained were cut into dimensions of 10 mm x 10 mm strips and weighed before subjecting to enzymatic degradation. The weight and thickness of the cut films were found to be 3.5±0.5 mg and 0.1±.0.01 mm, respectively.

2.4. Lipase mediated PCL degradation:

The enzymatic degradation was performed by adding 10 mL of different concentration of lipases from *L. plantarum, L. brevis* and their co-culture to the PCL samples. The enzymes were taken in 0.01 M Tris-HCl buffer of pH 8.1 and the degradation studies were carried out at a constant temperature of 37 °C. The concentrations of the different lipases were varied from 0.5 mg/mL to 10 mg/mL. At regular intervals, the PCL film strips were removed from the vial, washed with distilled water and then dried in a desiccator at room temperature for 24 hr. The weight of the films was determined before and after enzymatic degradation**,** and the weight loss was expressed in relative terms using the following formula.

$$\text{Relative weight loss \%} = \frac{\text{Initial weight} - \text{Final weight}}{\text{Initial weight}} \times 100$$

2.5 Results and Discussion:

PCL films were incubated with each type of lipase in Tris-HCl buffer solution at different concentrations and their gravimetric analyses up to 10 days were carried out.

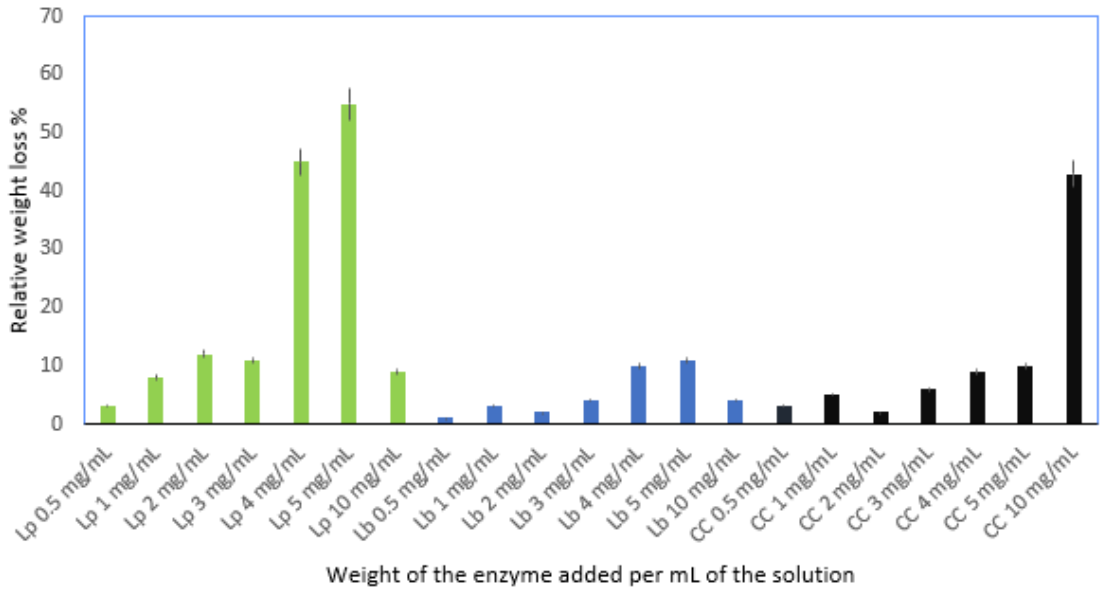

Fig. 2.1 Relative weight loss comparison after 10 day treatment of PCL film with different concentrations of *L. plantarum, L. brevis* and co-cultured (CC) lipases.

Fig 2.1 compares the relative mass loss percentage of PCL films before and after 10 days of enzymatic degradation. No significant mass loss of PCL film was found with different concentrations of *L. brevis* lipase. With 1 mg/mL loading of *L. brevis* lipase, there was only ~2 wt.% mass loss observed, which increased to a maximum of up to ~10 wt.% when the loading was increased to 4-5 mg/mL. However, when the *L. plantarum* lipase was employed, the PCL film degradation efficiency was found to be substantially higher. Interestingly, in this case, the PCL mass loss with 1 mg/mL loading of the lipase was found to be ~10%, which increased up to ~60% with the lipase loading of 5 mg/mL, beyond which the percentage mass loss was gradually decreased. This reveals that the *L. plantarum* lipase effectively degraded a major portion of the PCL film at an optimal loading of 5 mg/mL. On the other hand, the co-culture of *L. brevis* and *L. plantarum* showed almost 10% PCL degradation up to a loading of 5 mg/mL. However, with an increased lipase loading of 10 mg/mL, the percentage mass loss significantly increased to ~50%. This shows that the co-cultured lipase has good efficiency at a higher concentration when compared to the *L. plantarum* lipase. Thus, the overall polymer degradation was found to be dependent on the concentration and type of the enzyme. These results clearly show that the *L. plantarum* lipase exhibited the maximum PCL degradation efficiency among the three used in this study.

In order to further understand the enzyme action towards PCL degradation, we utilized thermogravimetric analysis (TGA) and differential thermal analysis (DTA) to study the thermal degradation behavior and crystallinity of the left-over PCL film after incubation with lipases. For this, the remained PCL films were removed at a time interval of 1, 5 and 10 days from each lipase culture, washed and dried well. These films were subjected to TGA and DTA analyses and the results are plotted in Fig 2.2 to 2.8.

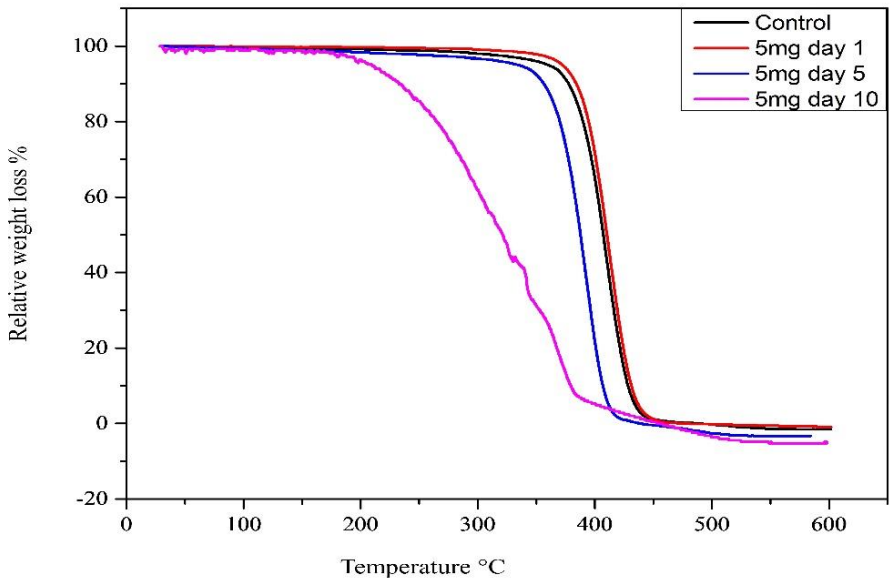

Fig. 2.2. TGA plot of the PCL film treated with *L. plantarum* lipase over different time periods.

Control experiments were also performed with pristine PCL films in order to compare their thermal behaviour after enzymatic degradation. It is expected that the onset of thermal degradation of the PCL films degraded by the enzymes would be lesser than the pristine films, as the degraded films would have been converted into lower molecular weight polymers. The onset of thermal degradation was measured at 5 wt% mass loss. The thermal stability of the pristine PCL film was found to be ~410 °C and the total mass loss was observed by 450 °C. The thermal degradation of the PCL films treated with each of the three different lipases for a period of 1 day was found to be identical to that of the pristine PCL film. This shows that there was no significant degradation occurred with all three enzymes in one day period. However, the PCL films that were subjected to 5 and 10 days of enzymatic degradation showed lesser thermal stability than the control. In case of *L. brevis*, the PCL films incubated with 5 mg/mL of lipase after 5 and 10 days were shown a thermal stability of ~389 °C. This shows that the lipase from *L. brevis* was not effective towards PCL degradation. On the other hand, the PCL films incubated with 5

mg/mL of the lipase from *L. plantarum* showed a clear trend in the thermal stability after 5 and 10 days of enzymatic degradation. In this case, the onset of PCL degradation after 5 and 10 days was found to be 343 and ~235 °C, respectively.

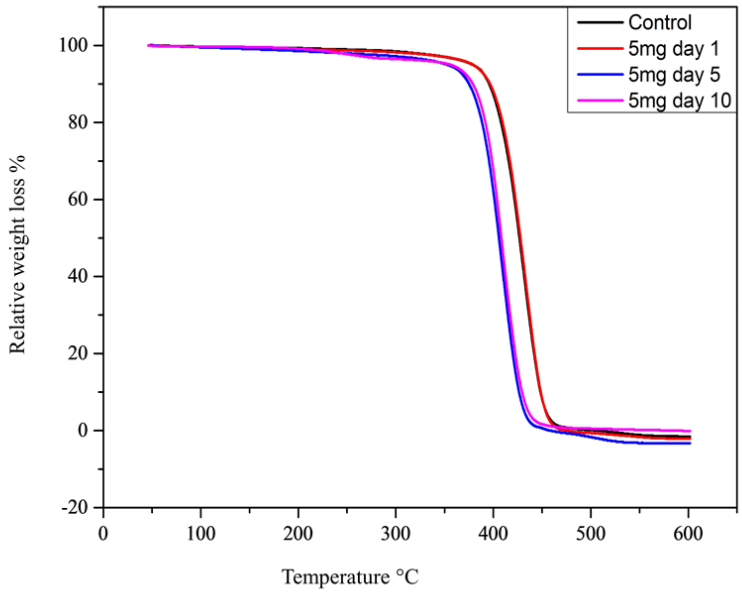

Fig. 2.3. TGA plot of the PCL film treated with *L. brevis* lipase over different time periods.

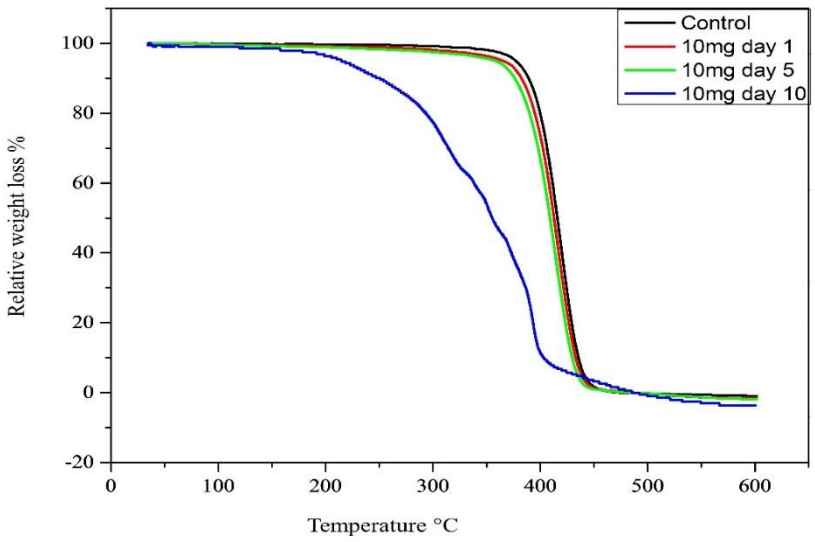

Fig. 2.4. TGA plot of the PCL film treated with co-cultured lipase over different time periods

This greater drop in the onset degradation temperature clearly shows that the lipase from *L. plantarum* possesses high efficiency towards PCL degradation. In case of the co-cultured lipase, with a loading of 10 mg/mL, up to day 5, the PCL degradation was almost identical to the control. However, the 10 day incubated PCL film showed a faster thermal degradation with the onset of degradation at ~232 °C. Thus, the higher loading of co-cultured lipase was found to be effective after 10 days. These results are very much in line with the earlier gravimetric analyses and corroborate that the *L. plantarum* lipase was the best among the three towards PCL degradation.

Since PCL is a semi crystalline polymer, DTA analysis can give insight to the regions that are degraded by the enzymes. The DTA results of the lipase degraded PCL films after 1, 5 and 10 days were compared with the pristine PCL film (Fig 2.6 To 2.8).

Table 2: Variation in percentage crystallinity analyzed from the DTA data

S.No	Day	Enzyme added	Percentage crystallinity
1	1	Lp 5mg/mL	60
2	5	Lp 5mg/mL	69
3	10	Lp 5mg/mL	93
4	1	CC 10mg/mL	60
5	5	CC 10mg/mL	77
6	10	CC 10mg/mL	93
7	1,5,10	Control	55

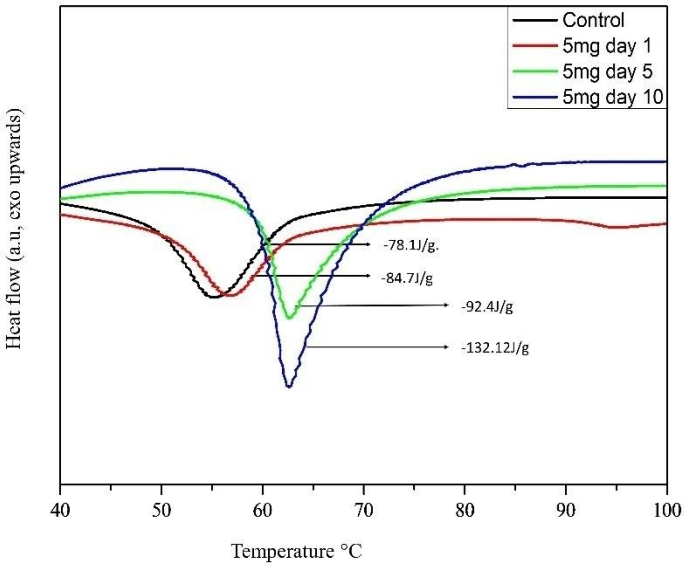

Fig. 2.5. DTA plot of the PCL film degraded by *L. plantarum* lipase over different time periods.

Table 2 summarizes the percentage crystallinity of the control and enzyme degraded PCL films. It has been observed that the pristine PCL film showed a percentage crystallinity of ~55 %. Similar to the TGA observation, the PCL films incubated with the three different enzymes for 1 day showed a very similar crystalline behaviour to that of the control. This shows that there was no significant polymer degradation by any of the enzymes in a period of 1 day. With *L. brevis*, the PCL films incubated with 5 mg/mL of lipase after 5 and 10 days also did not show a significant change in the crystallinity, indicating the poor enzymatic degradation of the polymer. On the other hand, the percentage crystallinity of the 5 and 10 days enzyme degraded PCL films with *L. plantarum* and co-cultured lipases showed a clear trend of increasing crystallinity. The PCL film subjected to enzymatic degradation with *L. plantarum* possessed a crystallinity of ~93% after 10 days. These observations clearly indicate that the amorphous regions of the PCL films have been degraded more effectively than the crystalline regions, which is in line with the literature reports [132, 146, 147, 148, 149].

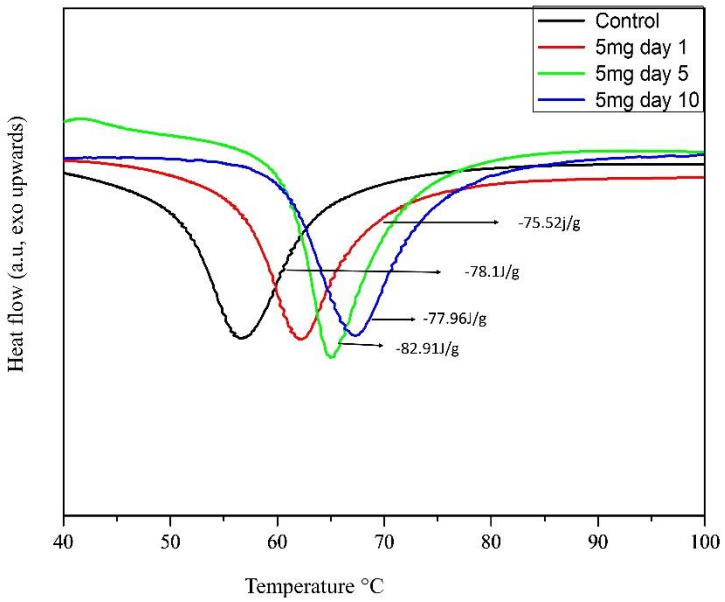

Fig. 2.6. DTA plot of the PCL film degraded by *L. brevis* lipase over different time periods.

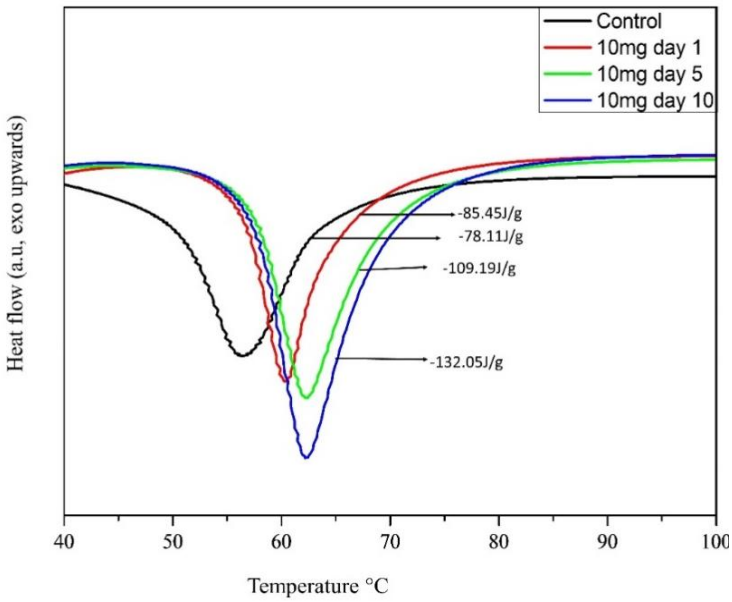

Fig. 2.7. DTA plot of the PCL film degraded by co-cultured lipase over different time periods.

To further confirm the enzymatic action on the PCL film, IR analysis was carried out with the pristine PCL film, and the films incubated with *L. plantarum* and co-cultured lipases for 10 days and the spectra are plotted in Fig 2.8.

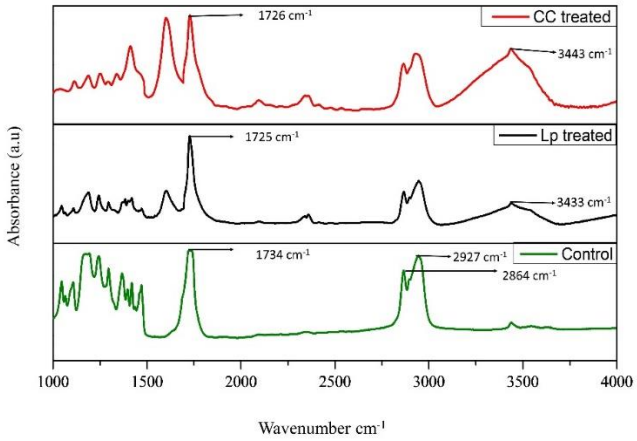

Fig. 2.8. FT-IR spectra of control and PCL films treated with *L. plantarum* and co-cultured (CC) lipases.

The pristine PCL film showed a characteristic ester carbonyl stretch at 1734 cm^{-1}. In addition, the characteristic C-H asymmetric and symmetric stretching peaks were observed at 2927 and 2864 cm^{-1}, respectively. After degradation by the enzymes, the carbonyl stretching peak was shifted to ~1725 cm^{-1}, which is a characteristic band of carbonyl from carboxylic acid. In addition, a broad peak in the range of 3000-3600 cm^{-1} was observed in the enzyme degraded PCL films, which is characteristic of hydroxyl groups of alcohol and carboxylic acid. These observations clearly indicate that the PCL films underwent chemical decomposition by the enzymatic action. The formation of carboxylic acid clearly indicated the hydrolysis of ester bonds, which is the principal mode of action of lipase class of enzymes.

Finally, the SEM visualization of the pristine PCL film and the film incubated with *L. plantarum* for 10 days was performed to understand the change in morphology of the polymer film (Fig 2.9).

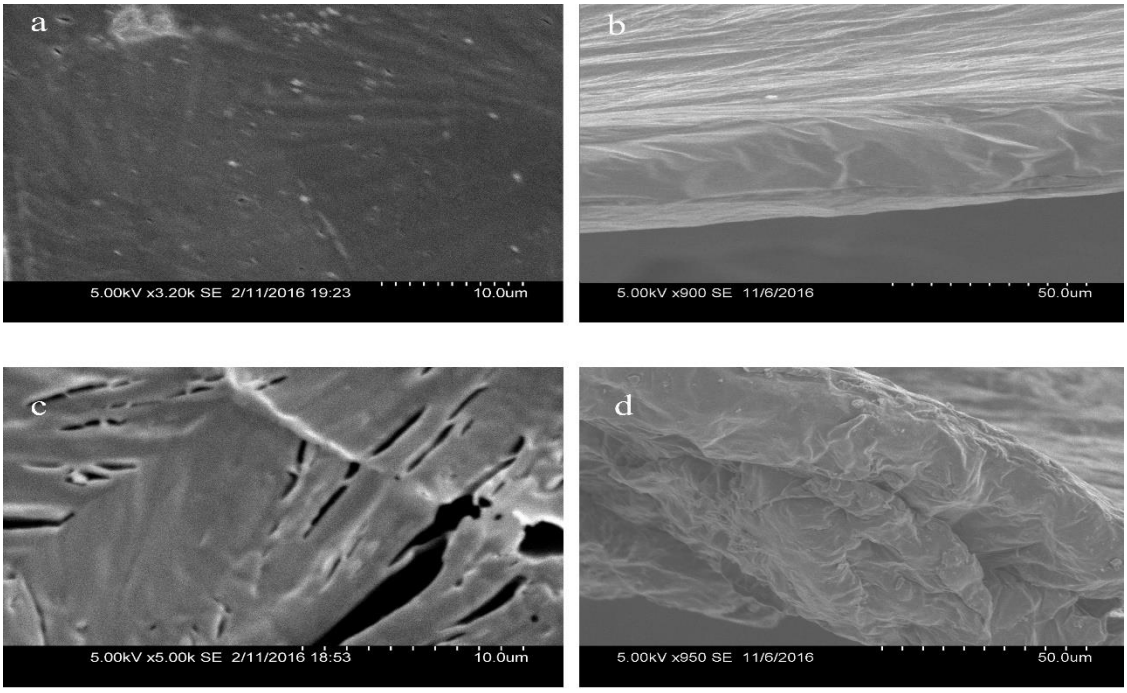

Fig. 2.9. SEM images of (a) control and (b) *L. plantarum* treated PCL film.

As seen from the Fig, the pristine PCL film was found to possess a smooth crack-free surface. On the contrary, the enzyme degraded film, under identical magnification to that of the control was found to contain several microscale cracks. This shows that a substantial amount of enzymatic polymer degradation has taken place. It appears to be that the PCL degradation has begun from the surface of the polymer film and progressed to the depth. In the process, the amorphous regions of the polymer were degraded at first that gave rise to increase in the percentage crystallinity of the polymer.

2.6 Conclusions:

The enzymatic degradation of the PCL film was performed by three different lipases obtained from *Lactobacillus brevis*, *Lactobacillus plantarum* and their co-culture. The enzymatic degradation was found to be significantly influenced by the concentration,

time of exposure and the type of the enzyme. Among the three enzymes screened in this study, the lipase from *Lactobacillus plantarum* was found to possess the maximum PCL degradation activity at a nominal loading of 5 mg/mL. Thermogravimetric analysis results showed that with increasing exposure time of enzyme, the thermal stability of the PCL films decreased due to the polymer degradation. The DTA analyses revealed that the enzyme preferentially degraded the amorphous regions at first, as evidenced by the increase in percentage crystallinity of the polymer. While the SEM analysis has shown the cracked polymer surface after enzymatic degradation, the FTIR analyses confirmed the hydrolytic action of the enzymes on the ester bonds of the PCL films. The study reveals the potential of genetically engineered probiotic *Lactobacillus* class of lipases towards polymer degradation with enhanced efficiency.

CHAPTER 3

EMBEDDED ENZYMATIC DEGRADATION OF PCL POLYMER

3.1 Introduction:

Polymer biodegradation is of paramount interest for several applications including drug delivery, tissue engineering and biomedical sutures [150]. Conventionally, polymer degradation was carried out either through chemical or thermal treatment [151, 152]. Chemical treatments often involve harsh conditions such as strong acids, bases or peroxides, which are not eco-friendly. Thermal degradation of polymers generally releases greenhouse gases and at times highly toxic gases such as dioxin [153]. On the other hand, biodegradation by microbial enzymes has emerged as an attractive alternate route for polymer degradation due to the mild conditions, and biocompatibility [154,155]. Due to its room temperature operation, enzymatic polymer degradation is also considered to be energy efficient [156].

Enzymes from various sources such as fungi and bacteria have been shown to have a great potential towards polymer degradation. Several enzymes like amylases, proteases and lipases are employed for polymer degradation due to their hydrolytic action on the functional groups such as glycosidic, amide and ester, respectively [157,158]. Bacterial lipases are generally considered to be one of the important classes of enzymes that can easily be genetically modified and produced at mass level. Also, they are promising over fungal lipases owing to their alkaline nature, thermal stability and tolerance to organic solvents [159]. Among the various bacterial strains, lactic acid bacteria like *Lactobacillus sp.* are established as probiotics, avirulent and part of human mucosal surfaces [160].

Since many of the preferred biodegradable polymers possess ester functionality, lipases are majorly used for such hydrolytic degradation [161]. Some of the preferred ester based bioresorbable polymers include poly(ε-caprolactone) (PCL), poly(glycolic acid), poly(L-lactic acid) and poly(lactide-co-glycolide) [162]. Among these polymers,

PCL has been identified as a promising candidate for various biomedical and environmental applications. In particular, PCL has been demonstrated for its enzymatic biodegradation towards controlled drug delivery and tissue engineering applications [163]. It is a soft semi crystalline polyester having melting point in the range of ~60 °C. It has advantages such as easy processibility at low temperatures (~80 °C) and safe elimination of water soluble byproducts post hydrolysis [164]. Therefore, in this study, lipase from *Lactobacillus plantarum* has been chosen to degrade PCL due to enzyme's probiotic nature and high efficacy towards ester hydrolysis.

Most of the enzymatic polymer degradation studies utilized the application of lipase over the surface of polyesters to result in a top-down fashion degradation [165]. In this approach, enzymes have to penetrate from the surface to the bulk of the polymer matrix in order to degrade it efficiently. This approach warrants frequent changing of enzyme containing buffer solution, yet providing only a low degradation rate [166]. On the other hand, a new embedded enzymatic polymer degradation was reported by Ganesh and Gross that utilized a fungal derived enzyme *Candida antarctica* Lipase B (CALB). They have demonstrated that embedding of enzyme into the polymer matrix helped in initiating the hydrolysis simultaneously in the surface as well as in bulk and thus resulting in rapid degradation [167]. In their further work, the polymer degradation using CALB embedded PCL films was optimized under shaking and flow conditions [168]. Despite the high potential of this approach, it is still in its infancy and no further studies were followed. In this current work, we have studied the embedded enzymatic degradation of PCL using lipase obtained from the probiotic source *Lactobacillus plantarum*. In addition, we have chosen static conditions without changing the enzyme containing buffer solution in order to get insights on the efficacy of the probiotic lipase on polymer degradation in the absence of any additional physical variables. The change in thermal

mass loss behavior, percentage crystallinity, and morphology have been studied as a function of enzymatic polymer degradation.

3.2 Material and Methods

3.2.1 Materials:

3.2.2 Sources: *L. plantarum* (MTCC 4461) was purchased from IMTECH, Chandigarh, India. PCL pellets (average molecular weight of 45,000 Da), chloroform and tween 20 were purchased from Sigma-Aldrich and used as received. Lipase was extracted from *L. plantarum* and purified using previously reported literature. [169] The change in the percentage crystallinity and thermal mass loss behavior of the samples were studied by differential thermal and thermogravimetric analyses using Shimadzu DTG-60. For this, the enzyme embedded PCL films were subjected to heating in nitrogen atmosphere from 35 to 600 °C at a heating rate of 10 °C/min under a steady nitrogen flow rate of 20 mL/min. X-ray diffraction (XRD) analyses over selected PCL films were performed using Rigaku Ultima IV with Cu K_α radiation (λ = 1.5418 A) at a scan rate of 0.3 °/min. The morphology and cross-sectional aspects of the enzyme degraded polymers at various intervals were studied using FEI Apreo field emission scanning electron microscopy (FE-SEM). Gel permeation chromatography (GPC) for molecular weight analyses were performed using Waters GPC instrument equipped with 2414 RI detector.

3.2.3 Preparation of Lipase:

Lipase gene from the bacterial cultures procured was isolated and amplified using thermal cycler. A recombinant expression vector was constructed using plasmid pMALc5X and the amplified Lipase gene, after transformation was heterologously expressed in *E.coli* strain BL21 (DE3) pLysS for lipase expression (Bionova). Since the vector contains Maltose binding protein (MBP), the fusion of a target protein (lipase) to MBP permits its one-step purification using amylose resin [142].

3.2.4 Preparation of PCL film:

The PCL films used for the embedded enzymatic degradation were prepared by solvent casting method [145]. Briefly, a solution was made by dissolving the PCL pellets in chloroform (1% w/v), with stirring at 37 °C for 30 minutes at 600 rpm. To this solution, lyophilized powder of enzyme 2, 4, 6 8 % (wt/wt) with respect to the PCL was added to and then poured onto culture dishes and dried overnight in order to get PCL thin films. The casted films thus obtained were cut into dimensions of 10 mm x 10 mm strips and weighed before subjecting to enzymatic action degradation. The weight and thickness of the cut films were found to be 3.5±0.5 mg and 0.1±.0.01 mm, respectively.

3.2.5 Lipase mediated PCL degradation:

The embedded enzymatic degradation was performed by adding 10 mL of 0.01 M Tris-HCl buffer of pH 8.1 and the degradation studies were carried out at a constant temperature of 37 °C. The concentrations of the lipase loaded was varied from 2, 4, 6 8 % (wt/wt) with respect to the polymer film. At regular intervals, the PCL film strips were removed from the vial, washed with distilled water and then dried in a desiccator at room temperature for 24 hr. The weight of the films was determined before and after enzymatic degradation**,** and the weight loss was expressed in relative terms using the following formula.

$$\text{Relative weight loss \%} = \frac{\text{Initial weight} - \text{Final weight}}{\text{Initial weight}} \times 100$$

3.2.6 Characterization:

Thermogravimetric and differential thermal analyses (TGA & DTA) of the samples were carried out on DTG-60, Shimadzu in order to understand the thermal degradation behaviour and percentage crystallinity. The specimens were heated in nitrogen atmosphere from 35 °C to 600 °C with a heating rate of 10 °C/min and a nitrogen flow rate of 20 mL/min. To follow the chemical changes in the PCL polymer, Fourier

transform infrared (FT-IR) spectra of the biodegraded and non-degraded samples in KBr pellets were recorded in the frequency range of 400 to 4000 cm^{-1} using Shimadzu 8400S instrument. X-ray diffraction (XRD) analysis of the PCL films was performed with Rigaku Ultima IV with Cu K_α radiation (λ = 1.5418 A) at a scan rate of 0.3 °/min. Field emission scanning electron microscopy (FE-SEM) images of the PCL films were obtained using the FEI Apreo instrument.

3.3 Results and Discussion:

In order to understand the polymer degradation through this embedded approach, the experiments were performed under static conditions, as shaking could assist leaching of partially degraded polymer chains into the aqueous medium. In addition, no further enzyme has been supplemented during the entire process so as to realize the degradation effect solely from the initially loaded enzyme. Thus, we have employed very mild conditions that could mimic a polymer substrate in a static environment.

First, to study the efficiency of the enzyme embedded approach towards polymer degradation, PCL films embedded with lipase of different percentages (2, 4, 6, and 8) were incubated in Tris-HCl buffer solution. TGA and DTA studies were performed on these samples in order to understand the thermal degradation behavior and crystallinity of the left-over PCL film after degradation. For this, the remained PCL films were removed at regular time intervals of 2, 4, 6, and 8 days from each incubated plate, rinsed and dried well. Control experiments were also performed with PCL films that were not subjected to enzymatic degradation, but embedded with the corresponding amounts of lipase. Figure 3.1 shows the TGA analyses of all the samples used in this study. It is expected that the onset mass loss of the PCL films degraded by the enzymes would be lesser than the control ones, as the enzyme degraded films would have been converted into lower molecular weight polymers. It can be seen that the 2% control film yielded

~10% of mass loss (considered as onset) at 383 °C and 93% of mass loss at 480 °C. After the enzymatic degradation with 2 to 8% of lipase loading, the onset decomposition temperature was found to be in the range of 195 to 300 °C and the complete decomposition was observed by 395 to 460 °C with a residual mass of <2%. It is also evident from the graph that the thermal stability of the degraded film was less at any point of temperature, when compared to the control. Such a decrease in thermal stability is in line with the expected trend. With 4% lipase embedded films, the onset of the thermal mass loss in 2 to 6 days of enzyme degraded films was in the range of 300 to 330 °C, while the 8 days degraded film started to decompose from 257 °C onwards. With these samples also ~98% of the thermal decomposition was found to occur by 460 °C. Further increase in the enzyme loading as in 6 and 8% resulted in further decrease of the onset thermal mass loss of PCL much below 300 °C (~195-250 °C), while 98% of thermal decomposition was observed in ~400 °C. The substantial decrement in the thermal stability of the lipase embedded PCL films clearly indicate the efficient enzymatic polymer degradation at 6-8% of enzyme loading.

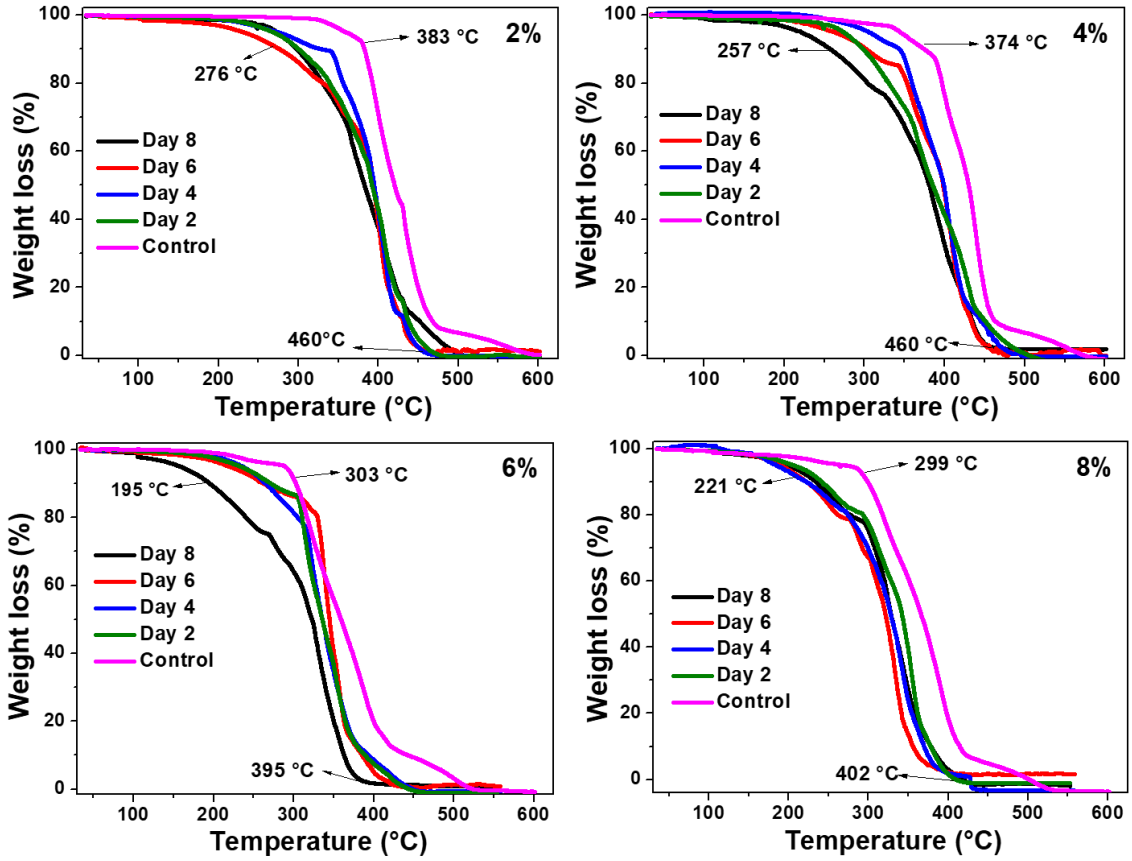

Figure 3.1. TGA mass loss analyses of 2, 4, 6, and 8% lipase embedded PCL films before (control) and after enzymatic polymer degradation.

The semicrystalline nature of PCL allows one to probe the change in crystallinity as a function of polymer degradation. DTA analyses on all the PCL samples used in this study were performed before and after enzymatic degradation (Figure 3.2). The 2 to 8% of lipase embedded PCL films possessed melting points in the range of 50 to 65 °C. In all the samples, the melting point was found to be increased to the tune of 5 to 10 °C after the enzymatic degradation due to the increase in crystallinity. Table 3 summarizes the variation in percentage crystallinity of the enzyme degraded PCL films as a function of time and compared against the corresponding controls. It can be noted that the pristine PCL film without any embedded enzyme was reported to possess a percentage crystallinity of ~55 % [169]. The enthalpy of fusion for the 100% crystalline PCL is known to be 139.5 J/g, using which the percentage crystallinity of our samples were

calculated from the enthalpy of fusion values obtained from DTA analyses [148]. The percentage crystallinity of 2 to 8% lipase embedded PCL films was found to be in the range of 30 to 39%. Thus, the embedding of enzymes in the PCL matrix caused a significant degree of amorphization that could be due to the incorporation of enzymes into the polymer matrix and thereby disrupting the crystalline regions. The amorphization was more pronounced with the 2% lipase embedded PCL film. After 2 days of enzymatic degradation, the percentage crystallinity of the residual PCL films was found to be significantly increased to the range of 55 to 75%. This substantial increase in the percentage crystallinity indicates the efficient enzymatic degradation of amorphous regions in the PCL matrix even by 2 days. It is known that the enzymatic degradation of semicrystalline polymers mainly occur at amorphous regions [149,150]. With further incubation of the PCL films for a longer duration up to 8 days resulted in gradual increase in the percentage crystallinity. By 8 days of degradation, the percentage crystallinity with varying enzyme loaded PCL films was found to increase to the range of 70 to 95%. These observations clearly indicate that the amorphous regions of the PCL films have been degraded more effectively than the crystalline regions and the 8% lipase embedded PCL film subjected to 8 days of enzymatic degradation was found to be the most efficient.

Table 3. Variation in percentage crystallinity obtained from DTA measurements with varying enzyme loading against number of incubation days.

Enzyme loading	2%	4%	6%	8%
Day	**Percentage Crystallinity**			
Control	33	37	38	39
2	70	73	79	80
4	75	78	81	83
6	82	86	88	89
8	93	95	97	98

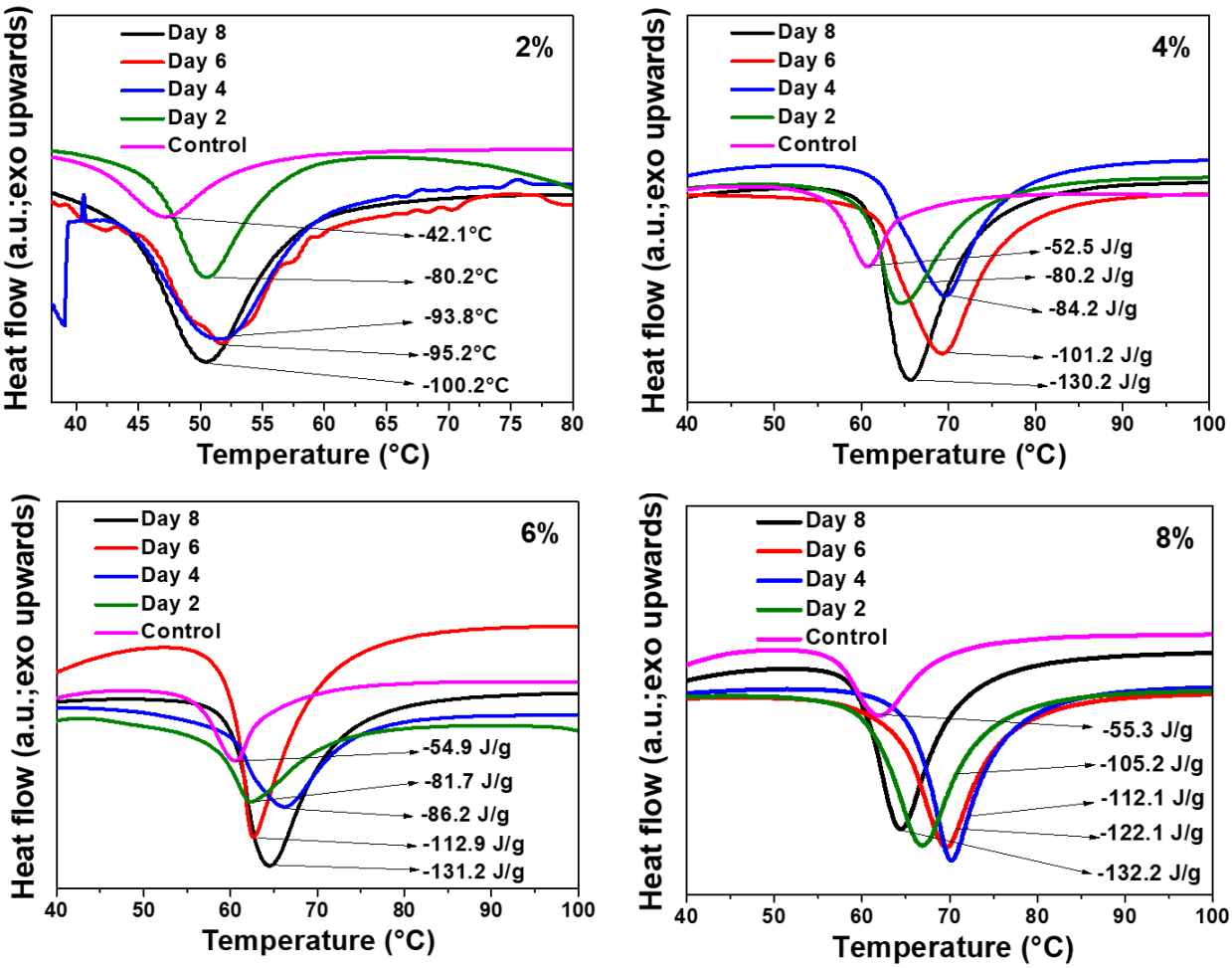

Figure 3.2. DTA percentage crystallinity analyses of 2, 4, 6, and 8% lipase embedded PCL films before (control) and after enzymatic polymer degradation.

In order to further ascertain the enzymatic degradation of the amorphous PCL regions, we have performed XRD analyses of the 8% lipase embedded polymer film before and after subjecting to 8 days of degradation (Figure 3.3). As seen from the figure, the pristine PCL film exhibited peaks corresponding to (110), and (200) planes at 21.6 and 23.8° 2θ values, respectively. [171] In addition, a small shoulder at 22.2° 2θ corresponding to (111) plane was observed, proving the characteristic semicrystalline nature of PCL. The crystallite size of the (110), and (200) peaks calculated using Scherrer's formula was 23.2, and 11.7 nm, respectively. The 8% enzyme loaded PCL control film, on the other hand, exhibited a gentle decrease in the crystallinity with a crystallite size of 16.8, and 10.8 nm for the (110), and (200) peaks, respectively. The

decrease in the percentage crystallinity with enzyme loading was corroborating the amorphization of the PCL matrix with the embedding of lipase, as indicated by DTA analyses. However, after 8 days of degradation, the percentage crystallinity was found to be substantially increased. The crystallite sizes corresponding to the respective (110), and (200) peaks in this case were found to be 26.5, and 22.8 nm. These results additionally corroborate the mechanism that the amorphous regions of the polymer films were degraded by the lipase and thereby increasing the percentage crystallinity of the remaining PCL films.

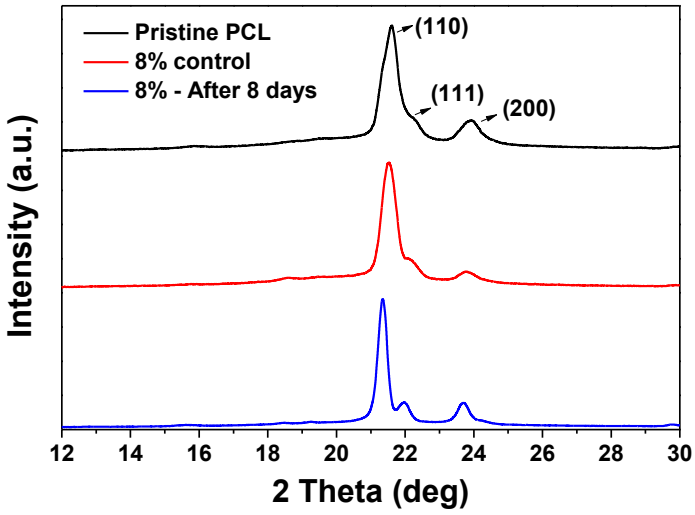

Figure 3.3. XRD patterns of pristine PCL film, 8% lipase embedded PCL film (control), and 8% lipase embedded PCL film after 8 days of incubation.

Enzyme release kinetics of the lipase embedded PCL films were studied in order to quantify the amount of enzyme leached from the polymer matrix to the buffer solution (Figure 3.4a). Simultaneously, percentage mass loss of the lipase embedded PCL films was studied to follow the polymer degradation (Figure 3.4b). For this, PCL films embedded with 2 to 8% of the *L. plantarum* lipase were incubated for different time periods of 2 to 8 days in the Tris-HCl buffer. The supernatant solution was collected and analyzed for the amount of enzyme leached. It was observed that 50-65 % of the

embedded lipase leached out of the PCL matrix in 2 days. With further incubation as in 4 days, additional 2-5% of lipase leaching to the buffer solution was observed. Similar magnitude of enzyme release from the PCL matrix was observed on days 6 and 8 as well. Thus, a significant portion of the embedded enzyme was released to the buffer solution over a course of time. It is presumed that the enzyme leaching from the PCL matrix was assisted by the rapid polymer degradation within 2 days. The percentage mass loss studies of enzyme embedded PCL films revealed a clear trend of increasing polymer degradation with the progress of time as well as with higher loading of lipase. The lowest mass loss of 11% was observed with 2% of lipase embedded PCL film in 2 days. During the same period of time the observed mass losses with 4, 6, and 8% of lipase embedded PCL films were 27, 32, and 35%, respectively. This shows that a significant portion of the polymer matrix got degraded within 2 days, which could also have assisted in leaching of the embedded lipase. Among all the enzyme loadings, 2 to 6% yielded a steady increase in the percentage degradation. Between 6 and 8% loadings, the latter showed only a marginal increment in the percentage mass loss. The percentage mass loss after 8 days was observed to be 71 and 73% with 6 and 8% of lipase loadings, respectively. Correlating with the DTA studies, it is obvious that the enzymes efficiently hydrolyzed the amorphous regions of the PCL film. These results show the high efficacy of the *L. plantarum* lipase in degrading the PCL films, when embedded in the matrix.

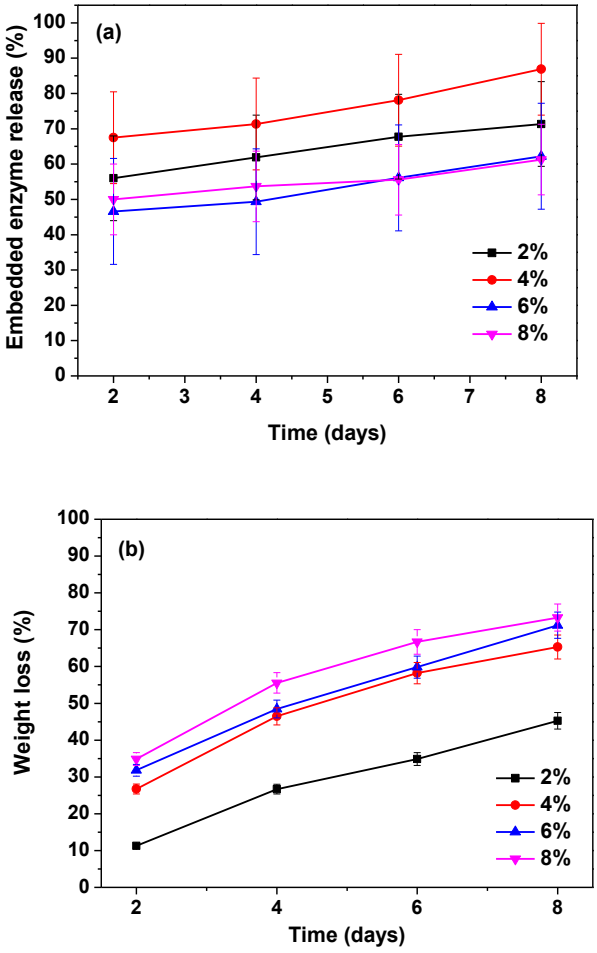

Figure 3.4. (a) Lipase release kinetics, and (b) polymer mass loss analyses of 2, 4, 6, and 8% lipase embedded PCL films after 2, 4, 6, and 8 days of incubation.

FE-SEM images on the lipase embedded PCL films were obtained with different quantities (2 to 8 wt.%) of lipase loaded samples against the degradation time to follow the surface and cross-sectional morphological changes. Figure 3.5 presents the FE-SEM images of lipase embedded control samples before subjecting to enzymatic degradation. It can be seen from the images that the non-degraded samples possessed a relatively smooth surface morphology as well as cross-section. The cross-sectional views also revealed the average thickness of the films in the range of ~100-120 µm. After 2 days of polymer degradation, the FE-SEM imaging on 2 and 4 wt% lipase loaded PCL films revealed a little amount of degradation on the surface and cross-sectional morphology (Figure 3.6). However, the 6 and 8 wt% lipase loaded PCL films possessed relatively a

greater amount of polymer degradation that was evidenced by the cracks on the surface and cross-sectional views. After 4 days, the polymer degradation was more evident with all the lipase loadings (Figure 3.7). In this case, the surface of the polymer films was found to have macropores that were in the range of ~2-3 μm. The cross-sectional imaging revealed a greater degree of polymer degradation in 4 days. Macropores, whose dimensions are in several 10s of μm were also observed. A similar surface and cross-sectional morphologies were observed in polymer samples that were subjected to 6 days of degradation as well (Figure 3.8). In our earlier work, we employed pouring strategy of enzymes on the polymer surface that did not result in formation of any pores in the bulk of the PCL film [169]. It is obvious that such a strategy results in slower polymer degradation, as the enzymes have to penetrate from top to bottom in a two-dimensional fashion. Such a top to bottom fashion of degradation was employed for enzymatic lithography to fabricate micron to sub-micron scale patterns in PCL. Using micro-contact printing and polymer pen lithography techniques, enzymes have been applied over selective regions on the PCL film surface, which resulted in enzymatic hydrolysis to create patterns in a top-down fashion [165,166]. On the other hand, in the embedded approach, the enzymes present in the bulk of the polymer film start to degrade the matrix in a three-dimensional fashion, resulting in micron-scale pores. This was evidenced by the enzyme leaching studies, which indicate that the lipase can freely approach the surface and the bulk of the polymer, thereby, leading to faster degradation. The PCL samples subjected to 8 days of degradation were found to be highly brittle and therefore could not be obtained as free-standing films for the FE-SEM observation. Hence, the obtained crumbled pieces were used for morphological analyses (Figure 3.9). In this case also, the surface of the remaining crystalline powders possessed micron-scale pores. In all the cases, the 6 and 8 wt% lipase loaded samples exhibited relatively higher degree of

degradation than the lower enzyme loadings. All these results corroborated the TGA and DTA analyses. The degradation of the PCL films into crumbled pieces by 8 days of incubation clearly indicated the high efficacy of the lipase embedded degradation approach.

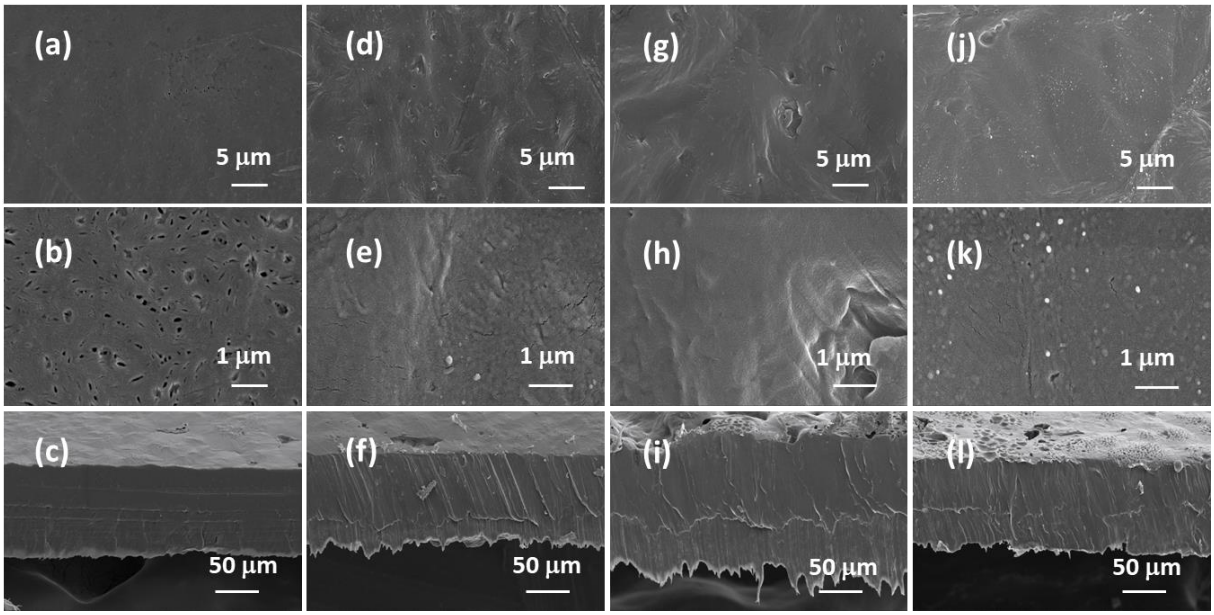

Figure 3.5. FE-SEM images of the (a-c) 2%, (d-f) 4%, (g-i) 6%, and (j-l) 8% of lipase embedded PCL films before subjecting to enzymatic degradation. Top row ((a), (d), (g), and (j)), middle row ((b), (e), (h), and (k)), and bottom row ((c), (f), (i), and (l)) images correspond to the respective low, high magnifications of the surface, and cross-section of the PCL film sections.

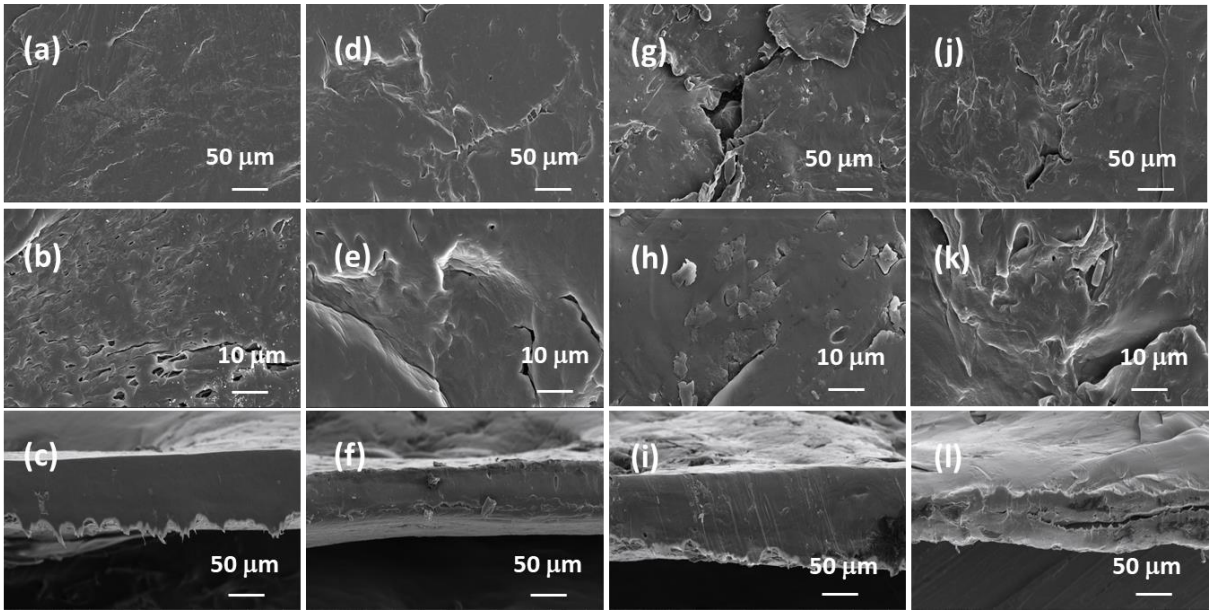

Figure 3.6. FE-SEM images of the (a-c) 2%, (d-f) 4%, (g-i) 6%, and (j-l) 8% of lipase embedded PCL films after subjecting to 2 days of enzymatic degradation. Top row ((a), (d), (g), and (j)), middle row ((b), (e), (h), and (k)), and bottom row ((c), (f), (i), and (l)) images correspond to the respective low, high magnifications of the surface, and cross-section of the PCL film sections.

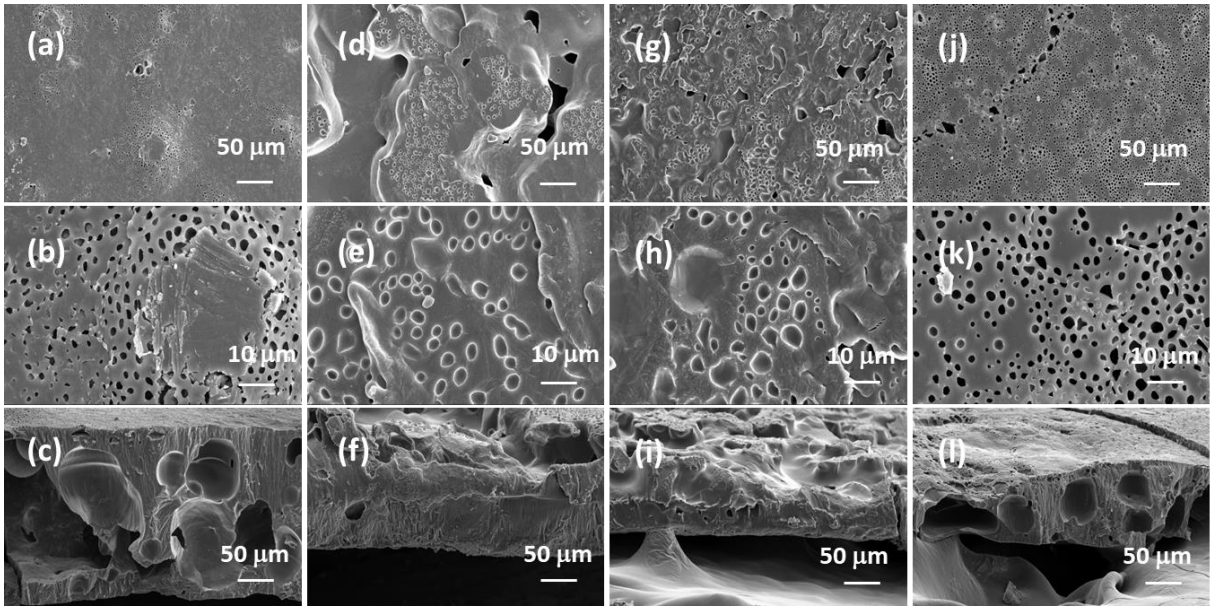

Figure 3.7. FE-SEM images of the (a-c) 2%, (d-f) 4%, (g-i) 6%, and (j-l) 8% of lipase embedded PCL films after subjecting to 4 days of enzymatic degradation. Top row

((a), (d), (g), and (j)), middle row ((b), (e), (h), and (k)), and bottom row ((c), (f), (i), and (l)) images correspond to the respective low, high magnifications of the surface, and cross-section of the PCL film sections.

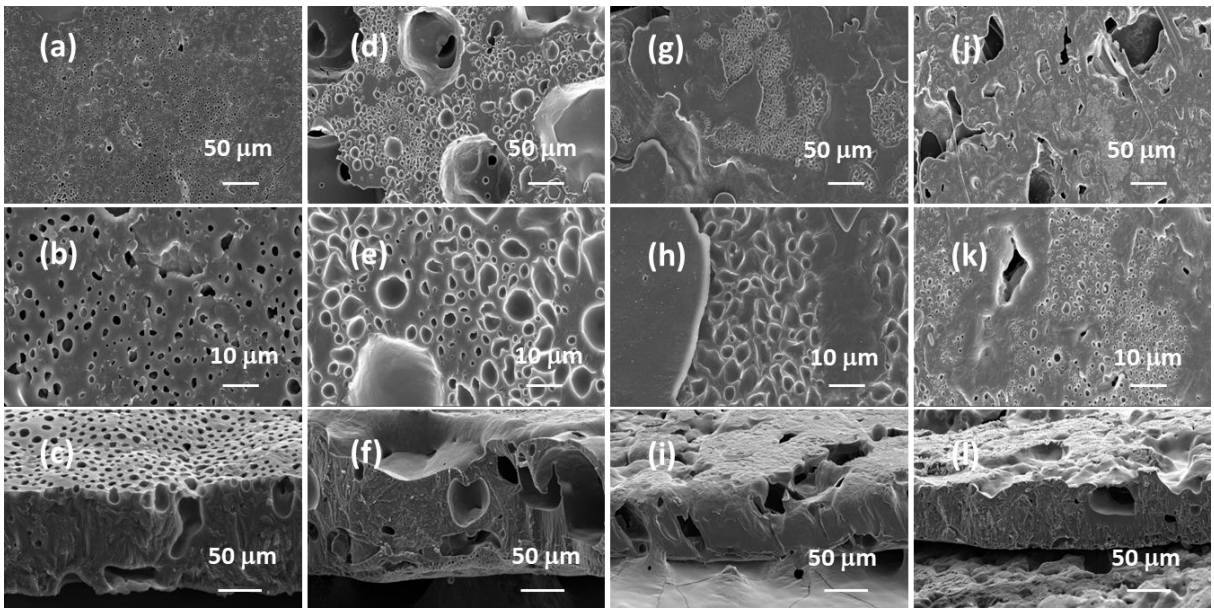

Figure 3.8. FE-SEM images of the (a-c) 2%, (d-f) 4%, (g-i) 6%, and (j-l) 8% of lipase embedded PCL films after subjecting to 6 days of enzymatic degradation. Top row ((a), (d), (g), and (j)), middle row ((b), (e), (h), and (k)), and bottom row ((c), (f), (i), and (l)) images correspond to the respective low, high magnifications of the surface, and cross-section of the PCL film sections.

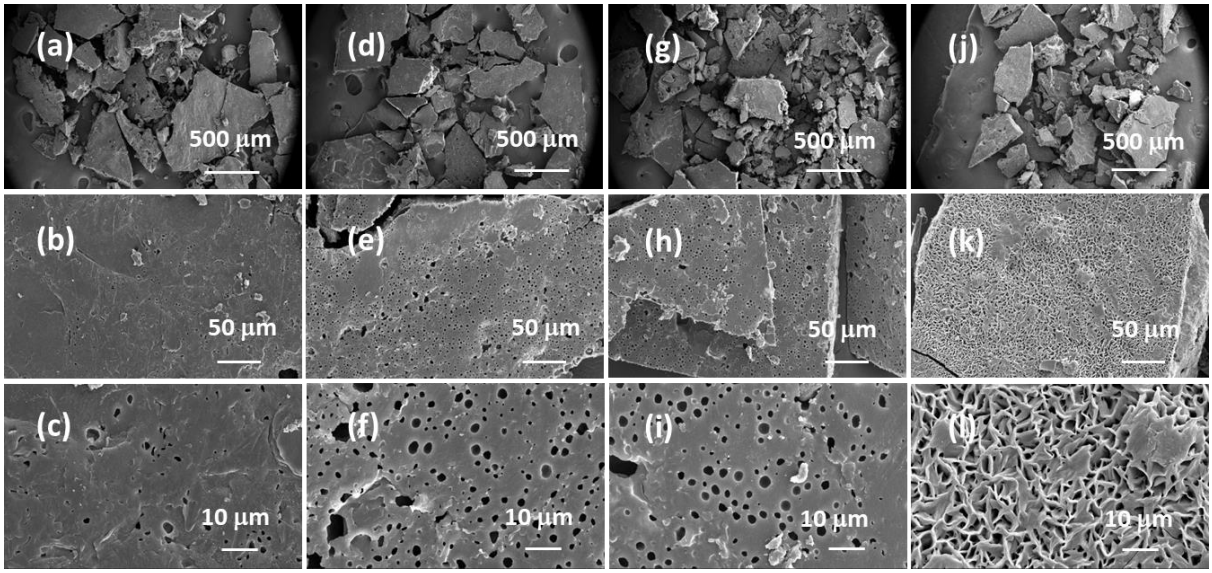

Figure 3.9. FE-SEM images of the (a-c) 2%, (d-f) 4%, (g-i) 6%, and (j-l) 8% of lipase embedded PCL films after subjecting to 8 days of enzymatic degradation. Top row ((a), (d), (g), and (j)), middle row ((b), (e), (h), and (k)), and bottom row ((c), (f), (i), and (l)) images correspond to the respective ultra-low, low, and high magnifications of the PCL film surfaces.

Gel permeation chromatography (GPC) analyses were carried out with 8% lipase embedded PCL samples to understand the change in molecular weight as a function of polymer degradation. Table 4 lists the number average molecular weight (M_n), weight average molecular weight (M_w) and polydispersity index (PDI) of the lipase embedded PCL films before and after subjecting to varying times of incubation. It can be seen from the table that the control sample exhibited M_n and M_w values of 36500 and 53030, respectively. With the left-over PCL films after enzymatic degradation, the M_n and M_w values were found to be significantly lower than the control, indicating efficient degradation of the polymer films.

Table 4. GPC analyses of 8% lipase embedded PCL films before (control) and after 2 to 8 days of enzymatic degradation.

Sample	Number average molecular weight (M_n)	Weight average molecular weight (M_w)	Polydispersity Index (PDI)
Control	36500	53030	1.5
2 days	21200	35060	1.7
4 days	25210	36890	1.5
6 days	10250	28030	2.7
8 days	17260	27600	1.6

CONCLUSIONS

PCL films embedded with 2 to 8 wt% of lipase derived from a probiotic source *Lactobacillus plantarum* were studied for their enzymatic degradation. TGA analyses showed a substantial decrease (~100 °C) in the onset thermal decomposition temperature, when compared between the lipase embedded PCL film before and after subjecting to 8 days of incubation. With increase in lipase content from 2 to 8%, the thermal decomposition temperature for complete mass loss was found to decrease from 460 to 395 °C. It was found from the DTA analyses that the lipase embedded control PCL films exhibited percentage crystallinity in the range of 30 to 39%. Among the different loading of lipase, 8% exhibited the highest enzymatic activity on the amorphous regions of the PCL films that resulted in increasing the crystallinity from 39% to 75% by 2 days and to 95% by 8 days. XRD analyses on 8% lipase embedded PCL film confirmed that the crystallite sizes of the respective (110), and (200) peaks calculated using Scherrer's formula were increased by ~1.5 to 2.1 times after enzymatic polymer degradation. The

enzyme release kinetics revealed leaching of ~50-65% of the embedded lipase into the buffer solution by 2 days. Such a leaching was found to be beneficial in generating micron-scale pores in the bulk of the polymer film, which provided greater accessibility to the enzymes to freely approach the surface as well as the bulk of the PCL film. The gravimetric analyses revealed that the lowest mass loss of 11% was exhibited by 2% lipase embedded polymer film after 2 days and the highest mass loss of 73% was observed with 8% of lipase loading after 8 days of incubation. FE-SEM studies revealed three-dimensional fashion of polymer degradation through the surface and cross-sectional morphological imaging. The micron-scale pores were clearly visible in case of 4 and 6 days of incubated samples, while the PCL films incubated for 8 days were found to be crumbled that indicated efficient polymer degradation through this enzyme embedded approach. GPC analyses further corroborated the efficient enzymatic polymer degradation through the substantial decrease in the number average molecular weight of the 8% lipase embedded control PCL film from 36500 to 17260 post degradation. It is noteworthy that the present work reports the enzymatic polymer degradation under static conditions, wherein no further lipase was added apart from the initial loading. Thus, the polymer degradation rates reported in this work can substantially be improved by employing shaking conditions and replenishing with additional enzymes periodically. Furthermore, the enzyme embedded polymer degradation approach shows potential to be extended for polymers containing ester functionality using lipases from various microbial sources.

CHAPTER 4

TOWARDS SINGLE CRYSTALLINE, HIGHLY MONODISPERSE AND CATALYTICALLY ACTIVE GOLD NANOPARTICLES CAPPED WITH PROBIOTIC *LACTOBACILLUS SPS.* DERIVED LIPASE

4.1 Introduction:

The integration or attachment of biological macromolecules with non-biological nanomaterials in functional devices helps in understanding the interface between the two on a molecular scale [172]. This attachment is of great practical relevance to biosensors, tissue engineering, drug and gene delivery. Among the several metal nanomaterials, silver and gold nanoparticles are one of the most commercialized candidates because of their unique optical, electrical, and photo-thermal properties. Metallic nanoparticles can be induced to aggregate into a solid at relatively lower temperatures, leading to improved and easy-to-create coatings for electronics applications [172,173]. Typically, nanoparticles possess a wavelength below the critical wavelength of light which renders them transparent and makes them very useful in cosmetics, coatings, and packaging. They can also be attached to single strands of DNA, which opens up avenues for theranostics applications [173]. Therefore, development of methods for the synthesis of stable metal nanoparticles has been an important area of research. Broadly, these nanoparticles can be synthesized by physical, chemical and biological means [174]. Generally, the chemical methods include contamination from precursor chemicals, use of toxic solvents and generation of hazardous by-products [175]. Hence, there is an increasing demand to develop high-yield, cheaper, nontoxic, and eco-friendly protocols for the synthesis of stable metallic nanoparticles. Therefore, a vast array of biological resources available in nature including plants and plant extracts, algae, fungi, yeast, bacteria, and viruses could all be employed for the synthesis of nanoparticles. The proteins/enzymes, amino acids, carbohydrates, phytochemicals present in the biomaterial are believed to be responsible for the reduction of metal ions into the nano form [176]. This has led scientists all over the world to further explore the biological green-synthesis routes, which can produce water-soluble, protein-capped, bio-compatible nanoparticles

with control over particle size by preventing agglomeration and at the same time posing no hazard to the ecosphere [177].

Protein-capped gold nanoparticles (GNPs) are particularly desirable due to their applications in sensors, catalysis, cardiac tissue engineering and drug delivery [178-183] This could be attributed to the enhanced biocompatibility, water solubility and amphoteric properties of proteins that offer flexibility in bringing the desired functionality [184-190]. In addition, their zwitter ionic property facilitates recovery of the protein-capped nanoparticles through anchoring over various supports, which is important from the perspective of sustainability and toxicity [191]. It is known that the size of the nanoparticles is greatly dependent on the nature of the capping agent. The conventional citrate-stabilized GNPs through Turkevich method range from 9-120 nm in size [192]. A few literature reports indicate that proteins can act as efficient capping agents in the synthesis and stabilization of highly monodisperse sub-10 nm GNPs [193, 194].

In this study, we chose the lipase isolated from non-pathogenic *Lactobacillus plantarum* bacteria for conjugating and stabilizing GNPs. Unlike commonly used stabilizers, lipases remain highly resistant over a wide range of pH alterations and to various chemical treatments [184, 195]. Furthermore, as opposed to fungal derived lipases, the probiotic lipases are considered to be eco-friendlier as they are part of the human mucosal microflora. Here, we show the synthesis of highly monodisperse lipase-capped GNPs of average size <5 nm and their catalytic reduction of 4-nitrophenol (4-NP) to 4-aminophenol (4-AP). In addition, we demonstrate the facile recovery of the GNPs through anchoring over magnetite nanoparticles, which show the efficient reusability of the GNPs without releasing into the environment.

4.2 Experimental

Lipase from *Lactobacillus plantarum* (MTCC 4461) was isolated as per our previous reports [170, 196, 197]. Hydrogen tetrachloroaurate (III) hydrate ($HAuCl_4$), 4-Nitrophenol (4-NP), Sodiumborohydride ($NaBH_4$), glutaraldehyde, 3-aminopropyltriethoxysilane (APTES) were purchased from Sigma Aldrich.

In a typical GNPs synthesis, 1 mL of 1 mM $HAuCl_4$ solution was added to a 500 µL protein solution of different concentrations (0.5, 1, 2, 6, and 10 mg/mL) in Tris-HCl buffer. To this mixture, 300 µL of 25 mM $NaBH_4$ solution was added, which resulted in rapid reduction of $AuCl_4^-$ to yield lipase-capped GNPs. The synthesized lipase-capped GNPs were characterized using UV-visible spectrophotometer (Shimadzu UV-3600 plus), Fourier Transform infrared (FT-IR) spectroscopy (Shimadzu 8400S) and dynamic light scattering (DLS) (Zetasizer Nano-ZS, Malvern) techniques. The morphological characteristics were analysed using high-resolution transmission electron microscopy (HR-TEM, FEI, Tecnai G2, F30).

The synthesis of magnetite nanoparticles through co-precipitation method and their subsequent amine-functionalization were performed by the following the literature procedure [198]. Briefly, 25 mg of pristine magnetite (Fe_3O_4) was added to a 95/5 vol% of ethanol/water mixture containing 5% of APTES and the resulting solution was incubated with gentle shaking at room temperature for 2 h. After this time, the Fe_3O_4 nanoparticles were magnetically recovered and sequentially washed three times with ethanol and finally one time with deionized water. Thus obtained amine-functionalized Fe_3O_4 nanoparticles were treated with 5 mL of 2.5% glutaraldehyde in PBS buffer for 2.5 h at room temperature, followed by washing with PBS buffer. To this, 1.5 mL of lipase-capped GNPs solution was poured and the mixture was incubated for 6 h in order to anchor the GNPs onto Fe_3O_4 via aldehyde-amine coupling [199, 200].

To carry out the reduction of 4-NP, 250 µL solution of lipase-capped GNPs was added to an aqueous mixture containing 1 mL of 40 ppm 4-NP and 1 mL of 0.5 M $NaBH_4$[201]. The progress of the reduction was monitored by UV-vis spectroscopy at different time intervals. For recyclability studies, the GNPs-anchored Fe_3O_4 nanoparticles were recovered magnetically and re-suspended in Phosphate buffer saline (PBS). The recycled GNPs-anchored Fe_3O_4 nanoparticles were studied for their catalytic activity till five cycles.

4.3 Results and Discussion

The schematic representation of synthesis of lipase capped GNPs, and their applicability towards catalytic and magnetic recoverability is shown in Figure 4.1.

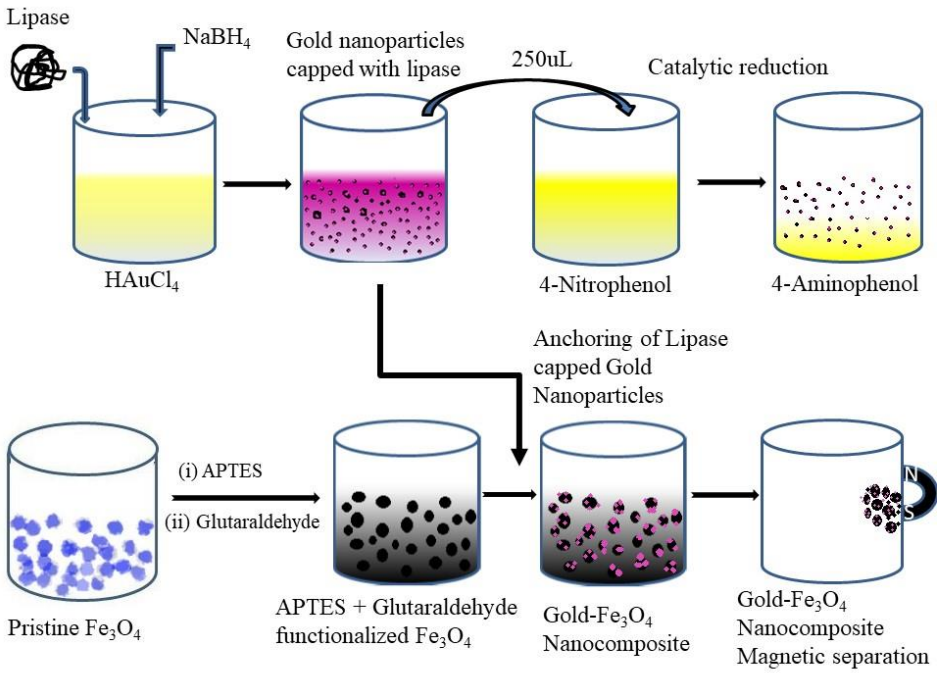

Figure 4.1. Pictorial representation of the synthesis of GNPs and their anchoring over amine-functionalized Fe_3O_4 nanoparticles for magnetic recoverability

The work mainly aims at the effect of variation in lipase quantity in the controlled synthesis and catalytic properties of GNPs. Therefore, in study this, we have chosen the working protein solution with varying concentrations of 0.5 to 10 mg/mL, while keeping the concentration of the gold precursor and the reducing agent constant. The UV-visible spectra of the synthesized GNPs capped with various amounts of lipase are shown in Figure 4.2.

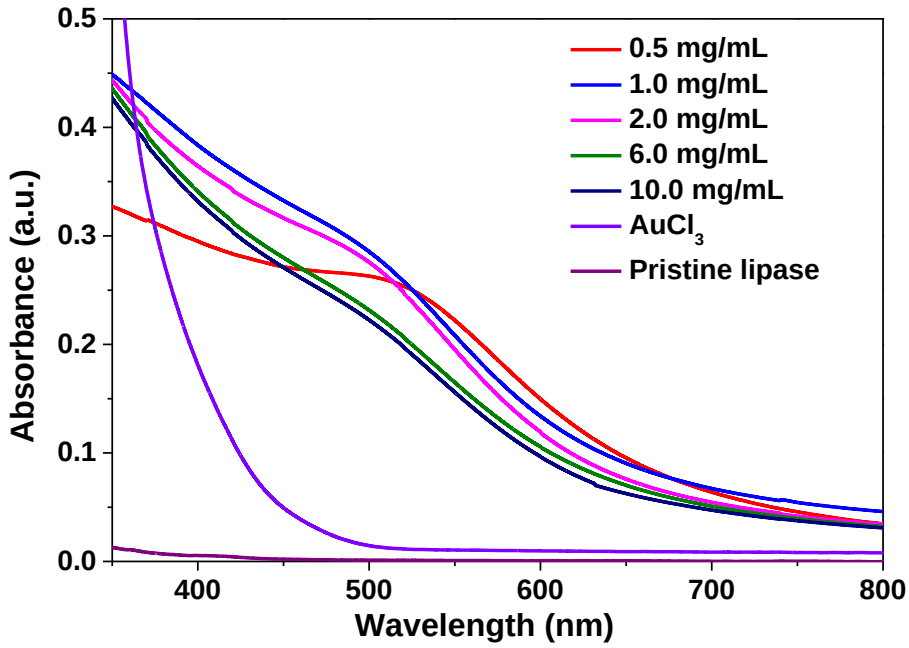

Figure 4.2. UV-Vis absorption spectra of GNPs capped with varying amount of lipase.

As seen from the figure, the GNPs stabilized with 0.5 mg/mL of lipase showed a characteristic plasmonic absorption peak at 518 nm. With the increase in concentration of the lipase, a gentle shift in the plasmonic peak from 518 to 531 nm associated with a broadening of the plasmonic peak was observed. It is known that the surface plasmons are sensitive to the environment and thus the characteristic peak has weakened and broadened with increasing quantity of lipase as capping agent. This behaviour is consistent with the literature and clearly indicates the efficient capping of GNPs with

lipase [190, 202]. The capping of lipase onto GNPs was further monitored by FT-IR analysis of pristine (uncapped) GNPs, pristine lipase and the GNPs stabilized with 10 mg/mL of lipase (Figure 4.3).

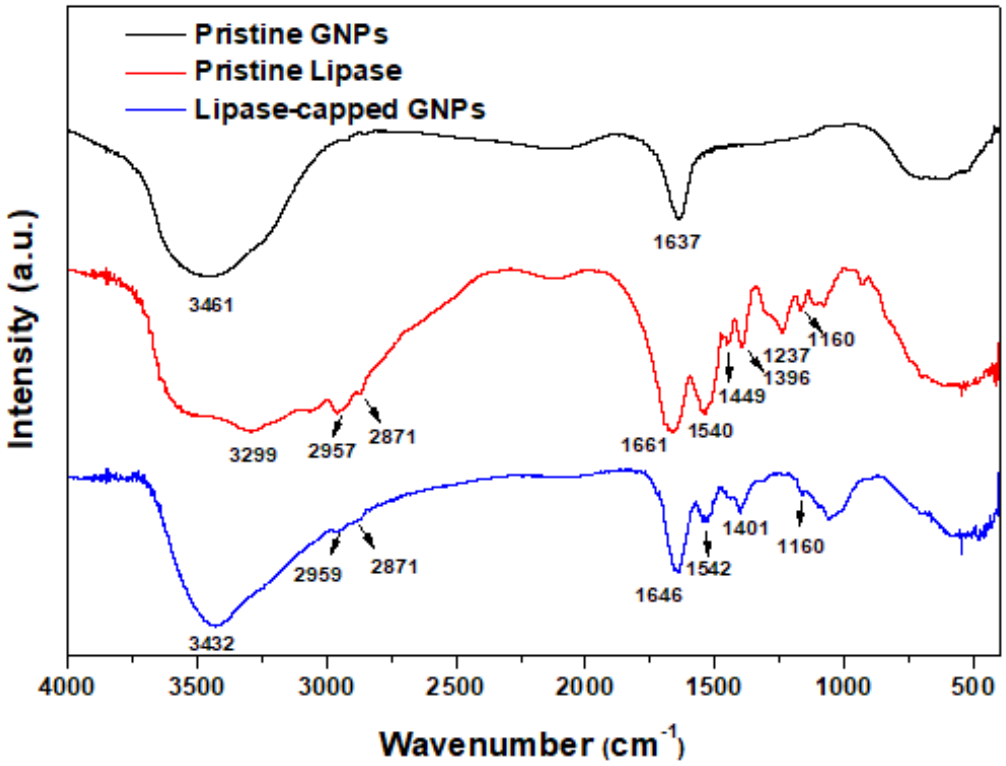

Figure 4.3: FT-IR spectra of pristine (uncapped) GNPs, pristine lipase and lipase-capped GNPs.

The pristine GNPs synthesized through the $NaBH_4$ reduction method in the absence of the lipase capping agent showed a broad stretching peak at 3461 cm^{-1} in the hydroxyl region and a peak at 1637 cm^{-1}, which could be due to the by-products of $NaBH_4$such as metaborate adsorbed onto the GNPs. On the other hand, the pristine lipase exhibited the characteristic amide carbonyl stretching peak at 1661 cm^{-1} along with a broad band in the range of 3100-3600 cm^{-1} corresponding to the hydroxyl and amine functional groups of protein. In addition, the aliphatic C-H stretching frequencies at 2957 and 2871 cm^{-1} along with several stretching peaks in the finger print region were

observed. In case of 10 mg/mL lipase-capped GNPs, the FT-IR spectrum was found to have good resemblance to that of pristine lipase, which confirmed the successful conjugation of lipase over the nanoparticles. A little variation in the IR stretching frequencies in the finger print region of lipase-capped GNPs could be due to the possible denaturation and re-orientation of the protein over the surface of GNPs.

DLS measurements were executed to study the hydrodynamic diameter of the GNPs as a function of lipase capping quantity and the results are plotted in Figure 4.4. The results revealed that the average particle size of the GNPs in all cases were in the range of 5 to 10 nm. However, with 0.5 and 1 mg/mL of lipase capping, the polydispersity of the synthesized GNPs was found to be higher than the 2-10 mg/mL of lipase capped GNPs.

These results clearly indicate that the GNPs are efficiently capped with lipase, which is more pronounced with higher loading of lipase.

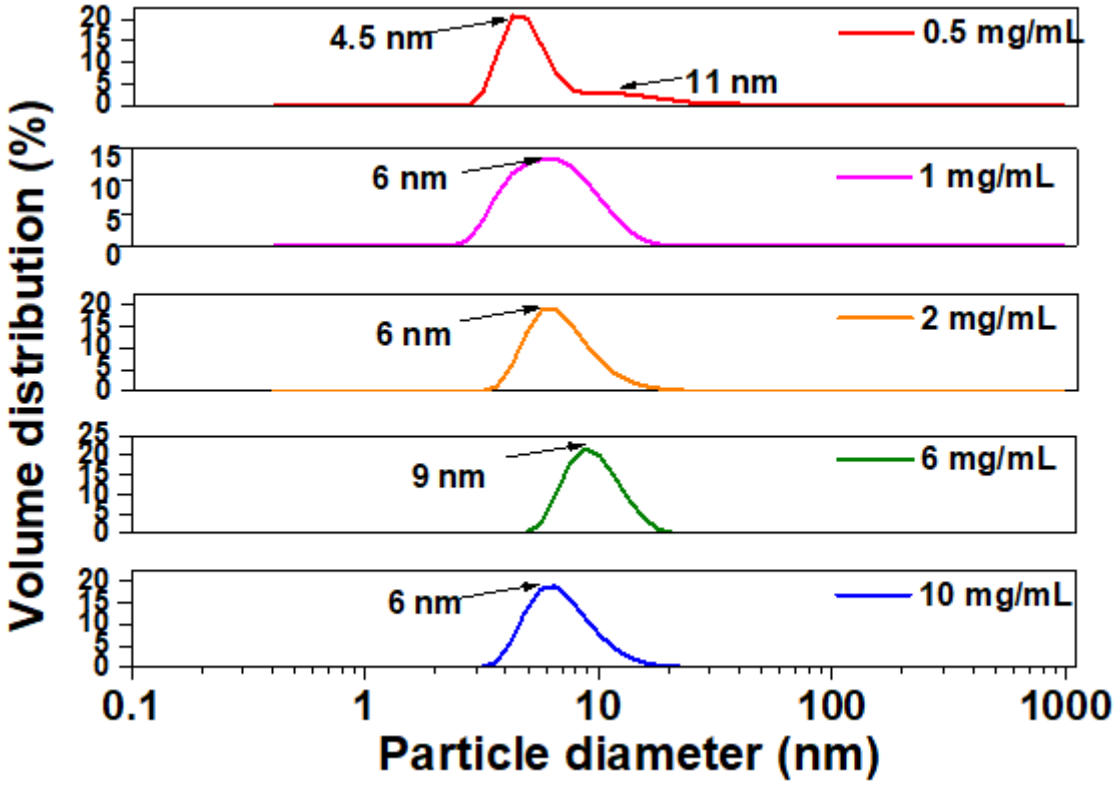

Figure 4.4: Size measurement of pristine lipase and GNPs with varying amount of lipase-capping.

The zeta potential (Figure 4.5) of the lipase capped GNPs was found to be in the range of ~ -12 to -14 mV at neutral pH. The pristine protein's zeta potential also lies in the same range due to the overall net negative charge. This close match in the zeta potential values confirm the capping of GNPs with lipase.

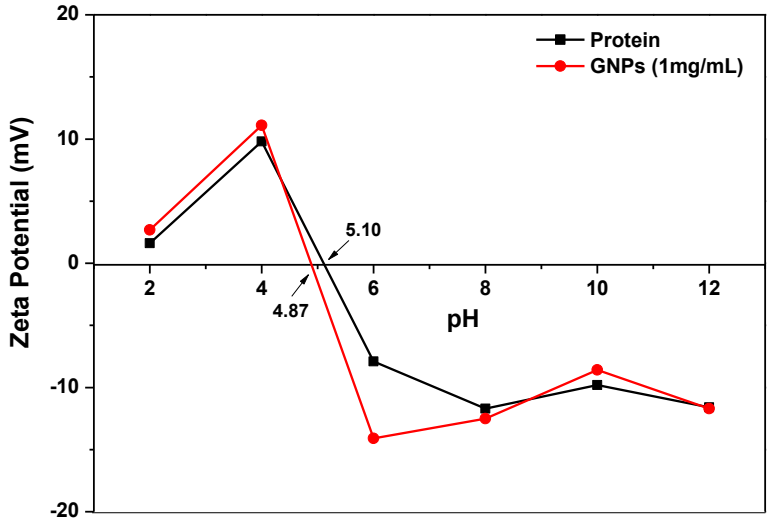

Figure 4.5: Zeta potential measurement over pristine lipase and lipase-capped GNPs as a function of pH.

The values also reveal that in addition to the steric repulsion, the GNPs capped with lipase might impart electrostatic repulsion as well, contributing to better solubility and high stability. The zeta potential of pristine Fe_3O_4, APTES-functionalized Fe_3O_4 and Fe_3O_4-GNP nanocomposite was measured as a function of pH and the results are presented in Figure 4.6. As seen in the figure, the pristine Fe_3O_4 exhibited zeta potential values of ~50 mV and ~ -30 mV at acidic and alkaline conditions, respectively. After surface functionalization, the zeta potential at acidic condition was found to be even higher (>60 mV) at pH 2, indicating the successful anchoring of amine groups that can be easily protonated at acidic pH and thus contributing to the higher value. After capturing lipase-capped GNPs, the zeta potential of Fe_3O_4-GNP nanocomposite at acidic pH was found to further decrease to ~ 25 mV. These changes additionally indicate the successful anchoring of lipase-capped GNPs over Fe_3O_4.

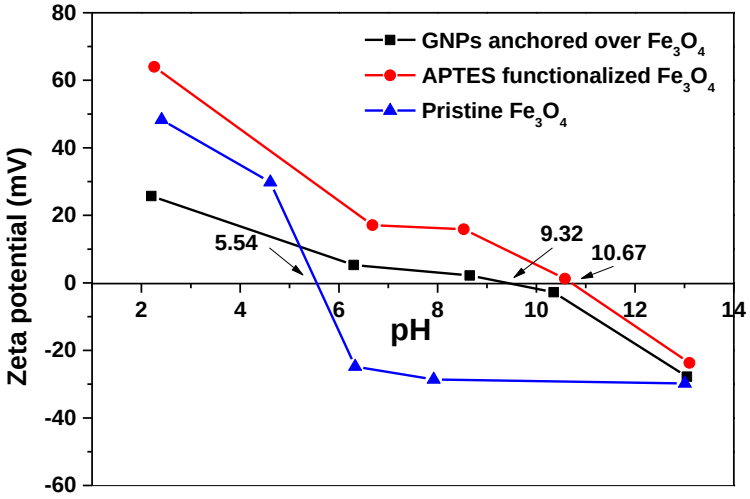

Figure 4.6: Zeta potential measurements over pristine Fe_3O_4, APTES-functionalized Fe_3O_4 and GNPs anchored over Fe_3O_4 as a function of pH.

HR-TEM studies were performed in order to understand the particle size and morphology of the lipase capped GNPs (Figure 4.7(a-e)). The synthesized GNPs with varying amounts of lipase were observed to be nearly spherical, whose size varied in the range of 2 to 8 nm with an average size of <5 nm. Interestingly, the selected area electron diffraction (SAED) studies shown in Figure 4.8 revealed that the GNPs that are capped with 0.5 mg/mL of lipase were highly polycrystalline in nature, as indicated by the diffuse rings. When the lipase amount was increased to 1 mg/mL, the SAED patterns were found to be modestly less polycrystalline. With further increase of lipase content as in 2-10 mg/mL, the SAED patterns showed distinct spots rather than a continuous ring, which indicate that the GNPs capped with higher loading of proteins were much less polycrystalline in nature and thus close to well-ordered single crystalline nanoparticles. This could be attributed to the efficient capping of lipase at higher loadings that restricted the growth of single crystalline GNPs into polycrystalline ones [198, 199, 200].

One of the major challenges in the lyophilic nanoparticles system is the recovery, as they are highly soluble and difficult to be filtered. Surface immobilization strategy has been identified to be a promising approach to effectively anchor the nanoparticles on a surface or support and thereby extracting from the solution. Furthermore, such a strategy is highly useful for several biological applications. A brief anchoring study of lipase capped GNPs over magnetite nanoparticles was performed that would allow facile magnetic recoverability of GNPs. The HR-TEM (Figure 4.7f) of the sample revealed the successful anchoring of GNPs over the magnetite nanoparticles, as marked by the distinct Fe_3O_4 and GNP domains.

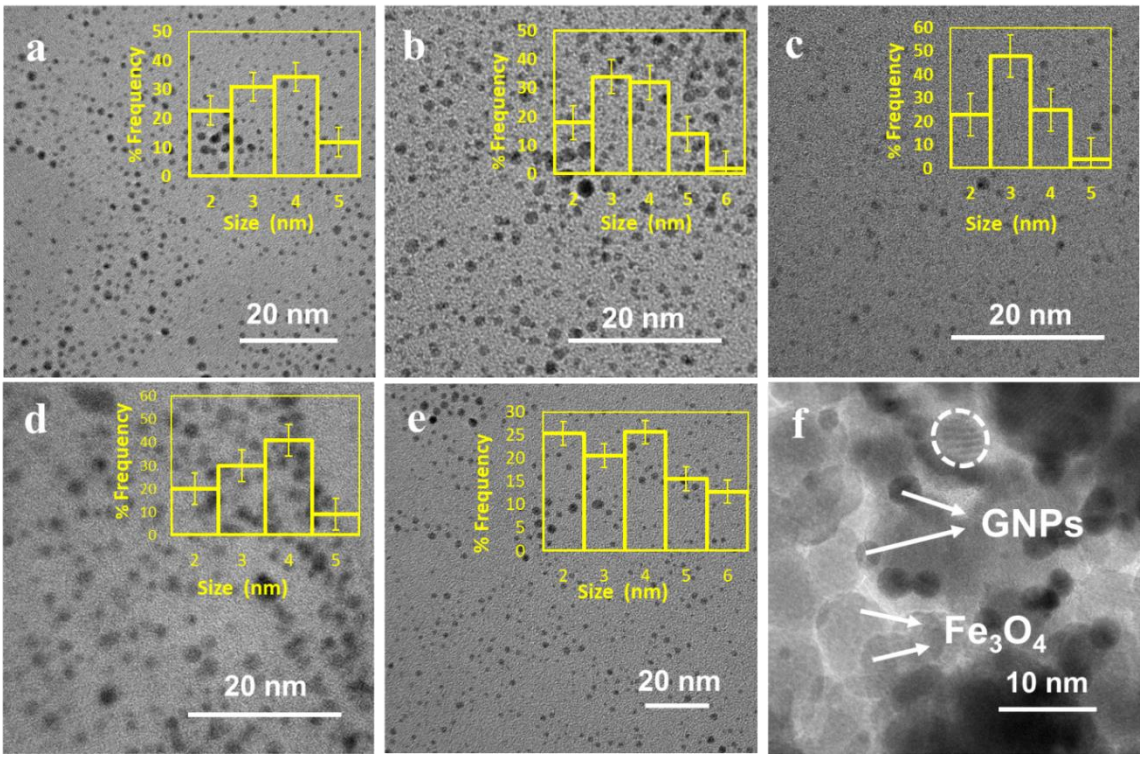

Figure 4.7: Composite HR-TEM images of (a) 0.5 mg/mL, (b) 1 mg/mL, (c) 2 mg/mL, (d) 6 mg/mL and (e) 10 mg/mL lipase-capped GNPs. Inset shows the particle size distribution. HR-TEM image of GNPs anchored over Fe_3O_4 nanoparticles is given in (f). The dotted circle shows the Moiré patterns arising from Fe_3O_4 support.

The merged SAED patterns also confirmed (Figure 4.8) the presence of both Fe_3O_4 and GNPs in the composite.

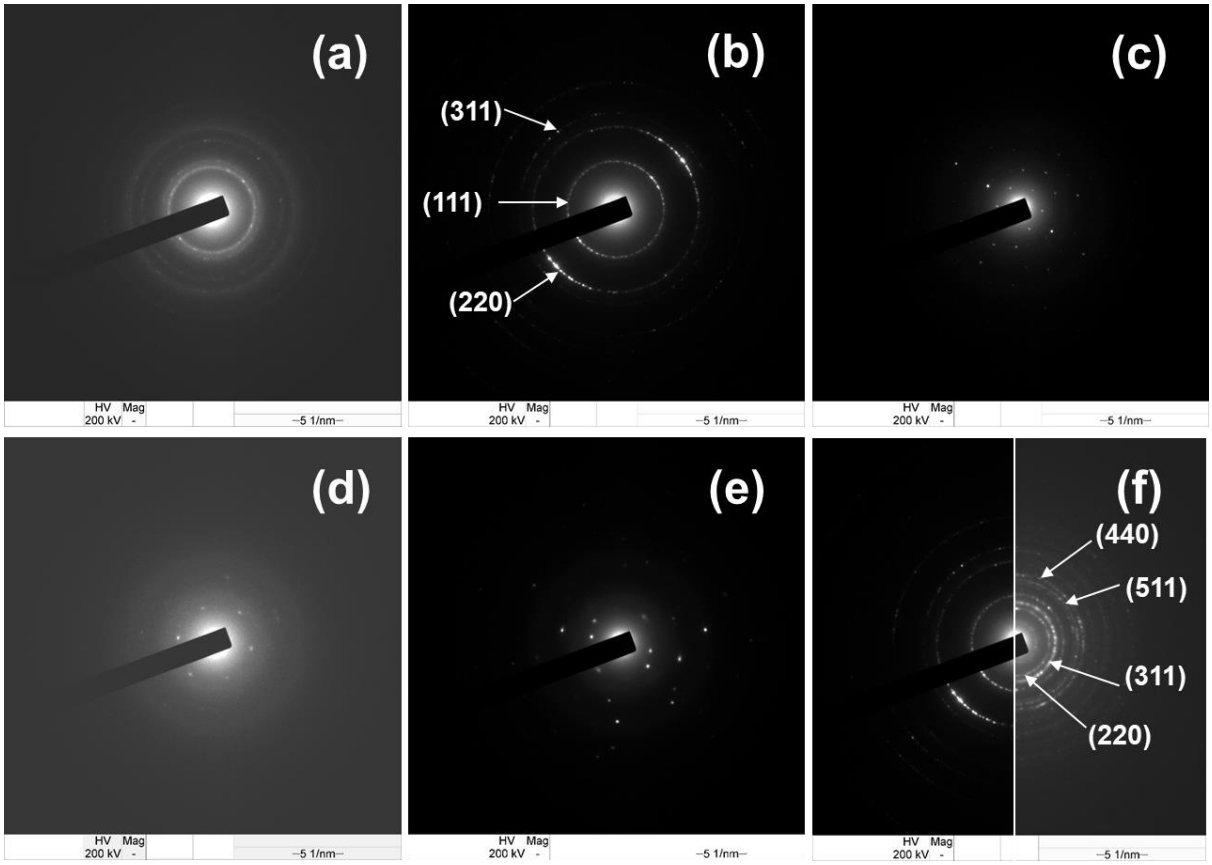

Figure 4.8 SAED patterns of (a) 0.5 mg/mL, (b) 1 mg/mL, (c) 2 mg/mL, (d) 6 mg/mL and (e) 10 mg/mL lipase-capped GNPs. Merged SAED image of 1 mg/mL lipase-capped GNPs and the same anchored onto Fe_3O_4 nanoparticles for comparison (f).

The catalytic conversion of 4-NP to 4-AP has been considered to be a benchmark reaction to study the efficacy of the GNPs. This conversion is deemed to be industrially important, as the former is an environmental pollutant, while the latter is the precursor for an important drug, *paracetamol*. Therefore, the catalytic reduction of 4-NP to 4-AP was performed using the GNPs capped with varying amount of lipase to probe their surface catalytic properties (Figure 4.9) [201, 202].

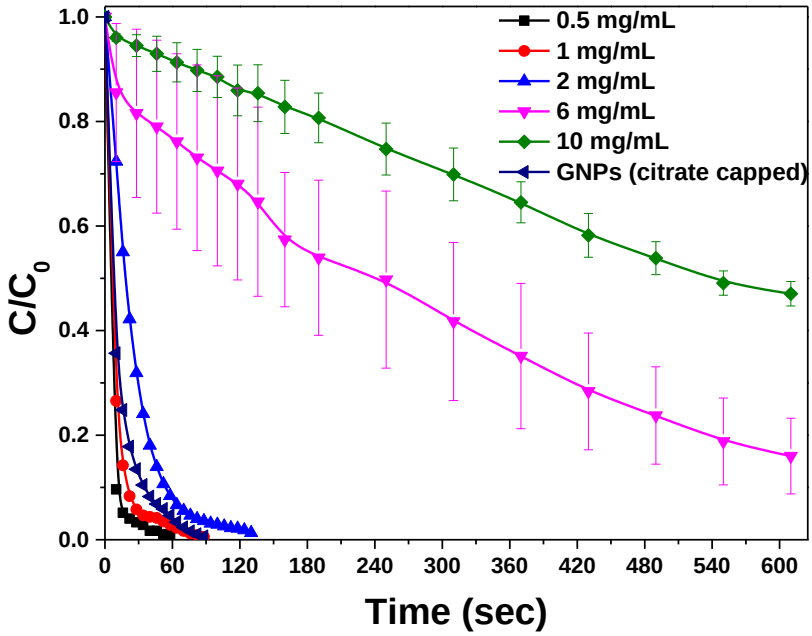

Figure 4.9: Catalytic reduction of 4-NP over GNPs capped with varying amount of lipase

A higher catalytic efficacy would therefore indicate higher availability of the catalytically active sites. With the reaction progress, the absorbance of the peak at 400 nm was decreasing, while a subsequent peak corresponding to 4-AP was appearing at 290 nm [201, 202, 203]. Though, all the GNPs used in this study exhibited high catalytic activity, the GNPs capped with 0.5 mg/mL of lipase was found to be the most active one that accomplished the reaction in less than one min. This could be attributed to the higher availability of the catalytically active sites due to the lesser amount of lipase capping. Clearly, the catalytic efficiency of the GNPs capped with 6 and 10 mg/mL is poorer compared to 0.5 mg/mL, which could be due to the efficient capping of lipase that decreases the available GNPs' surface for the catalysis. The turnover frequency (TOF) was also calculated for the catalytic reactions using lipase-capped GNPs and the results are shown in Figure 4.10.

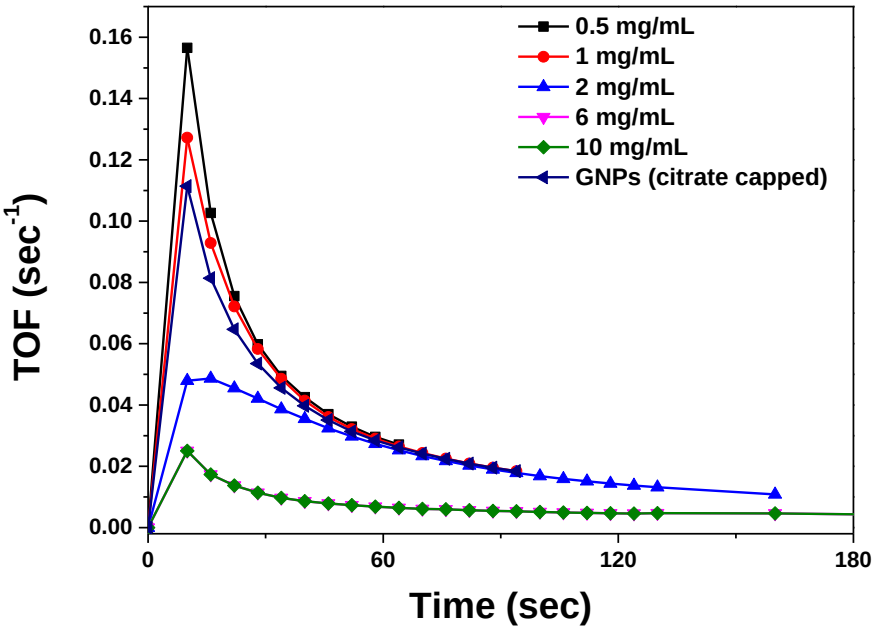

Figure 4.10: Turn over frequency of GNPs for the catalysis

The TOF is the number of completed catalytic cycles per atom of the catalyst, calculated as a function of time [201, 203]. The TOF of all the lipase-capped GNPs is found to be maximum at 10 s and the highest TOF is observed with 0.5 mg/mL of lipase capping. A control experiment with citrate capped GNPs synthesized by the Turkevich method exhibited slightly lesser TOF than 1 mg/mL lipase-capped GNPs, indicating the high catalytic efficacy of GNPs capped with less amount of lipase. To gain additional insight to the catalysis, the reaction parameters were fitted with different kinetic profiles and were found to fit well with pseudo-first order kinetics (Figure 4.11).

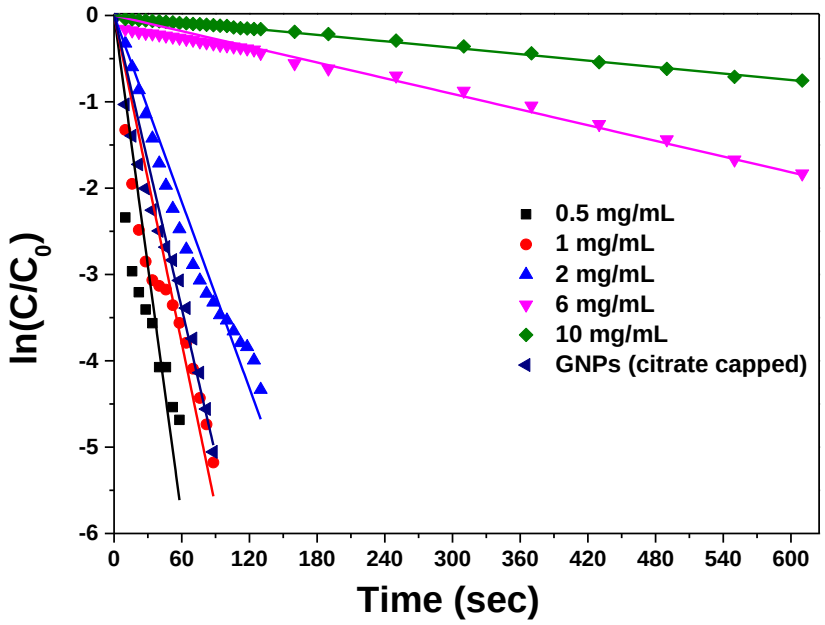

Figure 4.11: Pseudo-first order kinetics of catalytic reduction of 4-NP over GNPs capped with varying amount of lipase to Fe_3O_4 nanoparticles.

Table 5. Rate constants for 4-NP to 4-AP conversion using GNPs capped with varying amount of lipase.

Sample	Rate constant (sec^{-1})	% Standard Error (+/-)	R^2
0.5 mg/mL	0.0967	0.0078	0.938
1.0 mg/mL	0.0632	0.0031	0.964
2.0 mg/mL	0.0359	0.00007	0.990
6.0 mg/mL	0.00303	0.00006	0.988
10.0 mg/mL	0.00125	0.00001	0.996
Au NPs (Citrate capped)	0.0565	0.0014	0.990

Table 5 lists the rate constant calculated for GNPs capped with different amounts of lipase. The calculated rate constant was the highest (0.0967 s^{-1}) with 0.5 mg/mL lipase-capped GNPs, while the lowest rate constant (0.00125 s^{-1}) was obtained with 10 mg/mL lipase-capped GNPs. The recyclability of the lipase capped GNPs was demonstrated by anchoring them over Fe_3O_4. The 0.5 mg/mL lipase capped GNPs anchored over Fe_3O_4

were studied for their recyclability towards 4-NP reduction and the results are presented in Figure 4.12.

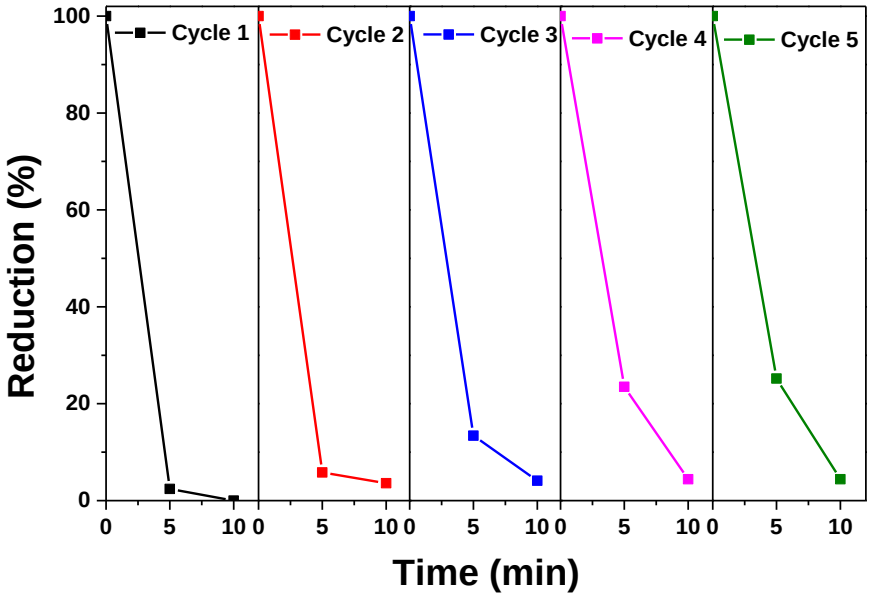

Figure 4.12: Catalytic reduction of 4-NP over GNPs capped with varying amount of lipase to Fe_3O_4 nanoparticles.

As evidenced from the figure, the catalytic efficiency was retained till five cycles. However, there was a modest decrease in the reaction rate, which could be due to the aggregation of magnetite over the recycling steps. Nevertheless, the study has shown the potential of recovering and reusing the lipase-capped GNPs in a facile manner.

4.4 Conclusion:

GNPs capped with varying amounts of lipase as stabilizing agent have been successfully synthesized, as confirmed by UV-visible and IR spectroscopy studies. Significantly, the tight size control and near-monodispersity of the lipase-capped GNPs have been revealed by HR-TEM and DLS analyses. In particular, with 0.5 and 1 mg/mL of lipase, the synthesized GNPs exhibited modest polycrystallinity, whereas with higher amount of lipase as in 2 to 10 mg/mL, the obtained GNPs were nearly monocrystalline [204]. The reduction of 4-NP to 4-AP studies revealed that the GNPs capped with 0.5

mg/mL of lipase exhibited the highest catalytic efficacy and the lowest catalytic efficacy was exhibited by 10 mg/mL lipase-capped GNPs. The clear trend showed that the catalytic sites of bare gold regions were more exposed and therefore available for efficient catalysis with 0.5 mg/mL lipase-capped GNPs. Indirectly, the results prove efficient capping of GNPs with lipase at higher loading, which minimizes the accessibility of bare gold regions for catalysis. The amine-functionalities of lipase enabled the anchoring of GNPs over Fe_3O_4 nanoparticles via glutaraldehyde conjugation. Such a strategy was found to be useful in recovering and reusing the GNPs. Further studies are directed to employ mild reducing conditions in order to preserve the activity of lipase anchored over GNPs, which would be useful for various applications including catalysis, sensing, drug delivery etc [205].

CHAPTER 5

IN VITRO HEMOCOMPATABILITY EVALUATION OF GOLD NANOPARTICLES CAPPED WITH *LACTOBACILLUS SPS* . DERIVED LIPASE

5.1 Introduction

Gold nanoparticles (GNPs) are emerging as potential agents for treatment in biomedical field. GNPs are unique due to their physiochemical properties such as smaller size, intense surface plasmon resonance in visible light wavelength region, excellent biocompatibility, and chemical stability. In this regard, the studies are currently being carried out with attention in many areas starting from targeted drug delivery in cancer treatment, antibacterial agents to tissue imaging agents [206–208]. Synthesis of GNPs involves reduction of Au (III) to Au (0) ions using different reducing solutions such as sodium citrate, $NaBH_4$, alcohols etc, which result in the size range of 3 to 200 nm depending on the synthetic route [209]. The synthesized GNPs are usually stabilized by the capping agents that prevent particle aggregation and provide interfacial properties [210]. The surface properties can be tailored by the judicial choice of capping agent. The use of biomolecules (proteins, carbohydrates) as capping agents will provide interaction via free end groups present in them. Till date much research has been focused on using GNPs for various applications and their clinical evaluation. However, relatively little is known about the potential biological risks associated with GNPs and several barriers such as chronic cytotoxicity, tumor targeting efficacy, ability to avoid generating an immune response for in vivo applications [211–213]. Thus recently several groups focused on risk assessment on clinical evaluation of medically applied nanoparticles and there is a shift in research focus towards probing the effect of GNPs on biological processes that are critical for the cell functions. Many studies have found that polymeric nanoparticles, dendrimers, quartz particles, carbon nanotubes are cytotoxic and induce blood clotting [214–219]. Extensive in vivo hemocompatibility analyses have been carried out only for a few nanoparticles; however, the data interpretation is complicated due to the lack of adequate nanoparticles' characterization in terms of surface charge,

size and variability of the experimental medium [220]. Recently, there is an upsurge in study on hemocompatability of GNPs with emphasis on blood coagulation factors [221]. It is known that the size, shape, surface charge, and capping agents influence the blood compatibility of GNPs [222–225]. Studies determining plasma binding profile of citrate-stabilized GNPs indicate that major blood proteins such as albumin, globulin, fibrinogen, interact strongly with GNPs and also results in hydrodynamic size doubling of nanoparticles [226]. Studies with chitosan, and pyrimidine functionalized GNPs show that platelets do not aggregate in the presence of nanoparticles thereby effecting thrombin, fibrin components of blood clotting factors and prolong the blood clotting time [222–225]. Since all the above studies were based on measuring prothrombin time, they avoided major cell components present in the whole blood. In this study, we carried out lipase capped GNPs' in vitro blood interaction studies using citrated whole blood (CWB) through monitoring the viscoelastic changes, platelets aggrometry tests, and plasma fibrinogen changes [227]. The results are significant in determining the effect of protein capped GNPs when come in contact with whole blood.

5.2. Materials and methods

5.2.1. Whole Blood Collection and Platelets isolation

All experiments were done with prior approval from ethical committee, Institutional Review Board (IRB:2016/11/009) of Deccan College of Medical Sciences, Hyderabad, Telangana, India and the written informed consent forms were collected from the healthy individuals participated in the study. Healthy volunteers were defined according to criteria of the Nordkem-Workshop. Blood was taken from healthy volunteers of age 18–30 who were free from platelet function affecting medication for a month. Donors suffering from any metabolic disorder or ailments were not included. The data of the donors such as (sex, age, height, weight, body mass index, blood pressure,

heart rate, haemoglobin percentage, WBC count) was collected and only the volunteers within the reference range for healthy humans were allowed to participate in the study [228].Whole blood samples were drawn from healthy volunteers using BD Vacutainer (3.8% sodium citrate). To isolate platelet rich plasma (PRP), the collected whole blood was diluted using Lymphoprep™ physiological saline at 1:1 ratio in a centrifuge tube and performed a soft spin at 130 g, 37^{o}C, 15 min. The obtained supernatant after centrifugation was collected into another sterile tube followed by haemocytometer count. The collected blood was again centrifuged at higher speed to obtain platelet poor plasma. Two fractions were obtained after centrifugation, the upper 2/3rd fraction is platelet-poor plasma (PPP) and the lower fraction is 1/3rd platelet rich plasma (PRP) [229, 230]. The PRP was dissolved in appropriate amount of PPP. The concentration of the platelets within the PRP was assessed, and standardized to 1200×10^3 platelets/mL by adding the appropriate amount of PPP and used for the study [231].

5.2.2 Synthesis and Characterization of Gold nanoparticles (GNPs)

The lipase used in this study was isolated from *Lactobacillus plantarum* (MTCC 4461) [232–234]. Hydrogen tetrachloroaurate (III) hydrate ($HAuCl_4$), and $NaBH_4$ were all purchased from Sigma Aldrich. Lipase capped GNPs were prepared by adding 1mL of 1mM HAuCl4 solution to solution of lipase in different concentrations (0.1, 0.5, 1, 1.5, and 2mg/mL) in Tris-HCl buffer, followed by addition of 300uL of 25mM $NaBH_4$ solution. The successful formation of GNPs was confirmed using UV visible spectrophotometer (Shimadzu UV-3600 plus), and dynamic light scattering (DLS) (Zetasizer Nano-ZS, Malvern). The size of the GNPs was also confirmed using high-resolution transmission electron microscopy (HR-TEM, FEI, Tecnai G2, F30). DLS experiments were done to determine changes in size of GNPs after incubation in PRP,

and PPP. Citrate-capped GNPs were synthesized using standard Turkevich method for comparison [235].

5.2.3 Platelet aggregation studies

Two different concentrations of GNPs namely 1.0 nM and 5 nM with respect to gold concentration was used to evaluate the blood coagulation properties at 37˚C. Aggregation studies were performed in glass cuvettes coated with silicon using the instrument platelet aggregometer (Chrono-Log 490 model, Chrono-Log corp). This spectrophotometer mimics the blood flow conditions, creates a shear stress using magnetic stirrers and measures the aggregation as function of difference between transmission wavelength of PPP and PRP with aggregation agonists (here L-GNPs, ADP) expressed in percentage aggregation. The recordings were carried out until ten minutes after adding lipase capped GNPs and 25uL of 2mL Adenosine Diphosphate (ADP) to PRP.

5.2.4 Plasma fibrinogen tests

Plasma fibrinogen tests were determined before and after incubation with lipase capped GNPs. Plasma fibrinogen test was performed based on sandwich Enzyme-Linked Immunosorbent Assay (AbFrontier, Catalog # LF-EK0153). This test was used to quantitatively determine the *in vitro* fibrinogen in human plasma. To make the standard curve, appropriate volume of standard solution with dilution buffers was added to microtiter wells and then human plasma was added to the sample wells, which was diluted by at least 4000 folds. Then the solutions were incubated for two hours, after which the incubation the solutions were discarded and the wells were washed adequately. About 100 microliter of working secondary antibody solution was pipetted into each well and incubated for 1 hour at room temperature. After incubation, the secondary antibody solutions from the wells were decanted, followed by washing of the wells. Then the

working Avidin-Horseradish Peroxidase solution was added to each well and incubated in dark for 1 h. After incubation, the wells were washed, the substrate solution was added and the plate was incubated at room temperature, followed by O.D. determination at 450 nm by the microtiter plate reader.

5.2.5 Blood clotting tests

Blood coagulation kinetics of lipase capped GNPs was studied employing Thromboelastography TEG®. The clotting time (R) was observed as a function of increase in clot strength upon Ca^{2+} activation of coagulation in the presence of GNPs until an increase in elasticity corresponding to 2 graphical mm was observed. A shorter R value indicates hypercoagulability. Clot strength (MA) is the measure of maximum clot strength (in mm) developed with function of time, which mainly depends on the activity of blood clotting cascade that is usually expressed in dynes/cm2. The clot kinetics is measured in terms of α-angle◦ (clot angle).

5.3 Results and discussion

The work primarily explores the effect of GNPs on blood with changing concentrations of lipase capping. Therefore, we have chosen 0.1 to 2mg/mL lipase capping solution, while keeping the gold solution and reducing agent concentrations constant. The samples are coded based on the amount of lipase capping agent used are as follows: 0.1mg/mL – (i); 0.5mg/mL – (ii); 1mg/mL – (iii); 1.5mg/mL – (iv); 2mg/mL – (v); and citrate-capped GNPs as reference – Citrate. Figure 5.1 depicts the strategy of the present hemocompatability study on human blood using lipase-capped GNPs.

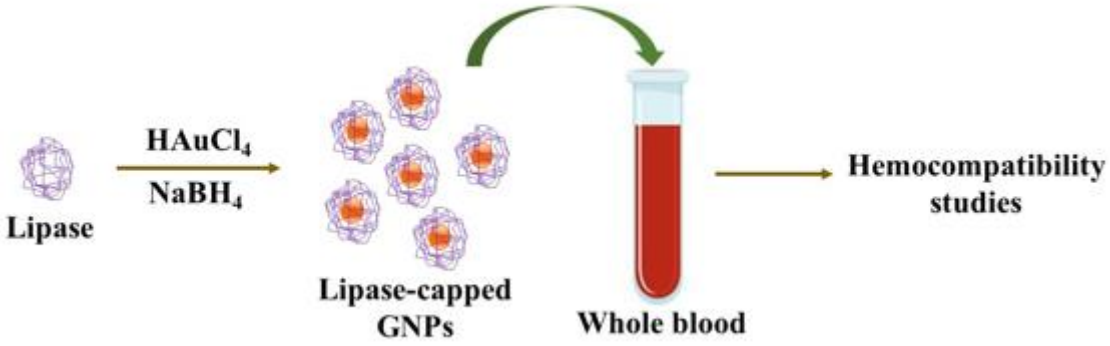

Figure 5.1: Study of Hemocompatibility of lipase capped GNPs on human blood

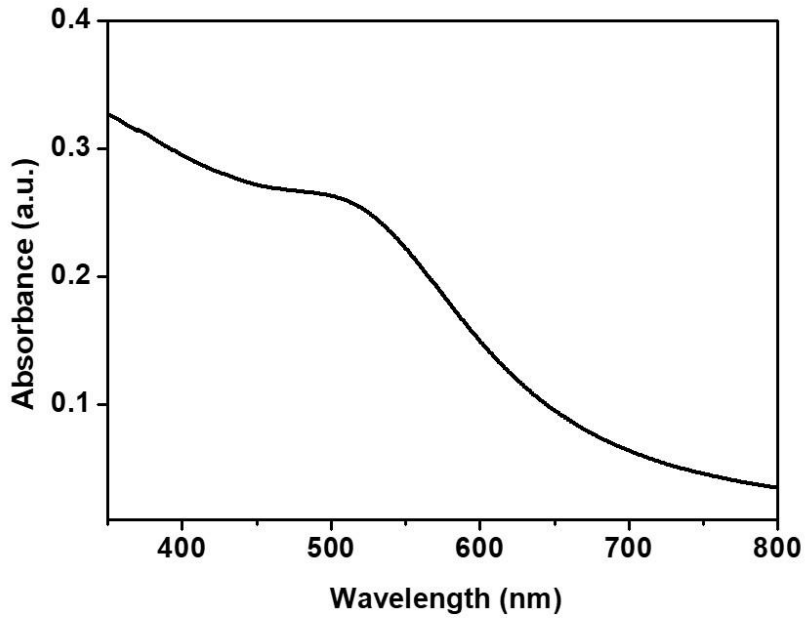

Figure 5.2. UV-VIS Spectra of Lipase capped GNPs

A gentle, but prominent plasmonic peak at ~521 nm reveals the successful formation of GNPs. The hydrodynamic size of the synthesized nanoparticles was evaluated before and after incubation with blood plasma by DLS measurements. Table 6 lists the mean particle diameter of the different amounts of lipase-capped GNPs employed in this study ranging from 7 to 10 nm.

Table 6: Particle size analysis using DLS for the lipase-capped and citrate-capped GNPs

Sample	Particle Diameter
(i)	9.4
(ii)	9.2
(iii)	8.8
(iv)	7.5
(v)	10.1
Citrate Capped	9.7

Note: (i) 0.1 mg/mL (ii) 0.5 mg/mL (iii) 1.0 mg/mL (iv) 1.5 mg/mL (v) 2.0 mg/mL Lipase capped and Citrate capped GNPs.

The hydrodynamic size of lipase capped GNPs after incubation with blood plasma (PPP) was also evaluated using DLS. It was found that the particle size remain unchanged even after 1 h of incubation in the blood plasma, suggesting that there was no aggregation of nanoparticles in blood plasma due to the efficient lipase capping which had stabilized the nanoparticles and prevented the aggregation in plasma solution. Representative HR-TEM images of 1mg/mL lipase capped GNPs are shown in Fig. 5.3.

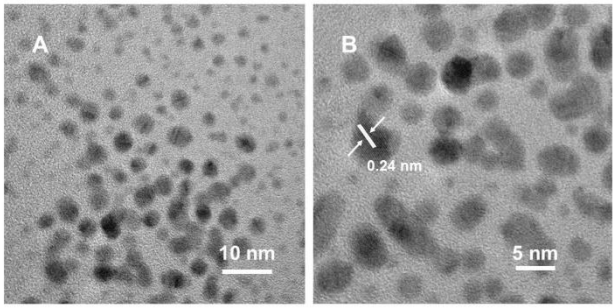

Figure 5.3. HR-TEM images of Lipase capped GNPs

It can be seen that the synthesized lipase capped GNPs were found to be in the sub-10 nm in size and the particle morphology was nearly spherical. Plasma fibrinogen

levels of plasma samples were evaluated after treatment with lipase capped GNPs and the results are presented in Fig. 5.4.

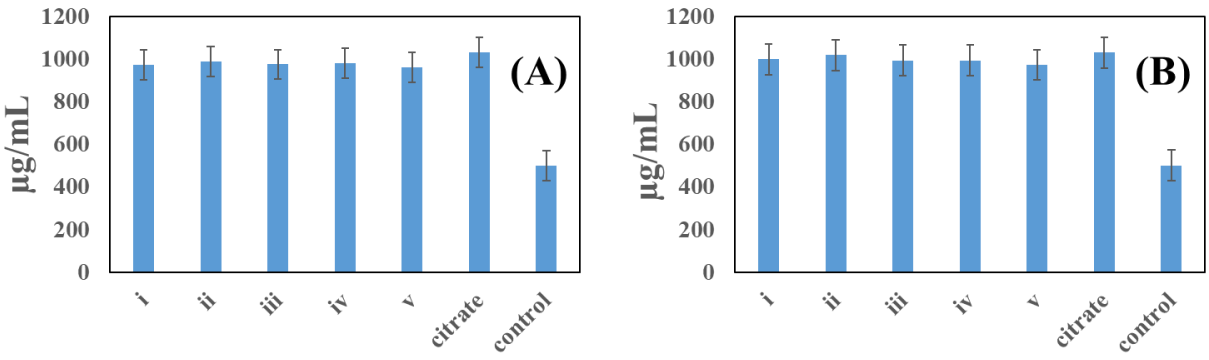

Figure 5.4. Plasma Fibrinogen test (A) 1 nM lipase capped GNPs treatment of whole blood (B) 5 nM lipase capped GNPs treatment of whole blood i) 0.1 mg/mL ii) 0.5 mg/mL iii) 1.0 mg/mL iv) 1.5 mg/mL v) 2.0 mg/mL Lipase capped GNPs, Citrate capped GNPs and Control

It was found that there was no significant difference among the GNPs at the two different concentrations used. However, compared to the control, a two fold increase in fibrinogen levels was observed post incubation with lipase capped GNPs. Several other studies have also reported that fibrinogen is one of the major components of blood that interacts with colloidal nanoparticles [236]. There may be several reasons; one of the differences could be attributed to the slight variation in protein charge in presence of nanoparticles. Therefore, it is imperative to study the effect of the increase in fibrinogen content towards strength and kinetics of blood coagulation. Thus, we further studied blood clot strength using Thromboelastography TEG® analysis in the presence of lipase GNPs (Figs.5.5).

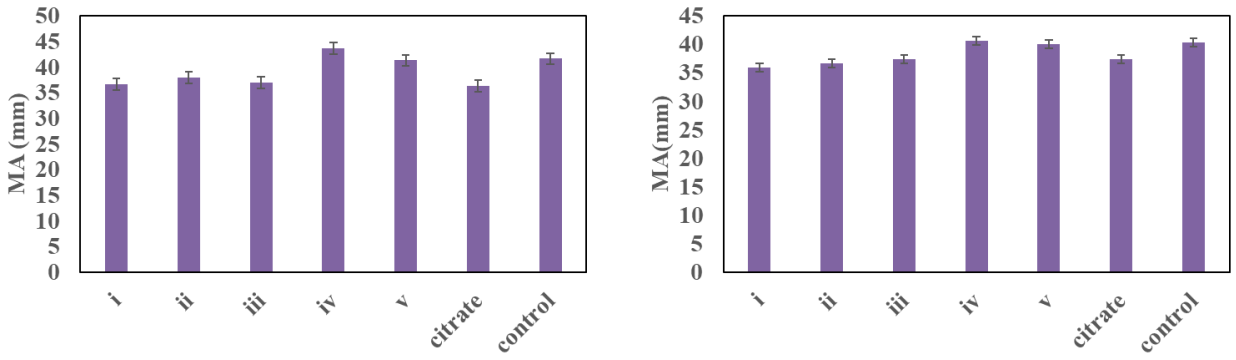

Figure 5.5. Estimation of Clot Strength (A) 1 nM lipase capped GNPs treatment of whole blood (B) 5 nM lipase capped GNPs treatment of whole blood i) 0.1 mg/mL ii) 0.5 mg/mL iii) 1.0 mg/mL iv) 1.5 mg/mL v) 2.0 mg/mL Lipase capped GNPs, Citrate capped GNPs and Control

In this experiment, *in vitro* blood coagulation experiments with gold concentrations of 1 nM and 5 nM with varying lipase (0.1, 0.5, 1.0, 1.5, 2.0mg/mL) capping agent was performed. We studied the effect of blood clotting on clot strength (MA), clotting time (R) (Figure 5.6) and clot kinetics

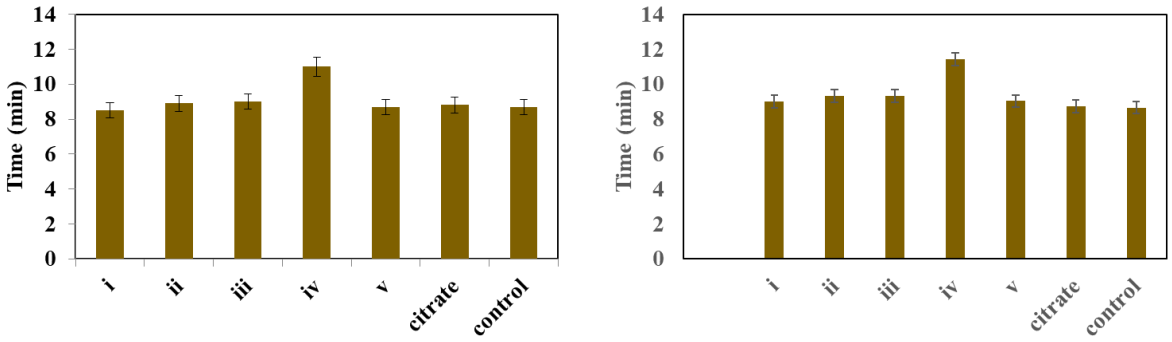

Figure 5.6. Estimation of Clot formation time (A) 1 nM lipase capped GNPs treatment of whole blood (B) 5 nM lipase capped GNPs treatment of whole blood i) 0.1 mg/mL ii) 0.5 mg/mL iii) 1.0 mg/mL iv) 1.5 mg/mL v) 2.0 mg/mL Lipase capped GNPs, Citrate capped GNPs and Control

(alpha-angle°) in the presence of GNPs along with $CaCl_2$ (Ca^{2+}) to activate blood coagulation since blood was collected using citrated vials. TEG® analysis of blood with 1 nM and 5 nM GNPs with varying lipase capping indicated that despite two fold increase in the fibrinogen levels, there was no significant effect on clot formation kinetics (α-angle) (Figure 5.7) clot strength and blood clotting time when compared with control [237].

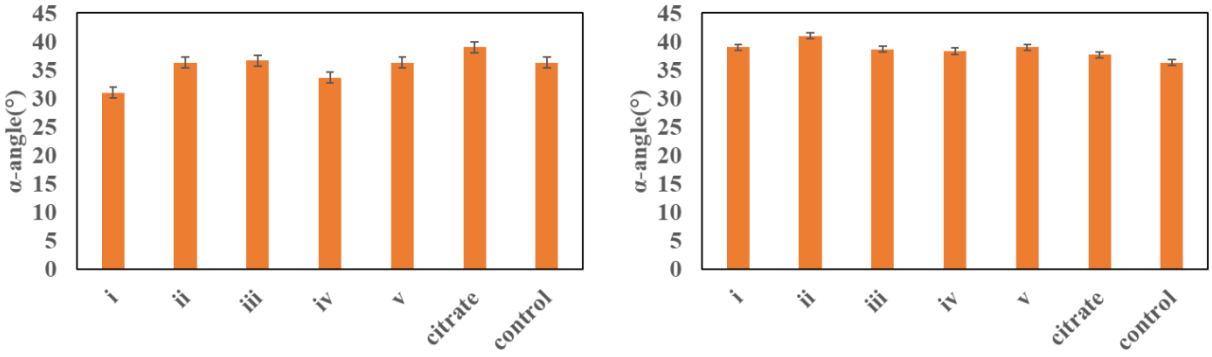

Figure 5.7. Estimation of Clot formation angle (A) 1 nM lipase capped GNPs treatment of whole blood (B) 5 nM lipase capped GNPs treatment of whole blood i) 0.1 mg/mL ii) 0.5 mg/mL iii) 1.0 mg/mL iv) 1.5 mg/mL v) 2.0 mg/mL Lipase capped GNPs, Citrate capped GNPs and Control

Furthermore, there was no clear trend in relation to the difference in lipase capping of GNPs and also the use of different concentrations of gold. This could be due to the smaller size of the nanoparticles which are usually in the range of sub-10 nm and their inability to hyperactivate the clotting cascade. Even after increasing the amount of nanoparticle concentration to 5 nM, we could not detect any significant effect on the blood coagulation process. Several studies reported that treatment with GNPs results in increase in fibrinogen, but there is no evidence that the GNPs are thrombogenic in nature. The increased fibrinogen binds to gold nanoparticle surfaces, which is usually size dependent and increases with decrease in particle size, but such a binding does not usually cause coagulation [238]. Studies have shown that citrate stabilized GNPs

potentiate ADP-induced platelet activation due to rapid internalization of smaller sized GNPs and subsequent fibrinogenesis [239]. In our study we used GNPs of size ~10 nm, which could have resulted in internalization by platelets and thereby increasing the fibrinogen content. The specific GNPs-protein corona has not been studied in detail so far and also the components and the parameters involved in blood clotting cascade that determine the clotting time and formation are not clearly understood [240–242]. The platelet aggregation in the presence of GNPs was evaluated with a positive control ADP. The percentage of platelet aggregation (%) in the presence of lipase capped GNPs was found to be significantly lower in the different concentrations tested in this study. The percentage aggregation of platelets after 10 minutes of incubation for different concentrations of lipase capped GNPs is presented in Fig. 5.8.

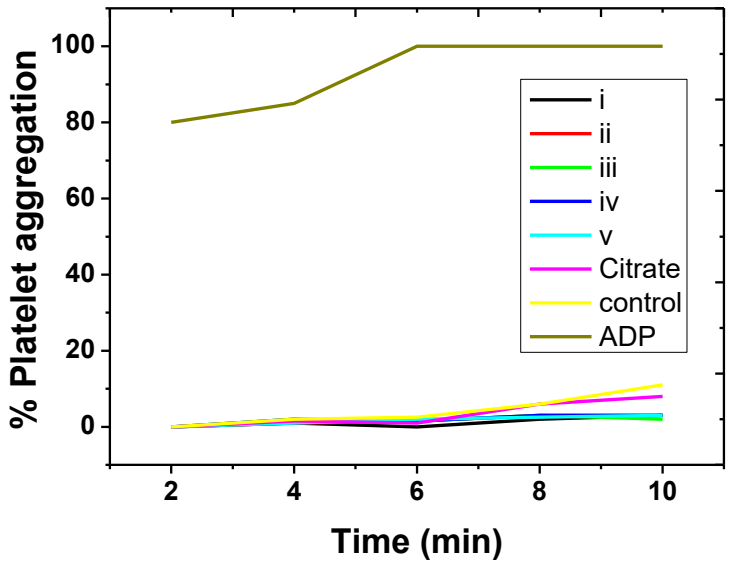

Figure 5.8. Estimation of Platelet aggregation in presence of lipase capped GNPs i) 0.1 mg/mL Lipase capped GNP's ii) 0.5 mg/mL iii) 1.0 mg/mL iv) 1.5 mg/mL v) 2.0 mg/mL, Citrate capped GNPs, Control

The results suggested that blood platelet aggregation was not activated in presence of GNPs. Earlier reports have shown that the nanoparticles of 20 nm size and

above were actively involved in platelet aggregation [240-242]. The lack of aggregation can be attributed to inactivation of platelets by the smaller size of the nanoparticles used for testing.

5.4 Conclusion

The present study revealed that lipase capped GNPs synthesized using $NaBH_4$ approach are stable and hemocompatible. It was found that there was two-fold increase in fibrinogen levels after the exposure to nanoparticles, which is consistent with other studies. However, the increase in fibrinogen levels was found not to have any adverse effect on the blood coagulation parameters such as clotting time, clot strength and clot formation kinetics. Furthermore, our study also revealed that there was no significant change in the platelet aggregation behaviour. The hemocompatability is attributed to the very small size regime (sub-10 nm) and the eco-friendly behavior of the probiotic lipase-capped GNPs. Future studies can be directed to determine the coagulation effects of GNPs as a function of size as well as at elevated concentrations.

CHAPTER 6

EXTRACELLULAR PROBIOTIC LIPASE CAPPED SILVER NANOPARTICLES AS HIGHLY EFFICIENT BROAD SPECTRUM ANTIMICROBIAL AGENTS

6.1 Introduction

Many ancient cultures have used several antimicrobial compounds based on selected plant materials, colloidal metals and specific mold extracts to treat infections [243]. These natural extracts and colloidal metals were replaced by the discovery of synthetic antibiotics by early 20th century. Since their discovery and commercial use, these antibiotics have saved innumerable lives [244]. In early 1940s, the antibiotic Penicillin was prescribed to control serious bacterial infections among World War II soldiers [245]. Ever since, antibiotics have played a major role in treating infections in cancer or immune compromised patients, diabetics, organ transplants, joint replacements, cardiac surgeries and thereby increasing the life spans across the world [246]. Their use is not limited to human, but have also been employed in bee-keeping, growth promoter in animal husbandry, horticulture, fish farming, food preservation and antifouling paints [247]. The use of antibiotics across various domains even at a low-concentration exposure to microbes results in selection and spread of antibiotic-resistant strains [248].

Apart from this, over prescription and misuse of antibiotics conferred resistance to clinically useful antibiotics as well. This is a threat to human healthcare system and therefore warrants key measures to tackle the risks posed by microbial resistance to antibiotics [249]. This rise in resistance of microbial organisms to various antibiotics in turn results in increasing the cost of health care. Thus, the need of the hour is to engage in developing effective and stable antimicrobial agents that are alternatives to antibiotics for combating microbial resistance. This has initiated the quest for new antimicrobial drugs that possess structures not related to the current active pharmaceutical ingredients in biological and medicinal chemistry.

Silver nanoparticles (Ag NPs), on the other hand, have become the popular choice recently for antimicrobial properties in several applications including food storage

containers, cosmetics, wound healing dressings etc [250]. It is reported that around 400 metric tons of Ag NPs have been produced annually [251]. Several reports exist on antimicrobial activity of Ag NPs due to the advantage that the microbes do not develop resistance against them easily, when compared to the antibiotics where they eventually develop resistance through genetic mutations [252]. Although Ag NPs can act alone as anti-bacterial agent, their aggregation in the absence of appropriate capping agents severely inhibits the antimicrobial action [253]. This can be overcome by employing an appropriate capping agent onto the Ag NPs. A variety of synthetic polymers, natural polymers, biomacromolecules and surfactants such as poly-(N-vinyl-2-pyrrolidone) (PVP), (polyethylene glycol (PEG), polyvinyl alcohol (PVA), starch, cellulose, sodium dodecyl sulfate (SDS), citrate, bovine serum albumin (BSA), fungal and plant protein extracts have been employed as capping agents for Ag NPs [254]. Among such various capping agents, bio-derived molecules such as enzymes, saccharides and plant derived molecules are considered to be more eco-friendly and bio-compatible. Proteinaceous capping agents have additional advantage of being amphoteric in nature, which could enable the interaction of the capping agent with poly cationic and poly anionic moieties present on the bacterial surface [255].

Despite the large scale industrial applications of Ag NPs, their utility also comes with a cost. Their excessive usage in the recent years has raised significant concerns among the researchers working in the field of environmental toxicology. While the permissible exposure limit set by Occupational Safety and Health Administration for soluble silver is 0.01 mg/m^3, the literature reports indicate the lethal dose 50 (LC_{50}) of Ag NPs (~80 nm in diameter) in zebra fish model is about 84 ng/mL, which is in the ppb concentration scale [256]. However, except a very few articles, majority of the studies reported in the literature used the concentration of Ag NPs in ppm scale. Thus, while in

the process of addressing antimicrobial resistance caused by antibiotics, the excess of Ag NPs released in the environment could result in a secondary health hazard and environmental threat. Furthermore, the Ag NPs are shown to affect the ammonia-oxidizing bacteria in biological nutrient removal and waste water treatment [257]. Therefore, it is imperative that the concentration of Ag NPs released in the environment should be very much in the acceptable level. In the present study, Ag NPs capped with lipase from probiotic source of *Lactobacillus plantarum* have been synthesized and studied for their antimicrobial properties against *Pseudomonas putida, Staphylococcus aureus and Aspergillus niger* [258]. Although lipases are present in various fungal and bacterial sources, Lactobacillus plantarum is preferable as they are probiotics and part of the human mucosal surface microflora. Due to this reason, they are known to be highly biocompatible. Recently, we have shown that Au nanoparticles capped with Lactobacillus plantarum lipase are hemocompatible [259]. Furthermore, it has also been shown that the functional groups such as –COOH present in the proteins are useful in chemically anchoring the nanoparticles onto Fe_3O_4 to facilitate facile magnetic recoverability and thereby minimizing the threat of releasing into the aquatic environment [260]. Therefore, we have studied the minimum inhibitory concentration (MIC) of the lipase capped Ag NPs against the microbial strains in the concentration range well below the LC50 values for zebra fish as a step toward absolute eco-friendly and biocompatible antimicrobial agent [261].

6.2 Materials and Methods

6.2.1 Materials:

Lipase from *Lactobacillus plantarum* (MTCC 4461) was isolated as per our previous reports. Silver [170]. Nitrate, $NaBH_4$ and PBS buffer (pH 7.4) used were

purchased from Sigma Aldrich. Pseudomonas putida, Staphylococcus aureus and Aspergillus niger culture were obtained from MTCC, Chandigarh, India.

6.2.2 Preparation of lipase-capped silver nanoparticles (Ag NPs):

About 0.2, 0.6 and 1.0 mM concentrations of silver nitrate solutions were freshly prepared in deionized water and used for the nanoparticles synthesis within 2 h of time. To 1 mL of the above mentioned silver nitrate solutions, 0.5 mL of lipase isolated from Lactobacillus plantarum was added such that the final lipase concentrations for each concentration of silver nitrate solution was 25, 50 and 100 μg/mL. Finally, the reduction of silver nitrate was accomplished by adding stoichiometric amount of sodium borohydride with respect to silver nitrate.

6.2.3 Characterization of lipase-capped Ag NPs

The formation Ag NPs capped with different concentrations of lipase was followed using UV-visible spectrophotometer (Shimadzu UV-3600 plus). Energy dispersive X-ray fluorescence (ED-XRF) studies were performed using Epsilon-1 Analytical instrument to ascertain the chemical identity of silver. Fourier Transform infrared (FT-IR) analyses of the synthesized Ag NPs were performed using Shimadzu 8400S spectrophotometer to confirm the lipase capping. Malvern Zeta Sizer Nano instrument was used to characterize the lipase capped Ag NPs to determine the hydrodynamic diameter. The morphological characteristics were analyzed using high-resolution transmission electron microscopy (HR-TEM, FEI, Tecnai G2, F30).

6.2.4. Evaluation of antimicrobial activity of the lipase capped Ag NPs on *Pseudomonas putida*

The *Pseudomonas putida* was cultured for 12 hours at 37 °C under shaking conditions (150 rpm) in Luria Bertani (LB) broth medium. To find the minimum inhibitory concentration (MIC), the initial cell concentration of 2.3×10^5 colony forming

units per mL (CFU/mL) culture was taken and treated individually with 10, 15, 20, 25 and 30 nM concentrations of the sample solution containing Ag NPs with three different concentrations of 0.2, 0.6 and 1.0 mM (with respect to elemental Ag) each separately capped with 25, 50 and 100 μg/mL of lipase. This culture mixed with Ag NPs was then incubated at 37 °C under shaking conditions (100 rpm) for 6 hours in dark. The positive control was the culture treated with 10 μg/mL of ampicillin. The negative controls were the cultures treated separately with pristine lipase and $NaBH_4$ (SB). The conditions for the positive and negative control were same as that of the former. The growth was recorded in terms of optical density at 600 nm using UV-Vis spectrophotometer after 6 hours of incubation. MIC was deduced by counting the CFUs to study the effect of lipase capped silver nanoparticles as compared to that of positive and negative controls. All the antimicrobial studies were performed in triplicates.

6.2.5 Evaluation of antimicrobial activity of the lipase capped Ag NPs on *Staphylococcus aureus*

The *S. aureus* was cultured for 24 hours at 37 °C under shaking conditions (150 rpm) in LB broth medium. About 2.8 x 10^5 CFU/mL was taken and treated with the nanoparticles in a similar fashion that of *P. putida* and the optical density at 600 nm was recorded using UV-Vis spectrophotometer after 6 hours of incubation with nanoparticles. MIC was deduced to study the effect of lipase capped Ag NPs as compared to that of positive and negative controls.

6.2.6 Evaluation of antimicrobial activity of the lipase capped Ag NPs on *Aspergillus niger*

The *Aspergillus niger* spores were inoculated in a media containing 8.76 mM of sucrose, 2.35 mM of sodium nitrate, 0.734 mM of potassium dihydrogen phosphate, 0.41 mM of magnesium sulphate, 0.067 mM of potassium chloride and 0.658 mM of ferrous

sulfate. The culture was incubated at 28 °C for 48 hours to reach the log phase. About 1 g of the biomass of fungi for control and sample grown after 48 hours of incubation was treated with 10, 15, 20, 25 and 30 nM Ag NPs separately in a similar fashion to P. putida. The cultures were incubated for 6 hours at 28 °C in dark condition and the dry weights of the treated biomasses were determined after drying in hot air oven at 60 °C for 15-20 minutes. The positive control was the culture treated with 10 μg/mL of Amphotericin B. From the bar graphs of dry weight of biomass versus concentration, the MIC values were obtained.

6.3. Results & Discussion

The synthesized lipase capped Ag NPs were initially characterized using UV-Vis spectrophotometer and the results are presented in Figure 6.1a-c. In all the three concentrations of $AgNO_3$ such as 0.2, 0.6 and 1.0 mM, the formation of strong plasmonic peaks in the range of 400-420 nm clearly indicated the successful synthesis of Ag NPs [262].

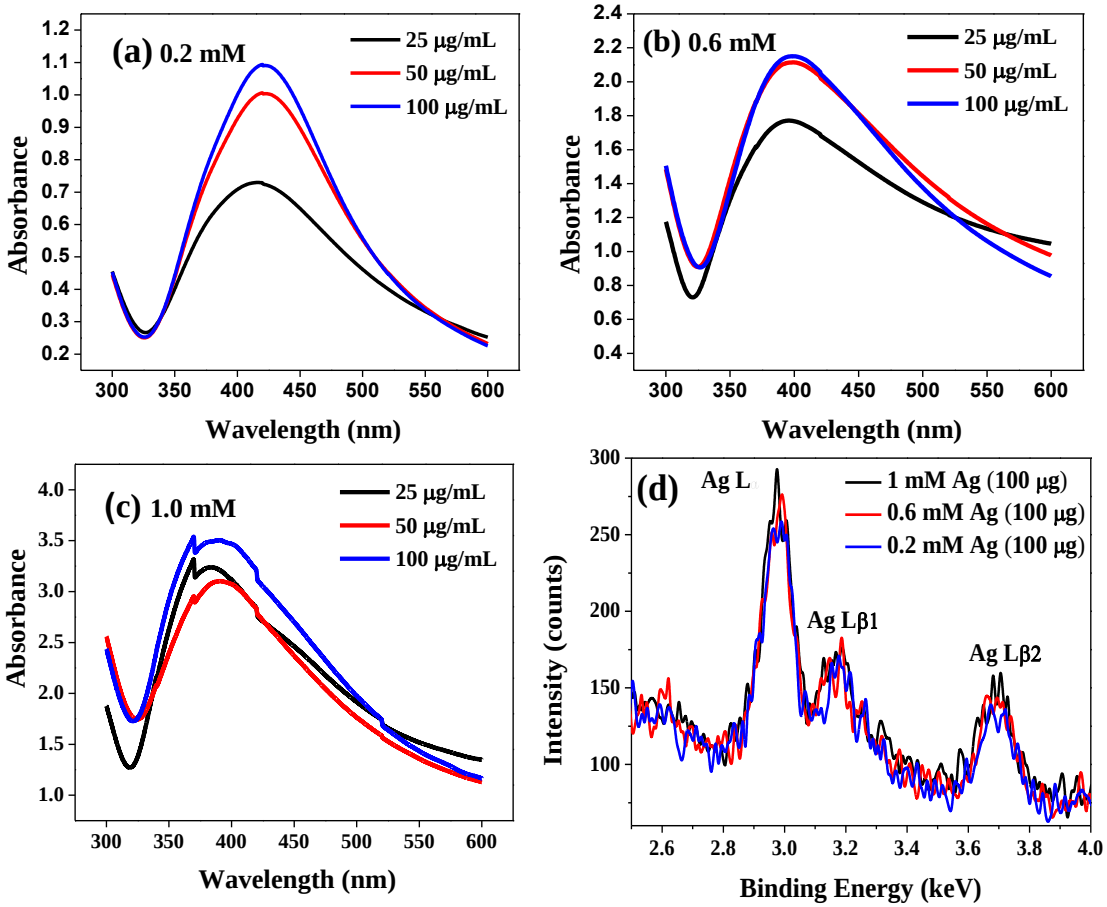

Figure 6.1: UV-Vis absorption spectra of Ag NPs synthesized from (a) 0.2mM, (b) 0.6 mM and (c) 1.0 mM $AgNO_3$ solutions with varying amount of lipase. (d) Energy dispersive X-ray fluorescence (ED-XRF) spectra of Ag NPs synthesized from the above mentioned $AgNO_3$ solutions with 100 µg/mL of lipase capping.

Interestingly, at a fixed concentration of $AgNO_3$, there is a trend of increasing plasmonic peak intensity with increasing the concentration of lipase capping agent. This is indicative of formation of smaller size and in turn larger number of Ag NPs with the systematic increase in lipase concentration. Furthermore, with the systematic increase in the concentration of $AgNO_3$, the absolute absorbance values of the plasmonic peaks were found to increase linearly, thus confirming the quantitative conversion of the starting materials into lipase capped Ag NPs**.** The chemical identity of the nanoparticles was

further ascertained using a powerful technique, energy dispersive X-ray fluorescence (ED-XRF) over the Ag NPs solutions synthesized from 0.2, 0.6 and 1 mM $AgNO_3$ solutions capped with 100 µg/mL of lipase (Figure 6.1d). It can be seen from the figure that the characteristic Ag L_{α}, Ag $L_{\beta 1}$ and Ag $L_{\beta 2}$ peaks were observed at 2.98, 3.17 and 3.68 keV, respectively, which corroborates the chemical identity of silver. In addition, a gentle increase in the peak intensity with increasing the concentration of silver additionally corroborates the observation from UV-vis spectroscopy studies.

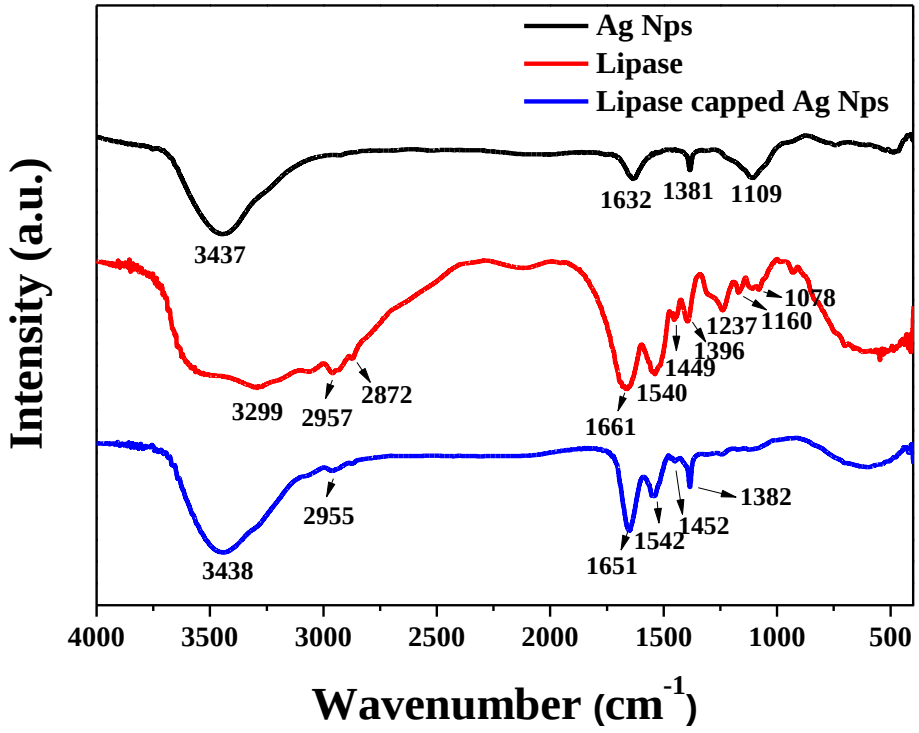

Figure 6.2: FT-IR spectra of pristine Ag NPs, pristine lipase and lipase-capped Ag NPs.

Fourier Transform infrared (FT-IR) analyses were performed in order to verify the capping of lipase over Ag NPs. Three samples such as pristine Ag NPs (reduced with $NaBH_4$ in the absence of any capping agent), pristine lipase and Ag NPs synthesized in the presence

of 100 μg/mL of lipase were subjected FT-IR analyses and the results are shown in Figure 6.2. The pristine Ag NPs showed a broad peak at 3437 cm^{-1} and a small peak at 1632 cm^{-1}, which could be attributed to the hydroxyl and other byproducts such as metaborate, respectively. The pristine lipase, on the other hand, exhibited characteristic stretching peaks in the range of 3200-3500 cm^{-1} corresponding to hydroxyl and amine groups, two stretching peaks at 2957 and 2872 cm^{-1} corresponding to –C-H functionality and a prominent amide stretching peak at 1661 cm^{-1} along with some additional stretching peaks in the finger print region. In case of Ag NPs synthesized in the presence of lipase, the IR spectrum was found to have a good resemblance to that of pristine lipase, which indicates the capping of lipase over the Ag NPs. The gentle shift in the amide stretching peak from 1661 cm^{-1} to 1651 cm^{-1} could be attributed to the electrostatic interaction between the surface of Ag NPs and the amide bonds of lipase that additionally confirms the efficient capping of lipase over Ag NPs. These results are in line with the literature [263].

The size of the as-synthesized lipase-capped Ag NPs were determined using dynamic light scattering (DLS) and the results are presented in Figure 6.3 The DLS analyses revealed that the hydrodynamic size of the nanoparticles possessed significant dependency on the concentration of the capping agent and a lesser dependency on the concentration of $AgNO_3$. When the concentration of $AgNO_3$ was fixed, the particle size was found to decrease with increasing amount of lipase capping agent (25-100 μg/mL), indicating the efficient capping by lipase and thus leading to smaller, stable and highly dispersible nanoparticles. When the concentration of $AgNO_3$ was increased from 0.2 to 0.6 mM, the particle size was observed to be increased at all concentrations of lipase used. It was noticed that the size of the Ag NPs obtained with 0.6 and 1.0 mM of $AgNO_3$

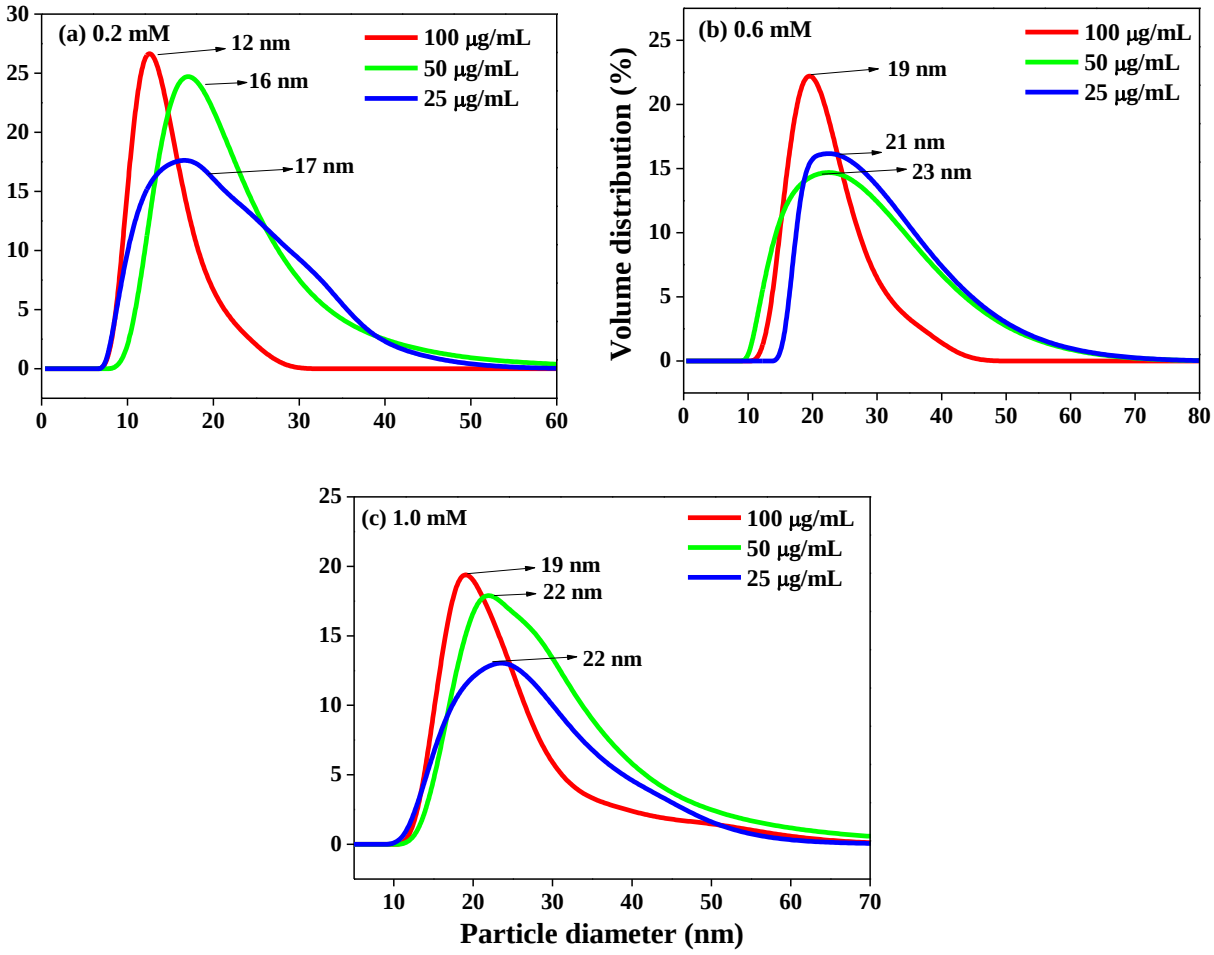

Figure 6.3: DLS size distribution of Ag NPs synthesized from (a) 0.2mM, (b) 0.6 mM and (c) 1.0 mM $AgNO_3$ solutions with varying amount of lipase.

was very comparable with equivalent amount of lipase capping agent. These results corroborate the observation from UV-Vis spectroscopy studies. Thus, the smallest AgNPs among the lot was observed to be obtained with 0.2 mM of $AgNO_3$ capped with 100 µg/mL of lipase. It was generally observed that at higher concentrations of $AgNO_3$ and lower concentrations of lipase the sizes as well as the polydispersity of the obtained Ag NPs were increased. HR-TEM imaging was performed over selected samples in order to understand the effect of lipase capping on the size and morphology of the Ag NPs and the results are presented in Figure 6.4(a-j). The Ag NPs synthesized from 0.2 mM $AgNO_3$ solution with varying lipase

concentration and the nanoparticles synthesized from varying initial $AgNO_3$ concentrations capped with a fixed lipase concentration of 100 µg/mL were chosen for the analysis.

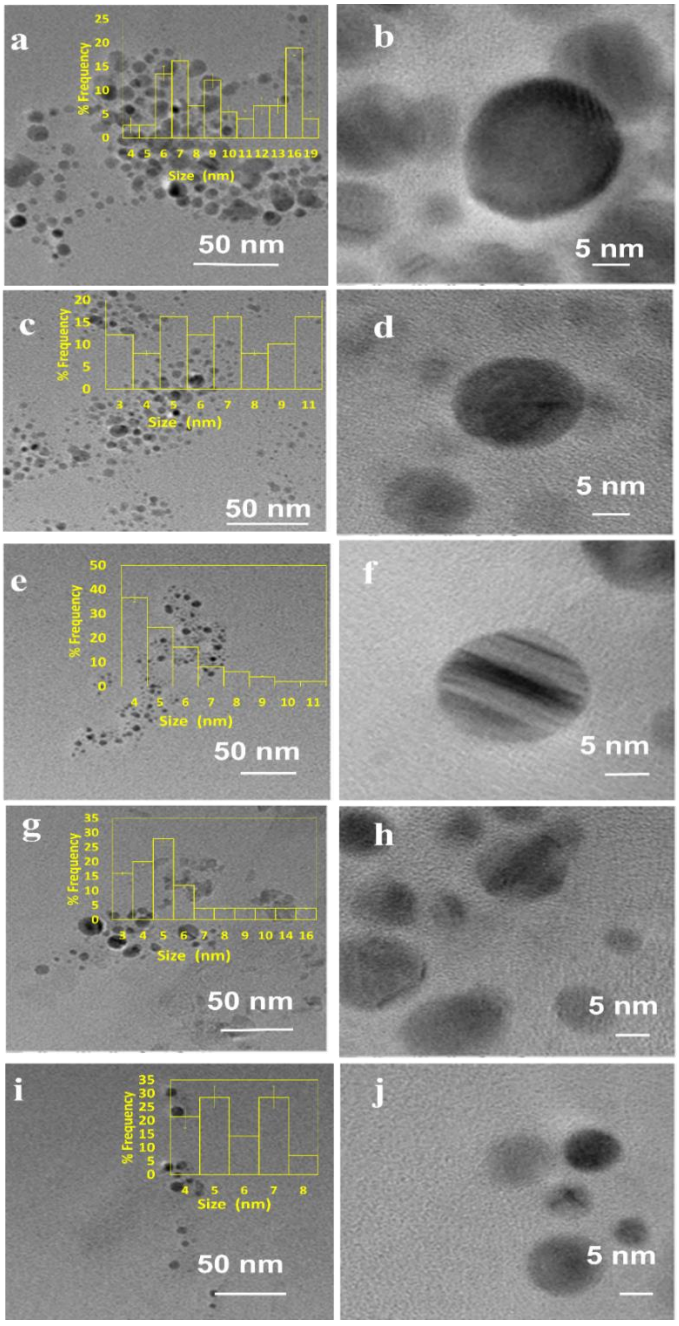

Figure 6.4 a-j: HR TEM images of a, b) 0.2 mM AgNPs capped with 25 µg of lipase c, d) with 50 µg of lipase e, f) 100 µg of lipase g, h) 0. 6mM AgNPs capped with 100 µg of lipase i,j) 1.0 mM AgNPs capped with 100µg of lipase

As can be seen from the figure, almost all the nanoparticles were found to be nearly spherical in shape. When the $AgNO_3$ concentration was fixed at 0.2 mM, with the increase in lipase capping amount from 25 to 100 μg/mL, the average size of the Ag NPs was found to decrease from ~10 to 5 nm. When the $AgNO_3$ concentration was varied from 0.2 to 1.0 mM with 100 μg/mL capping of lipase, the average size of the Ag NPs was found to be in the range of ~5 to 7 nm. Thus, the effect on the size was majorly influenced by the amount of lipase capping, not on the initial $AgNO_3$ concentration used in this study. These observations have clearly shown the efficient capping by lipase at 100 μg/mL and thus further corroborates the DLS analyses.

For studying the antimicrobial activity, the stock solutions of Ag NPs mentioned earlier were diluted to obtain the final working solutions having silver concentrations of 10, 15, 20, 25 and 30 nM (Figure 6.5). Several studies report that Ag NPs work effectively against gram negative bacteria. Therefore, we initially performed the antibacterial studies against the gram negative bacteria *Pseudomonas putida* (Figure 6.5(a-e)). Among the controls, pristine lipase and $NaBH_4$ did not exhibit any significant inhibition of the microbial growth, whereas the positive control ampicillin showed ~60% inhibition. With respect to the stock solution, the working solutions obtained from 0.2 mM solution of Ag NPs exhibited the best antimicrobial activity compared to the remaining two. This could be due to the smaller hydrodynamic size of the nanoparticles, as indicated by DLS analyses, that may have enhanced the permeation of the nanoparticles into the microbial cell. Among the working solutions, the antimicrobial activity of all the samples was found to be enhanced with increasing concentration from 10 to 30 nM, which could be attributed to the higher bioavailability of the nanoparticles. It is also observed that the antimicrobial activity was steadily increased with increasing lipase capping in most of

the cases. This could be due to the reason that the Ag NPs are highly stabilized and therefore well-dispersible, when capped with higher amount of lipase. With 20 nM and above concentrations, all the Ag NPs were found to exhibit ≥50% bactericidal effect. It is noteworthy that the most efficient MIC was achieved even at 10 nM concentration with Ag NPs obtained from 0.2 mM stock solutions.

We further explored the antibacterial effect of lipase capped Ag NPs against the gram positive bacteria *Staphylococcus aureus* (Figure 6.5(f-j). In this case also the lipase capped Ag NPs exhibited significant bactericidal effect, although the effect is slightly lesser than the *Pseudomonas putida*. The overall trend in terms of the effect of Ag NPs concentration and the lipase quantity towards bactericidal effect was found to be similar to the *Pseudomonas putida*. In this case too, the negative controls such as pristine lipase and $NaBH_4$ did not exhibit any significant bactericidal effect. However, the positive control ampicillin showed ~40% inhibition, which is significantly lesser than in the case of gram negative bacteria. It was found that at 30 nM concentration, all the Ag NPs sample solutions exhibited ≥50% antimicrobial activity. Again, the best MIC was achieved at concentration as low as 10 nM with Ag NPs capped with 100 μg/mL of lipase obtained from 0.2 mM stock solutions.

In order to explore the applicability of probiotic lipase capped AgNPs towards broad spectrum antimicrobial activity, we also studied the effect of the Ag NPs over a fungal strain *Aspergillus niger* (Figure 6.5(k-o)). It is known that the antibiotics are generally less effective against fungal strains and therefore the antifungal drug Amphotericin B was chosen as the positive control. This positive control exhibited ~50% of fungicidal activity, while the negative controls pristine lipase and $NaBH_4$ did not exhibit any significant fungicidal effect. As expected, the required amount of Ag NPs to exhibit significant antifungal effect was found to be higher than that against the bacteria.

The lowest concentration of Ag NPs required to exhibit the MIC was found to be at 15 nm concentration obtained from 0.2 mM stock solution of Ag NPs capped with 100 µg/mL of lipase. It is noteworthy that ~80% of fungicidal effect was exhibited by 30 nM solutions obtained from 0.2 mM stock solution of Ag NPs capped with 100 µg/mL of lipase.

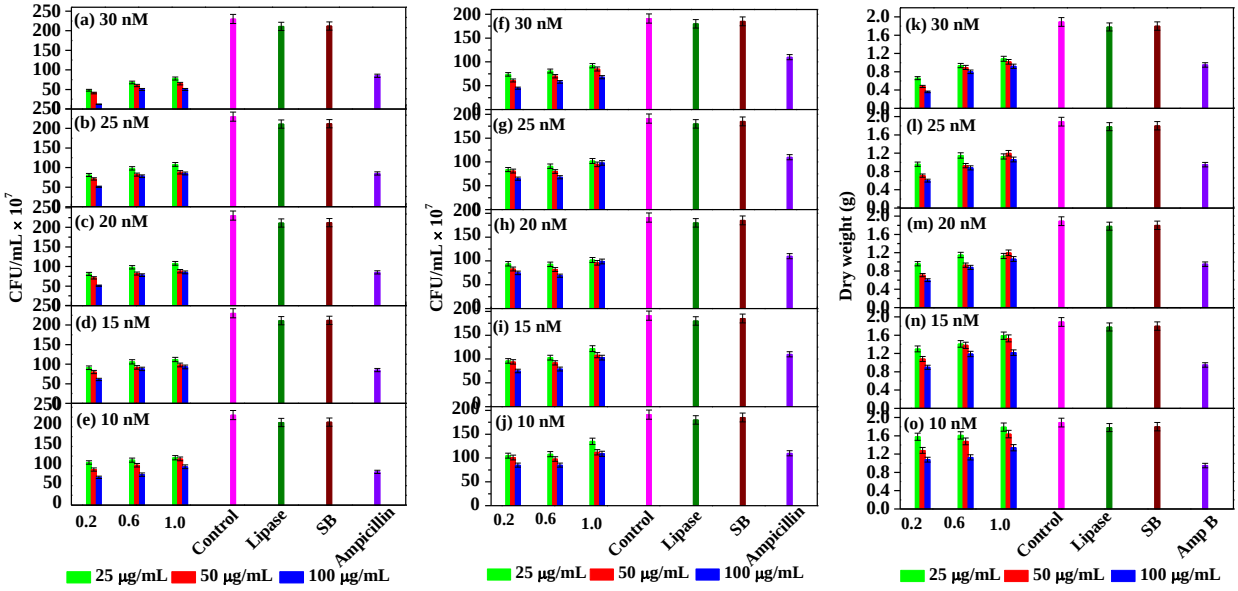

Figure 6.5: Antimicrobial activity of Ag NPs against (a-e) *P. putida*, (f-j) *S. aureus* and (k-o) *A. niger* tested against positive control of Ampicillin and Amphotericin B (in case of *A. niger*), untreated control and negative controls of Lipase treated culture and sodium borohydride (SB).

The above results clearly demonstrate the high antimicrobial efficacy of the Ag NPs stabilized with the probiotic lipase. Although it is not feasible to directly compare the MIC values reported in literature due to the differences in various influencing factors such as microbial strain, resistance level, initial microbial concentration, variation in the culture media, method adopted to calculate MIC, size/shape of Ag NPs and the stabilizing agent used, but our studies demonstrated the high antimicrobial activity in very low concentrations of Ag NPs much below the LC_{50} value of zebra fish [261, 264-266]. Table

1 shows the comparative MIC values of Ag NPs available in the literature against various microbial strains. As can be seen from the table, majority of the literature reported MIC values of Ag NPs against both bacteria and fungi in the μg/mL range. There are only a very few articles reporting the MIC values in the ng/mL range, which are closer to our current findings.

Although plethora of reports exist on the mechanistic studies of the antimicrobial activity of Ag NPs, the precise mechanisms are still unclear [267], but the following factors are considered to be the possible reasons for their activity. The Ag NPs are considered to bind initially to the cell membrane, gain entry into the cell and bind to the DNA, thereby believed to cause interference in the replication process [268,269]. Other theories state the binding of Ag NPs to the –SH group of the enzymes involved in electron transport chain (ETC) resulting in catalytic oxidation of the sulfhydryl group of the ETC proteins of the cell and further inactivating the proteins by forming disulfide linkages [270,271,272]. It is known that the surface of gram negative bacteria consist of lipopolysaccharides in its outer membrane, while the outer membrane of gram positive bacteria mainly consists of peptidoglycans. Since the proteins are amphoteric in nature that consist of both acidic and basic moieties, they can bind to a variety of surfaces to facilitate easy penetration of the Ag NPs through the outer membrane of the microbes and thereby initiate the cascade of chemical and biological changes, which could result in the enhanced antimicrobial activity. Thus, our results reveal that the capping of Ag NPs with probiotic lipase demonstrate high potential towards broad spectrum antimicrobial activity at very low concentrations in the range of ppb (ng/mL).

Table 7. Comparison of MIC values of Ag NPs against different microbes reported in the literature.

Microbes	Initial Concentration (CFU/mL)	MIC of Ag NPs	Reference
E. coli *Staphylococcus aureus* *Yeast*	10^7	0.56 ng/mL 5.6 ng/mL 2.24 ng/mL	264
B. subtilis, *S. aureus,* *P. aeruginosa* *E. coli*	N/A	6.8 µg/mL 5.1 µg/mL 1.70 µg/mL 3.4 µg/mL	273
Escherichia coli J53 *E. coli J53pMG101* *Salmonella sp.* *Staphylococcus aureus*	2.5 to 4 x 10^5	3.7 µg/mL 4.0 µg/mL 3.0 µg/mL 4.0 µg/mL	274
P. aeruginosa	10^6	2 µg/mL	275
E. coli *Staphylococcus aureus*	10^5	6.25 µg/mL 7.5 µg/mL	276
E. faecalis	10^8	5 mg/mL	277
E. coli MTCC 443, *E. coli MTCC 739,* *B. subtilis MTCC 441,* *S. aureus NCIM 5021*	10^5	20 µg/mL 60 µg/mL 30 µg/mL 70 µg/mL	278
Escherichia coli 116S, *J53* *E. coli J53pMG101*	10^8	0.216 ng/mL 8.64 ng/mL	279
Escherichia coli	5.0×10^6	5 µg/mL	280
BCG *Escherichia coli*	10^5	5 µg/mL 10 µg/mL	281
Escherichia coli, *Acinetobacter baumanii* *Pseudomonas aeruginosa* *Bacillus subtilis* *Mycobacterium smegmatis* *Mycobacterium bovis* *Staphylococcus aureus*	10^5	0.5 µg/mL 0.4 µg/mL 0.4 µg/mL 1.7 µg/mL 0.5 µg/mL 1.1 µg/mL 0.7 µg/mL	282
E. coli	10^8	1.35 ng/mL	283
S. enterica	10^5	9-14 µg/mL	284
E. coli, *S. aureus,* *Bacillus anthracis,* *Candida albicans.*	10^5	1.7 µg/mL 1.9 µg/mL 3.0 µg/mL 19 µg/mL	285
S.aureus, *P. aeruginosa,* *S. enterica,*	10^5	4.7 µg/mL 2.3 µg/mL 2.3 µg/mL	286

E. coli		1.2 μg/mL	
E. Coli *S. typhimurium*	10^5	4.0 μg/mL 6.0 μg/mL	287
Bacillus cereus *Bacillus subtilis* *Staphylococcus aureus* *Micrococcus luteus* *Enterobacter cloacae* *Serratia marcescens* *Shigella dysentery*	10^8	60 μg/mL 58 μg/mL 59 μg/mL 60 μg/mL 49 μg/mL 50 μg/mL 48 μg/mL	288
E. coli MTCC 443, *B. subtilis MTCC 441* *E. coli MTCC 739* *S. aureus NCIM 5021*	10^5	20 μg/mL 60 μg/mL 30 μg/mL 70 μg/mL	289
E. coli *S. aureus*	10^5	16.9 μg/mL 8.45 μg/mL	290
P. putida *S. aureus* *A. niger*	10^5	1.08 ng/mL 1.08 ng/mL 1.62 ng/mL	This work

6.4 Conclusion:

Probiotic lipase from *Lactobacillus plantarum* was employed as a stabilizing agent for Ag NPs synthesized through $NaBH_4$ reduction method. The concentrations of lipase and $AgNO_3$ were systematically varied from 25-100 μg/mL and 0.2-1.0 mM, respectively. While FT-IR studies revealed the successful capping of lipase over Ag NPs, UV-vis spectroscopic studies indicated the formation of smaller size nanoparticles with increased lipase concentration. The DLS and HR-TEM analyses revealed that the Ag NPs obtained from 0.2 mM $AgNO_3$ solution with 100 μg/mL of lipase capping were the smallest in size. Among all the combinations, the 100 μg/mL lipase capped Ag NPs synthesized from 0.2 mM $AgNO_3$ solution exhibited the best antimicrobial property against both gram positive (*S. aureus*) and gram negative (*P. putida*) bacteria at a MIC of 10 nM. In case of *A. niger*, the MIC exhibited by the same composition was found to be 15 nM. Thus, the combination of ultra-small size Ag NPs and lipase capping resulted in synergistic and efficient antimicrobial activity at concentrations much lower than the LC_{50} values of zebrafish. Furthermore, the efficient MIC values against the representative

bacteria and fungus reveals the high potential of the lipase capped Ag NPs as broad spectrum antimicrobial agents.

CHAPTER 7

BIODIESEL SYNTHESIS FROM WASTE COOKING OIL EMPLOYING FREE, IMMOBILIZED LIPASE FROM PROBIOTIC *LACTOBACILLUS SPS.*

7.1 Introduction:

The probiotic lipase from *L. plantarum, L. brevis* was further exploited for biodiesel production. Biodiesel is a mixture of alkyl esters made from renewable biological sources like vegetable oil mainly olive oil, cottonseed oil, jatropha oil, rapeseed oil, soyabean oil, sunflower oil, palm oil, corn oil, peanut oil and canola oil [292-295]. Biodiesel consumption has raised significantly over the decades as the fossil fuels reserves will be exhausting in a century at the current usage rate, apart from that, the gases emitted upon fossil fuel combustion are an environmental concern [296]. Biodiesel is a carbon neutral fuel as the carbon present in the exhaust was originally fixed from the atmosphere. These multiple factors contributed the regulatory agencies to encourage the use of biodiesel blends with fossil fuel [297]. The direct usage of vegetable oils as biodiesel is possible by blending it with conventional diesel fuels in a suitable ratio and these ester blends are stable for short term usages [298]. This blending process is simple which involves mixing alone and hence the equipment cost is low. But direct usage of these triglyceric esters (oils) is unsatisfactory and impractical for long term usages in the available diesel engines due to high viscosity, acid contamination and free fatty acid formation resulting in gum formation by oxidation and polymerization and carbon deposition [299]. Hence vegetables oils are processed so as to acquire properties (viscosity and volatility) similar to that of fossil fuels and the processed fuel can be directly used in the diesel engines available. To overcome, the problem associated with direct use of oil, lipase based transesterification is the best option [300]. Compared with chemical methods using alkaline or acid catalysts, utilization of lipase as a catalyst for biodiesel production has great potential because no complex operations are needed both for the recovery of glycerol and in the elimination of catalyst and salt [301]. In recent reports, several researchers have optimized the biodiesel production by altering reaction

conditions in many ways including (i) the effect of enzyme catalysts, heterogeneous catalysts [302-306]; (ii) the effect of operating parameters [307, 308] and acidic catalysts [309, 310]. The critical issues for biodiesel production are the high cost of raw material required and limited availability of vegetable oil feedstock which in turn will increase the manufacturing costs [310]. To minimize the production costs, waste cooking oils were used, subsequently, the total manufacturing cost of biodiesel significantly reduced. In addition to the production costs, the quality obtained by using waste cooking oils was at par with fresh vegetable oils [311]. Increase in food consumption lead to increase in usage and disposal of cooking oil [312]. This waste cooking oil can be converted to fuel that reduces the harmful disposal of these waste oils into drains thus decreasing environmental impact [313]. The reaction conditions required for biodiesel production are inconsistent, chiefly depends on the properties of waste cooking oil used. There is a need to optimize universally the reaction conditions of biodiesel production, resulting in consistent quality yields so that engine performances become superior with reduced emissions. The main problem associated with enzyme catalysis is the stability and recovery of enzyme from the reaction mixture for re-use. It can be overcome by immobilizing the enzyme, this enables the recovery of enzyme, better stability, thus better activity during reaction. The present study is focused on employing free and immobilized lipase isolated from probiotic source *Lactobacillus plantarum, Lactobacillus brevis* for biodiesel synthesis using waste cooking olive oil and to optimize the key process variables of transesterification.

7.2 Materials and Methods

7.2.1 Materials:

Lipase isolated from *Lactobacillus plantarum, Lactobacillus brevis* as described previously [170]. Used Olive oil, fresh olive was obtained from local restaurants and

purified with filters to eliminate food remains. Methyl oleate, methyl palmitate, methanol, hexane, sodium alginate were purchased from Sigma. All other chemicals were obtained commercially and were of analytical reagent grade.

7.2.2 Methods:

7.2.2.1 Preparation of immobilized enzyme using sodium alginate:

Sodium alginate gel was prepared by suspending 3 g of sodium alginate in 100 ml distilled water [314], stirred for 5 min and incubated for 30 min. To this suspension 0.5 ml of lipase enzyme was added and mixed thoroughly. Beads of uniform size were formed by dripping the solution in freshly prepared 250 ml of chilled 0.2 M calcium chloride. Beads were left in calcium chloride for 3-4 hrs and then resuspended in Tris-HCl buffer (pH 8.2). The beads were washed several times with the buffer to remove unbound enzyme.

7.2.2.3 Transesterification of waste cooking oil:

The enzymatic transesterification was carried out using free and sodium alginate encapsulated lipase enzyme as catalyst. Transesterification reaction to produce biodiesel was investigated by using waste cooking olive oil, methanol as reactants, free lipase and encapsulated lipase beads dissolved in hexane as catalyst. Transesterification was carried out in a reaction flask with temperature control and rpm controlled mechanical stirrer. The waste cooking oil was preheated until the desired temperature was reached. After that, a mixture of methanol and hexane with lipase as a catalyst was added to the oil and the transesterification reaction was done [315]. The influence of various reaction parameters such as molar ratio of oil to methanol, amount of lipase catalyst to methanol, reaction temperature and mixing intensity on the amount of biodiesel yields were investigated. All the parameters were optimized to produce maximum yield (Table 9). The reaction was stopped after 2h and then any excess methanol is evaporated by heating

the sample to 65 °C for 30 min. The obtained biodiesel was kept at 4 °C overnight to form two different layers, upper ester layer and the bottom glycerol layer. Then biodiesel is removed using a pipette. The biodiesel samples obtained were later subjected to analysis by Gas Chromatography (Shimadzu, Kyoto, Japan) to determine the quality, weight of the methyl esters was determined to obtain the quantity of yield. The properties of biodiesel such as viscosity, and density were determined to understand the quality of biodiesel obtained according to the ASTM D 6751(American Society for Testing and Materials) standard test methods.

7.3. Results:

7.3.1 Effect of molar ratio of oil to methanol:

In order to investigate **t**he effect of oil to methanol molar ratios on biodiesel yields, different molar ratios of fresh and used oil to methanol analysed were 1:1, 1:2, 1:3, 1:4, 1:5, 1:6, other parameters such as lipase catalyst concentration, reaction temperature 30 °C and agitation intensity of 120 rpm were kept constant (Table 8). It is evident (From Figure 7.1) that biodiesel yields alter with change in the oil to methanol ratios. The highest biodiesel yields (both the cases of fresh and used) obtained were for the oil to methanol molar ratio of 1:6 and the biodiesel yields gradually reduce from the 1:6 to 1:1 [316].

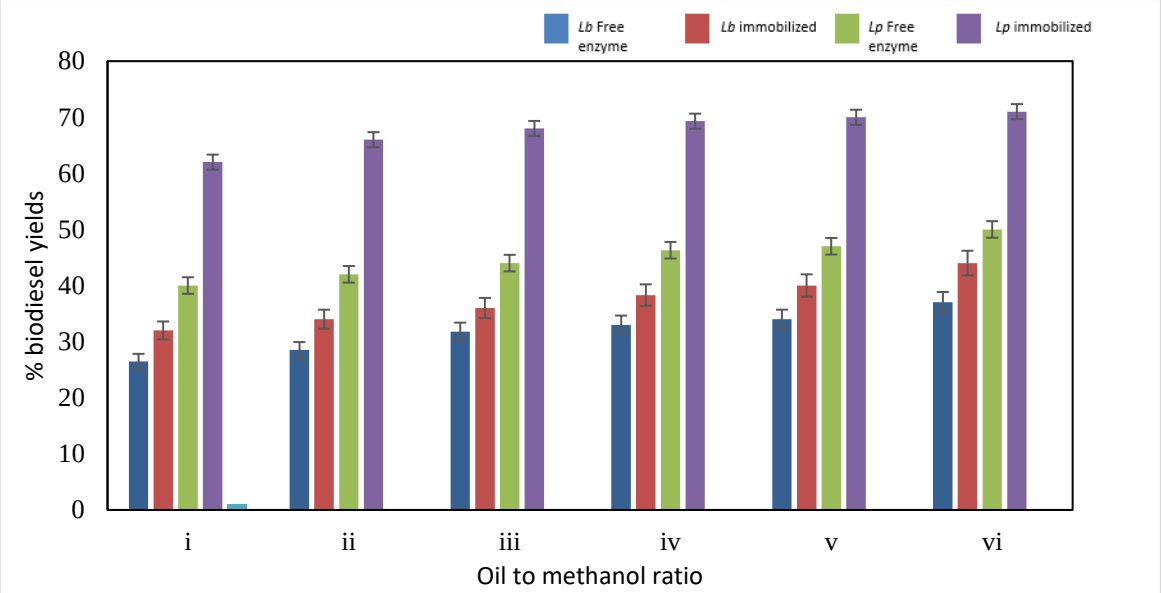

i=1:1, ii=1:2, iii=1:3, iv=1:4, v=1:5, vi=1:6 oil to methanol molar ratios, Temperature 30 ^{o}C, Mixing Intensity 120 rpm, Enzyme 2.5% *Lb: L. brevis, Lp: L. plantarum*

Figure 7.1a: Effect of molar ratio of alcohol to oil on transesterification of fresh olive oil by free and immobilized lipase

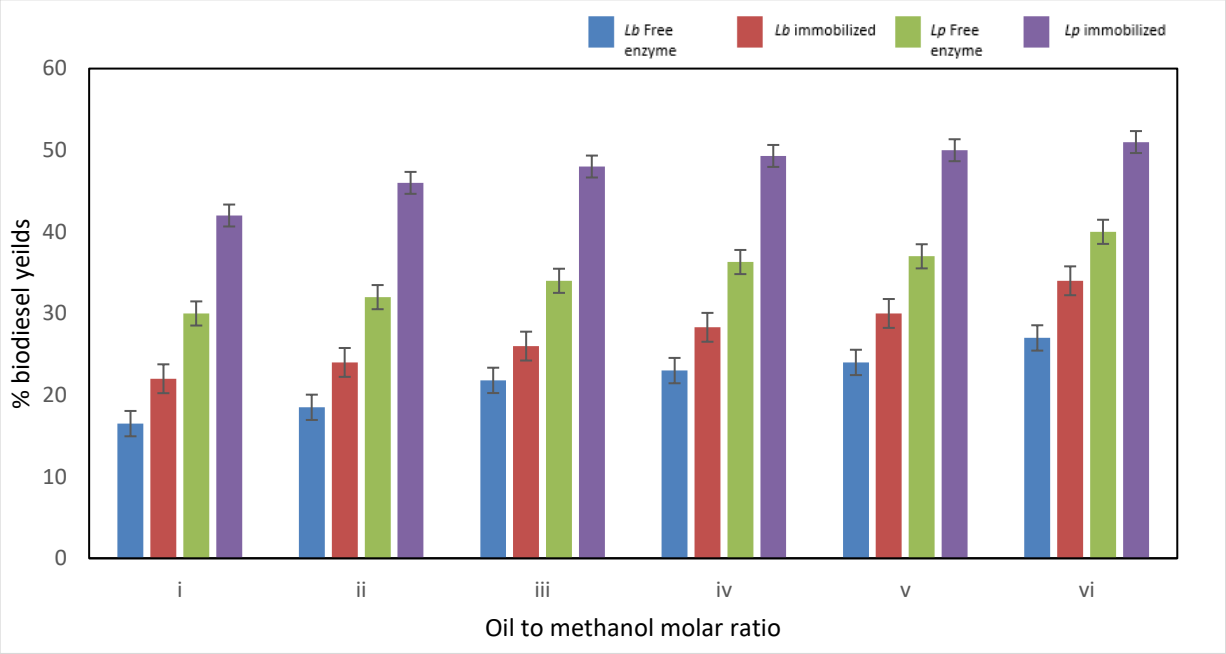

i=1:1, ii=1:2, iii=1:3, iv=1:4, v=1:5, vi=1:6 oil to methanol molar ratios, Temperature 30 ^{o}C, Mixing Intensity 120 rpm, Enzyme 2.5% *Lb: L. brevis, Lp: L. plantarum*

Figure 7.1b: Effect of molar ratio of alcohol to oil on transesterification of waste olive oil by free and immobilized lipase

Table 8: Parameters used for biodiesel production.

Variable Parameters	Parameters kept constant for free enzyme	Parameters kept constant for immobilized enzyme
Methanol to Oil Ratio 1:1 1:2 1:3 1:4 1:5 1:6	Amounts of Lipase: 2.5% (wt/v) Reaction Time: 2 h Mixing Intensity: 140 rpm Reaction Temperature:37 °C	Amounts of Lipase: 2.5% (wt/v) Reaction Time: 2 h Mixing Intensity: 140 rpm Reaction Temperature:37 °C
Lipase catalyst varied from 2.5, 3.0, 4.0, 5.0 % (wt/v)	Oil to Methanol Ratio: 1:6 Reaction Time: 2 h Mixing Intensity: 140 rpm Reaction Temperature:37 °C	Oil to Methanol Ratio: 1:6 Reaction Time: 2 h Mixing Intensity: 140 rpm Reaction Temperature:37 °C
Mixing Intensity: 120 rpm 140 rpm 160 rpm	Oil to Methanol Ratio: 1:6 Reaction Temperature:37 °C Amounts of Lipase: 2.5% (wt/v) Reaction Time: 2 h	Oil to Methanol Ratio: 1:6 Reaction Temperature:37 °C Amounts of Lipase: 2.5% (wt/v) Reaction Time: 2 h
Reaction Temperature 30 °C 37 °C 45 °C	Oil to Methanol Ratio: 1:6 Mixing Intensity: 140 rpm Amounts of Lipase: 2.5% (wt/v) Mixing Intensity: 140 rpm	Oil to Methanol Ratio: 1:6 Mixing Intensity: 140 rpm Amounts of Lipase: 2.5% (wt/v) Mixing Intensity: 140 rpm

7.3.2 Effect of the amount of catalyst used:

Lipase concentration is a crucial parameter for optimization of transesterification reaction, to make the biodiesel production more feasible, an optimum concentration should be found. The effect on biodiesel yields of the amount of catalyst (w/v) added to the reaction mixture were investigated. Figure 7.2 shows the biodiesel yields, the percentage weight of lipase catalyst to methanol. During the transesterification reaction, when the other parameters were kept constant, the catalyst loaded varied in the range of

2.5 to 5 % (w/v) of methanol (Table). There is a linear trend found with increase in the amount of catalyst (Figure 7.2). Smaller amount of lipase catalyst resulted in poorer biodiesel yields when compared to higher amount of lipase loading. This indicates that lipase at higher concentrations is more efficient catalyst. However further increase in lipase catalyst amount above 5% w/v didn't cause any significant rise in biodiesel yields [317].

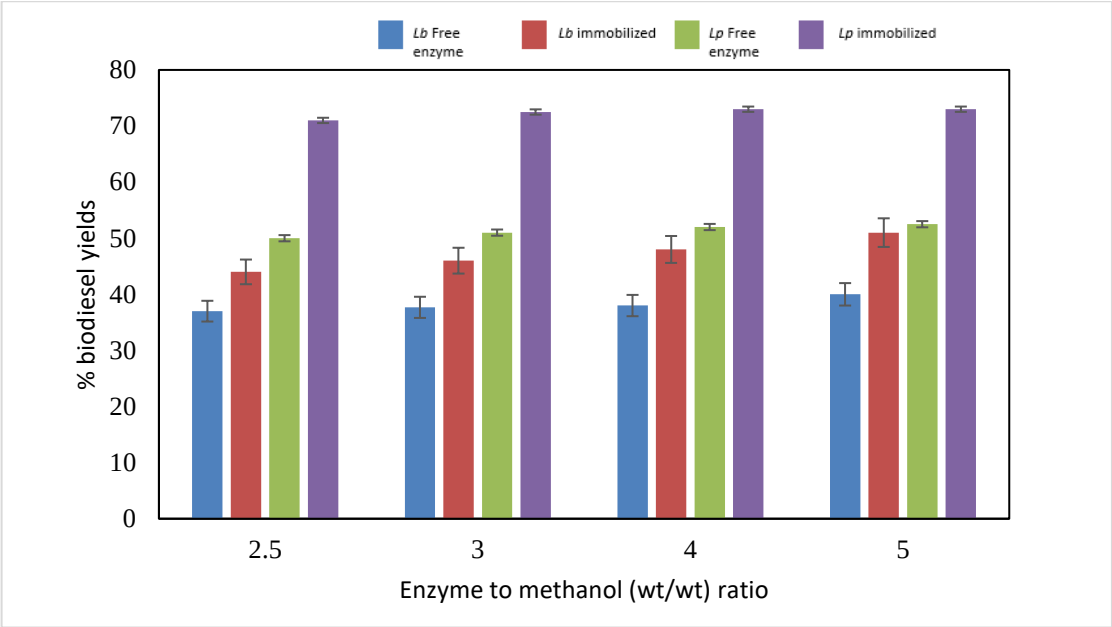

Figure 7.2a: Effect of enzyme to methanol ratio on transesterification of fresh olive oil by free and immobilized lipase

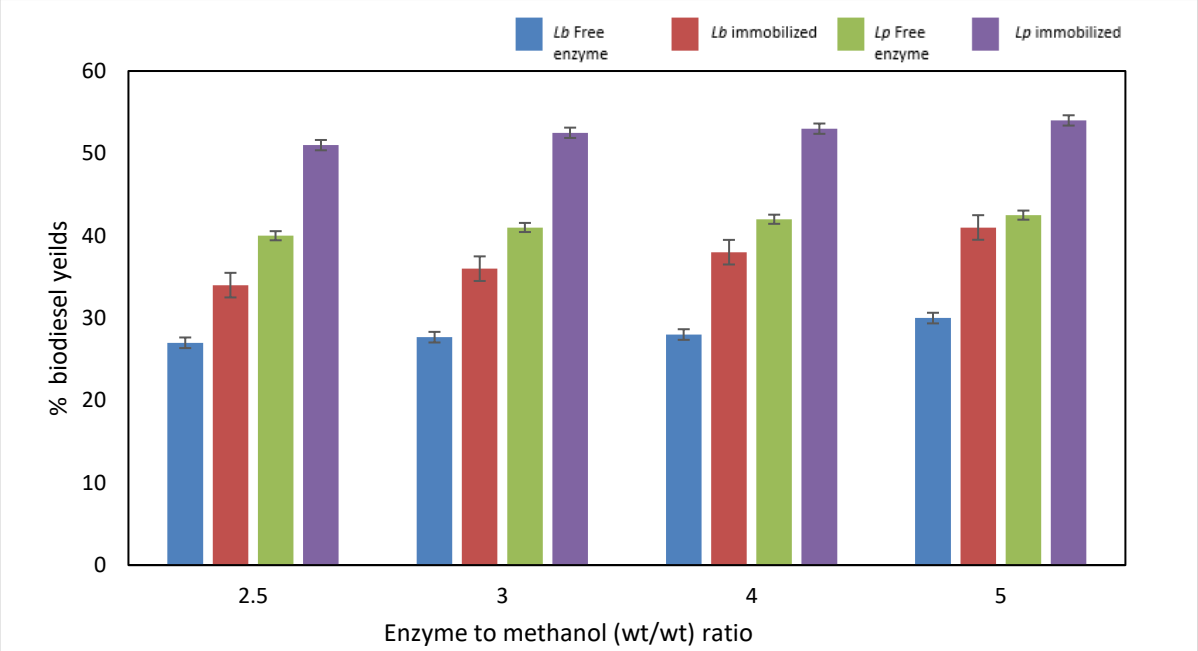

1:6 oil to methanol molar ratio, Temperature 30 ^{o}C, Mixing Intensity 120 rpm, *Lb: L. brevis, Lp: L. plantarum*

Figure 7.2b: Effect of enzyme to methanol ratio on transesterification of waste olive oil by free and immobilized lipase

7.3.3 Effect of reaction temperature:

To find the effect of reaction temperature on biodiesel yield the reaction temperatures were varied from 30, 37 to 45 ^{o}C keeping the other parameters constant (Table 8). It was found that the biodiesel production increased as the temperature increased from 30 to 45 ^{o}C with the highest yield obtained at 45 ^{o}C for the immobilized lipase when compared to the free lipase transesterification. The increase in temperature resulted in decrease in viscosity of oil and improved the catalytic site contact of the reactants and enhanced the enzymatic reaction, thus increasing the production [318, 319 and 320]. However, further increase in temperature resulted in decrease in production as a result of evaporation of methanol and thermal denaturation of the catalyst in case of free lipase, however sodium alginate encapsulated lipase showed a better biodiesel yield

when compared to free lipase. This could be attributed to the better stability of lipase resulting from immobilization. (Figure 7.3).

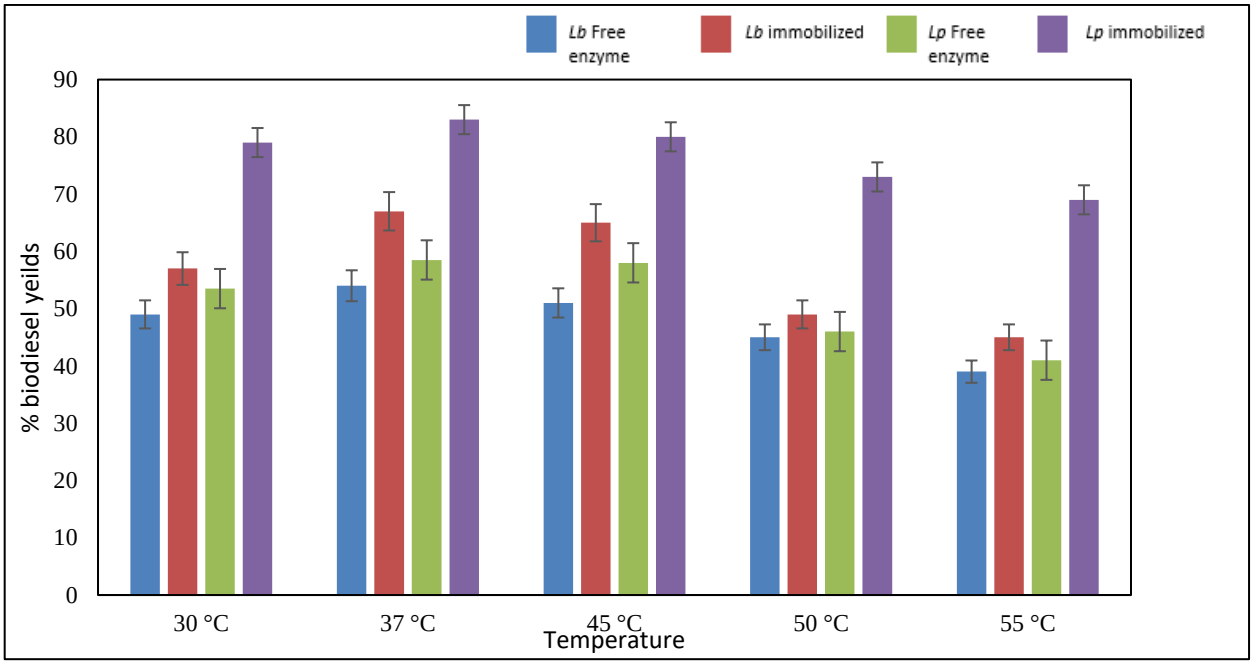

1:6 molar ratio, Mixing Intensity 160 rpm, Enzyme 5% *Lb: L. brevis, Lp: L. plantarum*

Figure 7.3a: Effect of temperature on transesterification of fresh olive oil by free and immobilized lipase

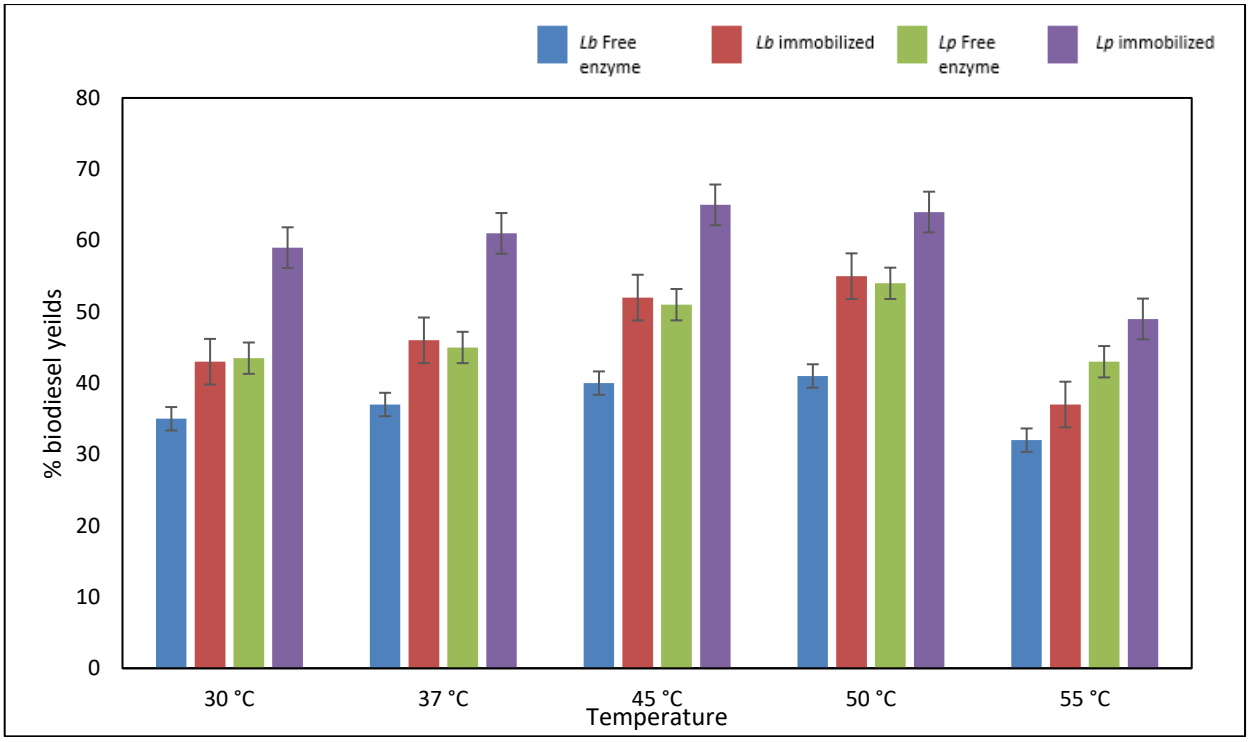

1:6 molar ratio, Mixing Intensity 160 rpm, Enzyme 5% *Lb: L. brevis, Lp: L. plantarum*

Figure 7.3b: Effect of temperature on transesterification of waste olive oil by free and immobilized lipase

7.3.4 Effect of mixing intensity of the reactants:

The mixing rate of reactants significantly effects the biodiesel yields, the reactants were mixed at two different agitation rates 120, 140, 160 rpm (refer to Table 8) while all other parameters were kept constant. The yields were higher at agitation rate of 160 rpm when compared to agitation rate of 120 rpm, 140 rpm. As the mixing intensity is increased, the reactants and the active site of catalyst have a better surface interaction, mass transfer, resulting in decreasing the activation energy of the reaction and diffusion from active site of the enzyme (Figure 7.4) [321].

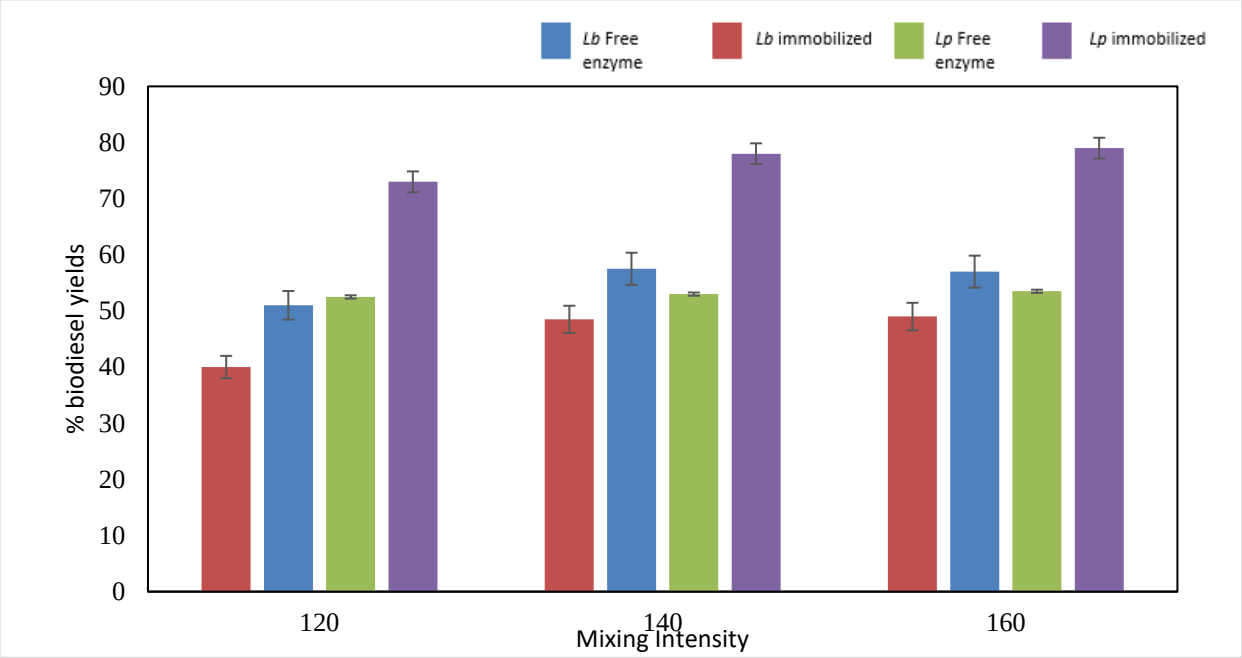

Figure 7.4a: Effect of mixing intensity on transesterification of fresh olive oil by free and immobilized lipase

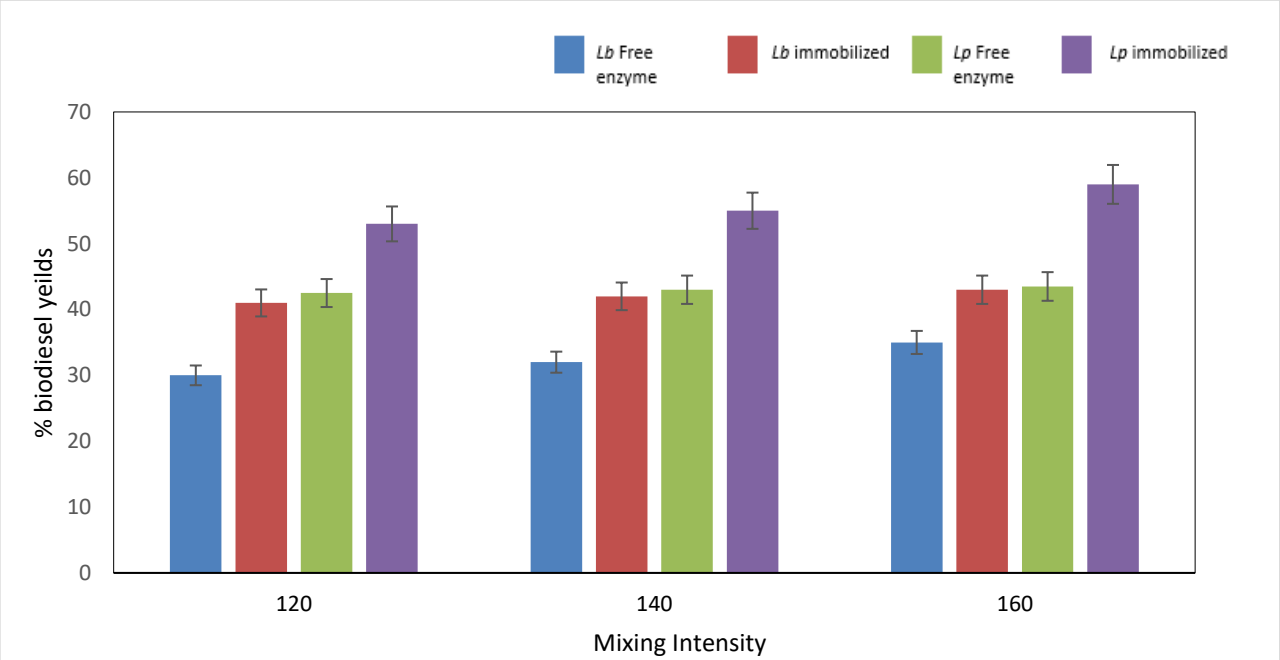

1:6 molar ratio, Temperature 30 ^{o}C, Enzyme 5%, *Lb: L. brevis, Lp: L. plantarum*

Figure 7.4b: Effect of mixing intensity on transesterification of waste olive oil by free and immobilized lipase

7.3.5 Viscosity and density properties of the biodiesel obtained:

One of the main objective of the transesterification reaction to produce biodiesel is to reduce the viscous nature of olive oil and to make it more suitable as fuel for engine. Table 9 & 10 shows the viscosity of biodiesel obtained from waste olive oil varying several reaction parameters employing lipase from *L. plantarum*. The biodiesel viscosity obtained was in the range of ASTM D 6751 standards when observed at 40 ^{o}C [24]. The lowest viscosity was found for oil to methanol molar ratios of 1:1, 1:2 and 1:3 after 2 hrs of incubation. Another important property of biodiesel is density. The density of the biodiesel at 15 °C obtained from waste cooking oil was in the range of 860-874 kg/m^3 varying different parameters. The standard density of the biodiesel as per report ranges between 860-874 kg m^{-3} which is as per EN 14214 published by the European Committee for Standardization of biodiesel. [322]

Table 9: Viscosity and density of biodiesel produced from waste cooking oil employing free lipase from *L plantarum*.

Sample (Amounts of Lipase: 2.5% (wt/v), Reaction Time: 2 h Mixing Intensity: 140 rpm)	**Density 15 °C (EN-14214, 860-874 kg m^{-3})**	**Viscosity at 40 °C (ASTM D6751 1.9-6.0 mm^2/s)**
1:1	861	4.8
1:2	873	4.9
1:3	865	3.9
1:4	878	4.1
1:5	869	6.12
1:6	871	6.39

Table 10: Viscosity, density properties of biodiesel produced from waste cooking oil employing immobilized lipase from *L plantarum*.

Sample (Amounts of Lipase: 2.5% (wt/v), Reaction Time: 2 h Mixing Intensity: 140 rpm)	**Density 15 °C (EN-14214, 860-874 kg m^{-3})**	**Viscosity at 40 °C (ASTM D6751 1.9-6.0 mm^2/s)**
1:1	860	2.1
1:2	872	2.8
1:3	866	4.1
1:4	870	5.7
1:5	864	5.9
1:6	880	5.2

7.4 Discussion:

The results obtained for all the biodiesel samples were significant and the maximum average value was 81%, 59 %, 67%, 54% using immobilized lipase, free lipase at 160 rpm, with 1:6 fresh olive oil to methanol ratios for immobilized lipases using *Lactobacillus plantarum, Lactobacillus brevis* respectively, whereas for used olive oil the maximum average value obtained was 65%, 58.5%, 55%, 41% using immobilized lipase, free lipase at 160 rpm, with 1:6 fresh olive oil to methanol ratios for immobilized lipases using *Lactobacillus plantarum, Lactobacillus brevis* respectively. This yields were expected as the substrate used for transesterification was used cooking olive oil. Waste cooking oil possess free fatty acids which will interfere with reactants and catalytic site of the enzyme. The free fatty acids of the waste cooking oil traps large amount of the esters formed and leads to biodiesel yield loss [323]. Based on the stoichiometric equation, 1 mole of triglyceride reacts with 3 moles of alcohol and gives rise to 3 moles of fatty acid ester and 1 mole of glycerine [324]. We optimized the oil to methanol ratios and found that oil to methanol ratio of 1:6 was optimum for the maximum yields of biodiesel and this was found to be in agreement with the other reported cases [325]. The

biodiesel yield gradually increased by increasing in the methanol to oil ratio from 1:1 to 1:6 [Figure 7.1]. Though the excess amount of methanol will result in forward reaction ensuring higher reaction rates minimizing diffusion of reactants from catalytic site but the excess oil to methanol ratio beyond 1:6 will bring down the catalytic efficiency of the free enzyme by partially inactivating it and leading to formation of glycerine layer, however in the case of encapsulated enzyme, the effect of glycerine is minimal and there is increase in biodiesel yields linearly when compared to free enzyme. The encapsulation prevents the reactants diffusion from the active to a certain extent [326] (can be seen in figure 7.1). To further understand the effect of enzyme (free and immobilized) dosage on the biodiesel yield, the enzyme concentration was varied from 2.5 to 5.0 % w/v with respect to methanol content of the reaction system. Figure 7.2 showed the gradual increase in biodiesel production with increase in concentration to a certain extent, thereafter biodiesel content stagnated without any further increase in lipase concentration in both cases of free and immobilized enzyme. It indicated that an excess of enzyme is not required when the reactants are a limitation and the lipase remained as a solid catalyst undissolved which became the rate limiting step [327]. Different reaction temperatures were also analysed to increase the biodiesel yield [Figure 7.3]. It was found that 45 ^{o}C was optimum for maximum biodiesel yield for free enzyme and for immobilized enzyme the reaction temperature was optimum till 50 ^{o} C,. If the temperature of reactants was increased further till 55 ^{o} C, it resulted in evaporation of methanol and decrease in viscosity of oil that resulted in reduced interaction of reactants with enzyme and also thermal denaturation of free enzyme, however the immobilized enzyme, the optimum temperature was from 45 to 50 ^{o}C, with further increase in temperature the same downwards trend of transesterification yields as in the case of free enzyme was observed. At lower temperatures the olive oil viscosity increases, which leads to difficulty in

agitation of the reaction mixture, resulting in poor catalysis and lower yield for both the free and immobilized enzyme. The effect of mixing intensity of reactants on biodiesel production was investigated using different stirring rates of 120 rpm, 140 rpm and 160 rpm, while other parameters were kept constant (Table 9). As indicated in Figure 7.4 a direct relation exists between agitation speed and biodiesel yield. The agitation speed of 140 rpm showed optimum biodiesel yield beyond which there is was no significant increase in the yield was observed for both the free and immobilized enzyme [328, 329]. Table 10 & 11 indicated the kinematic viscosity value range of the biodiesel obtained. The viscosity values obtained for biodiesel were far below the reactant olive oil, which can be adjusted by blending with petro-diesel. The viscosity values of biodiesel should range between 1.8-5.4 mm^2/s as per ASTM D 6751 standards and the values for the obtained biodiesel were 4.8-6.39 mm^2/s. The density values range between 860-874 kg m^{-3} as per the standards recommended by EN-14214. Density of biodiesel remained constant across various parameters used for transesterification reactions as can be seen in Table 8 & 9.

7.5 Conclusions:

The objective of this study was to optimize the reaction parameters required for the production of biodiesel exploiting used olive oil employing free and immobilized lipase isolated from *Lactobacillus plantarum* as a catalyst and to determine the viscosity, density properties of the obtained biodiesel. The results obtained for all the biodiesel samples were significant and the maximum average value was 81%, 59 %, 67%, 54% using immobilized lipase, free lipase at, 45 ^oC, 160 rpm, with 1:6 fresh olive oil to methanol ratios for immobilized lipases using *Lactobacillus plantarum*, *Lactobacillus brevis* respectively, whereas for used olive oil the maximum average value obtained was 65%, 58.5%, 55%, 41% using immobilized lipase, free lipase at, 45 ^oC, 160 rpm, with

1:6 fresh olive oil to methanol ratios for immobilized lipases using *Lactobacillus plantarum, Lactobacillus brevis* respectively. This yields were expected as the substrate used for transesterification was used cooking olive oil. Waste cooking oil possess free fatty acids which will interfere with reactants and catalytic site of the enzyme. The free fatty acids of the waste cooking oil traps large amount of the esters formed and leads to biodiesel yield loss. The immobilization allows easy recovery of the enzyme from the reactant mixture and its reuse for subsequent cycles of transesterification reactions. The biodiesel thus obtained is of superior grade with respect to viscosity and density as per international standards But it is further recommended to investigate the diesel properties such ash content, sulphur content, brake fuel efficiency and other parameters with prolonged operation conditions for better yield.

CHAPTER 8

SUMMARY AND CONCLUSIONS

8.1 Summary

Lipases possess good substrate specificity that exceeds any other known enzyme. This property of the lipase has led to its huge application potential that are literally boundless.

Hence, the present study aims to characterize the lipase isolated from probiotic species *Lactobacillus brevis* and *Lactobacillus plantarum* for different applications. Based on the gaps available from the existing literature, the objectives of the present work can thus be broadly divided into the following aspects:

- *Lactobacillus sps*. lipase mediated poly (ε-caprolactone) degradation by pouring method.
- *Lactobacillus sps*. lipase mediated embedded PCL degradation.
- To understand the effect of probiotic *Lactobacillus plantarum* derived lipase in synthesizing and capping, catalytically active gold nanoparticles.
- In vitro hemocompatability evaluation of gold nanoparticles capped with *Lactobacillus plantarum* derived lipase.
- Evaluation of antimicrobial Activity of Lactobacillus sps. lipase capped silver-nanoparticle
- *Lactobacillus sps*. lipase mediated conversion of waste cooking oil to Biodiesel.

8.2 Conclusions:

In conclusion the following observations are made about the results obtained in this study.

i) *Lactobacillus sps.* Lipase mediated poly (ε-caprolactone) degradation by pouring method

The enzymatic degradation of the PCL film was performed by three different lipases obtained from *Lactobacillus brevis, Lactobacillus plantarum* and their co-culture. The enzymatic degradation was found to be significantly influenced by the concentration, time of exposure and the type of the enzyme. Among the three enzymes screened in this study, the lipase from *Lactobacillus plantarum* was found to possess the maximum PCL degradation activity at a nominal loading of 5 mg/mL. Thermogravimetric analysis results showed that with increasing exposure time of enzyme, the thermal stability of the PCL films decreased due to the polymer degradation. The DTA analyses revealed that the enzyme preferentially degraded the amorphous regions at first, as evidenced by the increase in percentage crystallinity of the polymer. While the SEM analysis has shown the cracked polymer surface after enzymatic degradation, the FTIR analyses confirmed the hydrolytic action of the enzymes on the ester bonds of the PCL films. The study reveals the potential of genetically engineered probiotic *Lactobacillus* class of lipases towards polymer degradation with enhanced efficiency.

ii) Embedded enzymatic degradation of the PCL film

The embedded enzymatic degradation of the PCL film was performed by four different concentrations of lipase obtained from *Lactobacillus plantarum*. The enzymatic degradation was found to be significantly influenced by the concentration, time of exposure. Among the four enzyme embedding screened in this study, the 8% embedding lipase from *Lactobacillus plantarum* was found to possess the maximum PCL degradation activity. Thermogravimetric analysis results showed that with increasing exposure time of enzyme, the thermal stability of the PCL films decreased due to the

polymer degradation. The DTA analyses revealed that the enzyme preferentially degraded the amorphous regions at first, as evidenced by the increase in percentage crystallinity of the polymer.

iii) Towards single crystalline, highly monodisperse and catalytically active gold nanoparticles capped with probiotic *Lactobacillus plantarum* derived lipase

GNPs capped with varying amounts of lipase as stabilizing agent have been successfully synthesized, as confirmed by UV-visible and IR spectroscopy studies. Significantly, the tight size control and near-monodispersity of the lipase-capped GNPs have been revealed by HR-TEM and DLS analyses. In particular, with 0.5 and 1 mg/mL of lipase, the synthesized GNPs exhibited modest polycrystallinity, whereas with higher amount of lipase as in 2 to 10 mg/mL, the obtained GNPs were nearly monocrystalline. The reduction of 4-NP to 4-AP studies revealed that the GNPs capped with 0.5 mg/mL of lipase exhibited the highest catalytic efficacy and the lowest catalytic efficacy was exhibited by 10 mg/mL lipase-capped GNPs. The clear trend showed that the catalytic sites of bare gold regions were more exposed and therefore available for efficient catalysis with 0.5 mg/mL lipase-capped GNPs. Indirectly, the results prove efficient capping of GNPs with lipase at higher loading, which minimizes the accessibility of bare gold regions for catalysis. The amine-functionalities of lipase enabled the anchoring of GNPs over Fe_3O_4 nanoparticles via glutaraldehyde conjugation. Such a strategy was found to be useful in recovering and reusing the GNPs. Further studies are directed to employ mild reducing conditions in order to preserve the activity of lipase anchored over GNPs, which would be useful for various applications including catalysis, sensing, drug delivery etc.,

iv) In vitro hemocompatability evaluation of gold nanoparticles capped with *Lactobacillus plantarum* derived lipase.

The present study revealed that lipase capped GNPs synthesized using $NaBH_4$ approach are stable and hemocompatible. It was found that there was two-fold increase in fibrinogen levels after the exposure to nanoparticles, which is consistent with other studies. However, the increase in fibrinogen levels was found not to have any adverse effect on the blood coagulation parameters such as clotting time, clot strength and clot formation kinetics. Furthermore, our study also revealed that there was no significant change in the platelet aggregation behavior. The hemocompatability is attributed to the very small size regime (sub-10 nm) and the eco-friendly behavior of the probiotic lipase-capped GNPs. Future studies can be directed to determine the coagulation effects of GNPs as a function of size as well as at elevated concentrations.

v) Evaluation of Antimicrobial Activity of *Lactobacillus sps.* Lipase Capped Silver-Nanoparticle

Probiotic lipase from *Lactobacillus plantarum* was employed as a stabilizing agent for Ag NPs synthesized through $NaBH_4$ reduction method. The concentrations of lipase and $AgNO_3$ were systematically varied from 25-100 μg/mL and 0.2-1.0 mM, respectively. While FT-IR studies revealed the successful capping of lipase over Ag NPs, UV-vis spectroscopic studies indicated the formation of smaller size nanoparticles with increased lipase concentration. The DLS and HR-TEM analyses revealed that the Ag NPs obtained from 0.2 mM $AgNO_3$ solution with 100 μg/mL of lipase capping were the smallest in size. Among all the combinations, the 100 μg/mL lipase capped Ag NPs synthesized from 0.2 mM $AgNO_3$ solution exhibited the best antimicrobial property against both gram positive (*S. aureus*) and gram negative (*P. putida*) bacteria at a MIC of 10 nM. In case of *A. niger*, the MIC exhibited by the same composition was found to be 15 nM. Thus, the combination of ultra-small size Ag NPs and lipase capping resulted in synergistic and efficient antimicrobial activity at concentrations much lower than the

LC_{50} values of zebrafish. Furthermore, the efficient MIC values against the representative bacteria and fungus reveals the high potential of the lipase capped Ag NPs as broad spectrum antimicrobial agents.

vi) Biodiesel Synthesis from Waste Cooking Oil Employing Lipase Isolated from Probiotic *Lactobacillus plantarum*

The results obtained for all the biodiesel samples were significant and the maximum average value was 83.5% at 1:6 oil to methanol ratio for fresh olive oil used. This yields were expected as the substrate used for transesterification was fresh cooking olive oil. While with the waste cooking oil the highest yields obtained were 67%, as it possess free fatty acids which will interfere with reactants and catalytic site of the enzyme, thus decrease in yeild. The biodiesel production was found to be effective at 45 ^{o}C, 160 rpm, 2 hours of reaction time and 6:1 methanol to olive oil molar ratio using 5 wt% of lipase enzyme (based on the volume of methanol). This is an efficient process as it uses waste cooking oil with a significant amount of waste oil conversion, amount of catalyst loaded and reaction time. The transesterification reactions yielded biodiesel of superior grade with respect to viscosity and density properties.

8.3 Major contributions of the work

The following are the major contributions from the above work.

- There are several reports on degradation of PCL employing lipase obtained from single cultures of bacteria and fungi. But to the best of our knowledge this was the first report of eco-friendly approach degradation of PCL employing probiotic lipase obtained from single and co-cultures of *Lactobacillus plantarum* and *Lactobacillus brevis.*
- We have also been successful to show degradation of PCL by enzyme embedded approach which will pave the way for developing polymer with different

degradation times and properties that can be tailored according to the surgical applications.

- This is one of the first few approaches for green synthesis of catalytically active, single crystalline lipase capped gold nanoparticles, with superior catalytic activity.
- Synthesis of biocompatible gold nanoparticles were studied for their influence on blood clotting and found to be very hemocompatible.
- We successfully synthesized lipase capped silver nanoparticles and evaluated its antimicrobial activity and this provided us an estimate of the antimicrobial efficacy and efficiency of the silver nanoparticles in comparison to the antibiotics.
- We successfully optimized the reaction parameters for synthesis of biodiesel exploiting waste cooking olive oil employing free and immobilized lipase isolated from *Lactobacillus plantarum, L. brevis* as a catalyst.

8.4 Future scope of work

The future possibilities arising from the results of the present work are as given below:

- This study helps us to make polymer biomaterials with different half degradation times suiting different applications.
- Lipase capping of nanoparticles can be exploited for drug delivery approaches since the gold nanoparticles were synthesized in a greener, eco-friendly approach and the materials were proven to be hemocompatible.
- Other immobilization techniques can further be studied to check the functional efficacy of the lipase for synthesizing industrially important compounds.
- Synthesis of lipase mediated long chain fatty acid esters, amides and polymer degradation can further be studied.

REFERENCES

[1] Glick D, King C G. *The Protein Nature of Enzymes. An Investigation of Pancreatic Lipase*. ***J Am Chem Soc***. 1933, **55**, 2445-2449.

[2] Arnon D I. *Copper enzymes in isolated chloroplasts. Polyphenoloxidase in beta vulgaris*. ***Plant Physiol***. 1949, **24**, 1-15.

[3] Fischer E, Passmore F. *Uber kohlenstoffreichere Zuckerarten aus d. Mannose*. ***Berichte der Dtsch Chem Gesellschaft.*** 1890, **23**, 2226-2239.

[4] Fischer E. *Einfluss der Configuration auf dieWirkung der Enzyme*. ***Berichte der Dtsch Chem Gesellschaft.*** 1894**, 27**, 2985-2993.

[5] Schmid A, Hollmann F, Park JB, B¨uhler B. *The use of enzymes in the chemical industry in Europe*. ***Curr Opin Biotechnol.*** 2002, **13**, 359-366.

[6] Mateo C, Palomo JM, Fernandez-Lorente G, Guisan JM, Fernandez-Lafuente R. *Improvement of enzyme activity, stability and selectivity via immobilization techniques*. ***Enzyme Microb Technol.*** 2007, **40**, 1451-1463.

[7] Martina M, Hutmacher DW. *Biodegradable polymers applied in tissue engineering research A review*. ***Polym Int.*** 2007, **56**, 145-157.

[8] Kirk O, Borchert TV, Fuglsang CC. *Industrial enzyme applications*. ***Curr Opin Biotechnol.*** 2002, **13**, 345-351.

[9] Sheldon RA. *Enzyme Immobilization The Quest for Optimum Performance*. ***Adv Synth Catal***. 2007, **349,** 1289-1307.

[10] Sharma, S, Kanwar, S.S. *Purification of a novel thermophilic lipase from Bacillus licheniformis MTCC-10498*. ***ISCA J. Biological Sci.*** 2012, **1,** 43-48.

[11] Mohammad Badrud Duza, Mastan. S A. *Microbial enzymes and their applications – a review*. ***Indo Am J Pharm Res.*** 2013, **38**, 6208-6219.

[12] Ogawa J. *Microbial enzymes New industrial applications from traditional screening methods*. ***Trends Biotechnol.*** 1999, **171**, 13-20.

[13] Koch K, Vandenberg R, Nieuwland P, Wijtmans R, Wubbolts M, Schoemaker H, Rutjes F, and Vanhest J. *Enzymatic synthesis of optically pure cyanohydrins in microchannels using a crude cell lysate*. ***Chem Eng J*** 2008, **135**, 89-92.

[14] Teo E-L, Chuah G-K, Huguet ARJ, Jaenicke S, Pande G, Zhu Y. *Process intensification with biocatalysts Dynamic kinetic resolution and fluorous phase switch with continuous extraction*. ***Catal Today*** 2004, **974**, 263-270.

[15] Mu˜noz Solano D, Hoyos P, Hern´aiz MJ, Alc´antara AR, S´anchez-Montero JM. *Industrial biotransformations in the synthesis of building blocks leading to enantiopure drugs*. ***Bioresource Technol*** 2012, **115** 196-207.

[16] Premraj R, Mukesh Doble, *Biodegradation of polymers*. ***Indian J. Biotechnol*** 2005, **42**, 186-193.

[17] Wilhelm T, Wittstock G. *Generation of Periodic Enzyme Patterns by Soft Lithography and Activity Imaging by Scanning Electrochemical Microscopy*. ***Langmuir*** 2002, **18**, 9485-9493.

[18] Crookes-Goodson WJ, Slocik JM, Naik RR. *Bio-directed synthesis and assembly of nanomaterials.* ***Chem Soc Rev*** 2008, **37**, 2403-2412.

[19] Bhattacharya D, Gupta RK. *Nanotechnology and Potential of Microorganisms.* ***Crit Rev Biotechnol*** 2005, **254,** 199-204.

[20] Dur´an M, Silveira CP, Dur´an N. *Catalytic role of traditional enzymes for biosynthesis of biogenic metallic nanoparticles A mini-review*. ***IET Nanobiotechnol*** 2015, **9**, 314-323.

[21] Mukherjee P, Ahmad A, Mandal D, Senapati S, Sainkar SR, Khan MI, Parishcha R, Ajaykumar PV, Alam M,Kumar R, and Sastry M. *Fungus-Mediated Synthesis of Silver Nanoparticles and Their Immobilization in the Mycelial Matrix A Novel Biological Approach to Nanoparticle Synthesis*. ***Nano Lett.*** 2001, **110**, 515-519.

[22] Andexer JN, Langermann JV, Kragl U, Pohl M. *How to overcome limitations in biotechnological processes – examples from hydroxynitrile lyase applications*. ***Trends Biotechnol*** 2009, **27**, 599-607.

[23] Barros, M., Fleuri, L. F., Macedo, G. A. *Seed lipases sources, applications and properties – a review*. ***Braz. J. Chem. Eng***. 2010, **27**, 15-29.

[24] Gurung, N., Ray, S., Bose, S., Rai, V. *A broader view Microbial enzymes and their relevance in industries, medicine, and beyond.* ***BioMed. Res. Int***. 2013, **20**, 1-18.

[25] Gokbulut, A.A., Arslanoglu, A. *Purification and biochemical characterization of an extracellular lipase from psychrotolerant Pseudomonas fluorescens KE38.* ***Turk. J. Biol***. 2013, **37**, 538-546.

[26] Sugihara, A., Ueshima, M., Shimada, Y., Tsunasawa, S., Tominaga, Y. *Purification and characterization of a nevol thermostable lipase from Pseudomonas cepacia.* ***J. Bio. Chem.*** 1992, **112,** 598-603.

[27] Kukeraja, V., Bera, M.B. *Lipase from Pseudomonas aeruginosa MTCC 2488 Partial purification, characterization and calcium dependent thermostability*. ***Indian. J. Biotechnol***. 2005, **4**, 222-226.

[28] Kumar, A., Parihar, S.S., Batra, N. *Enrichment, isolation and optimization of lipase-producing Staphylococcus sp. from oil mill waste oil cake*. ***J. Exp. Sci.*** 2012, **3**, 26-30.

[29] Khan, I.M., Dill, C.W., Chandan, R.C., Shahani, K.M. *Bovine pancreatic lipase. II. Stability and effect of activators and inhibitors.* ***Biochem. Biophys. Acta***. 1967, **132**, 68-77.

[30] Ananthi, S., Immanuel, G., Palavesam, A. *Optimization of lipase production by Bacillus cereus strain MSU as through submerged fermentation* ***Plant. Sci. Feed***. 2013, **3**, 31-39.

[31] Sangeetha, R., Geetha, A., Arulpandi, I. *Concomitant production of protease and lipase by Bacillus licheniformis VSG1 production, purification and characterization*. ***Braz. J. Microbiol.*** 2010, **41**, 179–185.

[32] Ephraim, D.P., Bhat. S.G., Muthuswamy, C. *Lipase production by immobilized Bacillus smithii BTMS11 and its potential application in waste water treatment.* ***Int. J. Curr. Biotechnol.*** 2014, **2**, 1-8.

[33] Sekhon, A., Dahiya, N., Tewari, R.P., Hoondal, G.S. *Production of extracellular lipase by Bacillus megaterium AKG-1 in submerged fermentation.* ***Indian. J. Biotechnol.*** 2006, **5**, 179-183.

[34] Sabat, S., Krishna Murthy, V., Pavithra, M., Mayur, P., Chandavar, A. *Production and characterisation of extracellular lipase from Bacillus stearothermophilus MTCC 37 under different fermentation conditions.* ***Int. J. Eng. Res. Appl***. 2012, **2**, 1775-1781.

[35] Kumar, R., Sharma, A., Kumar, A., Singh, D. *Lipase from Bacillus pumilus RK31 Production, purification and some properties.* ***World. Appl. Sci. J***. 2012, **16**, 940-948.

[36] Liu, Z.., Zheng, X.B., Zhang, S.P., Zheng, Y.G. *Cloning, expression and characterization of a lipase gene from the Candida antarctica ZJB09193 and its application in biosynthesis of vitamin A esters*. ***Microbiol. Res***. 2012, **167**, 452–460.

[37] Pereira, E.B., DeCastro, H.F., DeMoraes, F.F., Zanin, G.M. *Esterification activity and stability of Candida rugosa lipase immobilized into chitosin.* ***Appl. Biochem. Biotechnol.*** 2001, **91**, 739-752.

[38] Chander, H., Chebbi, N.B., Ranganathan, B. *Lipase activity of Lactobacillus brevis*. ***Arch***. ***Mikrobiol***. 1973, **92**, 171-174.

[39] Uppada, S.R., Gupta, A.K., Dutta, J. R. *Statistical optimization of culture parameters for lipase production from Lactococcus lactis and its application in detergent industry*. ***Int J. ChemTech. Res***. 2012, **4,** 1509-1517.

[40] Lopes, Mde, F., Cunha, A.E., Clemente, J.J., Corrondo, M.J., Crespo, M.T. *Influence of environmental factors on lipase production by Lactobacillus plantarum.* ***Appl. Microbiol. Biotechnol.*** 1995, **51,** 249-254.

[41] Ramakrishnan, V., Goveas, L.C., Narayan, B., Halami, P.M. *Comparison of lipase production by Enterococcus faecium MTCC 5695 and Pediococcus acidilactici MTCC 11361 using fish waste as substrate Optimization of culture conditions by Response surface methodology.* ***ISRN Biotechnol***. 2013, **20**, 1-9.

[42] Dieve, F.J., Costas, M., Longo, M.A. *Production of a thermostable extracellular lipase by Kluyveromyces marxianus.* ***Biotechno. Lett***. 2003, **25**, 1403-1406.

[43] El-Sawah, M.M., Sherief, A.A., Bayoumy, S.M. *Enzymatic properties of lipase and characteristics production by Lactobacillus delbrueckii subsp. bulgaricus.* ***Antonie van Lueewenhoek***, 1996, **67**, 357-362.

[44] Rashmi, B. S., Gayathri, D. *Partial purification, characterization of Lactobacillus sp. G5 lipase and their probiotic potential.* ***Int. Food. Res. J.*** 2014, **21**, 1737-1743.

[45] Falony, G., Armas, J.C., Mendoza, J.C.D., Hernández, J.L.M. *Production of extracellular lipase from Aspergillus niger by solid-state fermentation*. ***Food Technol. Biotechnol***. 2006, **44**, 235–240.

[46] Basheer, S.M., Chellapan, S., Beena, P.S., Sukumaran, R.K., Elyas, K.K., Chandrasekharan, M. *Lipase from marine Aspergillus awamori BTMFW032 production, partial purification and application in oil effluent treatment.* ***N. Biotechnol.*** 2011, **28**, 627-638.

[47] Rajan, A., Soban Kumar, D.R., Nair, A.J. *Isolation of a novel alkaline lipase producing fungus Aspergillus fumigatus MTCC 9657 from aged and crude rice bran oil and quantification by HPTLC.* ***Int. J. Biol.Chem.*** 2011, **5,** 116-126.

[48] Maia, M.M., Heasley, A., Morais, M.M., Melo, E.H., Morais, M.E., Ledingham, W.M., Filho, J.L. *Effect of culture conditions on lipase production by Fusarium solani in batch fermentation.* ***Bioresour. Technol***. 2001, **76**, 23-27.

[49] Okafor, J.I., Gugnani, H.C. *Lipase activity of Basidiobolus and Conidiobolus species*. ***Mycoses.*** 1990, **33**, 81-85.

[50] Li, N., Zong, M.H., Ma, D. *Unexpected reversal of the regioselectivity in Thermomyces lanuginosus lipase-catalyzed acylation of floxuridine*. ***Biotechnol. Lett.*** 2009, **31**, 1241-1244.

[51] Hodgson J. *The changing bulk biocatalyst market.* ***Biotechnology.*** 1994, **128**, 789-90.

[52] Demain AL, Vaishnav P. *Production of recombinant proteins by microbes and higher organisms.* ***Biotechnol Adv*** 2009, **273,** 297-306.

[53] Jayati Ray Dutta P, Dutta K, Banerjee R. *Optimization of culture parameters for extra-cellular protease production from a newly isolated Pseudomonas sp. using response surface and artificial neural network models.* ***Process Biochem*** 2004, **391**, 2193-2198.

[54] Jayati Ray Dutta P, Dutta K, Banerjee R. *Modeling and optimization of protease production by a newly isolated Pseudomonas sp. using a genetic algorithm.* ***Process Biochem*** 2005, **402**, 2879-2884.

[55] Ulery BD, Nair LS, Laurencin CT. *Biomedical Applications of Biodegradable Polymers.* ***J Polym Sci B Polym Phys*** 2011, **4912**, 832-864.

[56] Santerre JP, Labow RS, Duguay DG, Erfle D, Adams GA. *Biodegradation evaluation of polyether and polyester urethanes with oxidative and hydrolytic enzymes.* ***J Biomed Mater Res*** 1994, **2810**, 1187-1199.

[57] Labow RS, Meek E, Santerre JP. *The biodegradation of polyurethanes by the esterolytic activity of serine proteases and oxidative enzyme systems*. ***J Biomater Sci Polym*** 1999, **107**, 699-713.

[58] Cho K, Lee J, Xing P. *Enzymatic degradation of blends of polye-caprolactone and polystyrene-co-acrylonitrile by Pseudomonas lipase*. ***J Appl Polym Sci*** 2002, **834**, 868-879.

[59] Zhou W, Wang X, Yang B, Xu Y, Zhang W, Zhang Y, Ji J. *Synthesis, physical properties and enzymatic degradation of bio-based poly butylene adipate-co-butylene furan dicarboxylate copolyesters*. ***Polym Degrad Stab*** 2013, **9811**, 2177-2183.

[60] Zhang J, Kasuya K, Hikima T, Takata M, Takemura A, Iwata T. *Mechanical properties, structure analysis and enzymatic degradation of uniaxially cold-drawn films of poly[R-3-hydroxybutyrate-co-4-hydroxybutyrate]*. ***Polym Degrad Stab*** 2011, **9612**, 2130-2138.

[61] Abe H, DoiY, Aoki H, Akehata T. *Solid-State Structures and Enzymatic Degradabilities for Melt-Crystallized Films of Copolymers of R-3-Hydroxybutyric Acid with Different Hydroxyalkanoic Acids*. ***Macromolecules*** 1998, **31**, 61791-61797.

[62] Iwata T, Doi Y. *Crystal structure and biodegradation of aliphatic polyester crystals*. ***Macromol Chem Phys*** 1999, **20011**, 2429-2442.

[63] Iwata T, Aoyagi Y, Tanaka T, Fujita M, Takeuchi A, Suzuki Y, Uesugi K. *Microbeam X-ray Diffraction and Enzymatic Degradation of Poly[R-3-hydroxybutyrate] Fibers with Two Kinds of Molecular Conformations.* ***Macromolecules*** 2006, **3917**, 5789-5795.

[64] Numata K, Abe H, Iwata T. *Biodegradability of Poly hydroxyalkanoate Materials.* ***Materials*** 2009, **23**, 1104-1126.

[65] Darwis D, Mitomo H, Enjoji T, Yoshii F, Makuuchi K. *Enzymatic degradation of radiation crosslinked poly α–caprolactone.* ***Polym Degrad Stab*** 1998, **62,** 2259-2265.

[66] Mahalik JP, Madras G. *Effect of the Alkyl Group Substituents on the Thermal and Enzymatic Degradation of Polyn-alkyl acrylates.* ***Ind Eng Chem Res*** 2005, **4412**, 4171-77.

[67] Williams DF. *Enzymic hydrolysis of polylactic acid.* ***Arch Eng Med*** 1988, **101**, 5-7.

[68] Lee SH, Song WS. *Enzymatic hydrolysis of polylactic acid fiber*. ***Appl Biochem Biotechnol*** 2011, **16,** 4189-4102.

[69] Fukuzaki H, Yoshida M, Asano M, Kumakura M. *Synthesis of co poly d,l-lactic acid with relatively low molecular weight and in vitro degradation.* ***Eur Polym J*** 1989, **2510**, 1019-1026.

[70] Mainil-Varlet P, Curtis R, Gogolewski S. *Effect of in vivo and in vitro degradation on molecular and mechanical properties of various low-molecular-weight poly lactides*. ***J Biomed Mater Res*** 1997, **363**, 360-380.

[71] Reeve MS, McCarthy SP, Downey MJ, Gross RA. *Polylactide stereochemistry Effect on enzymic degradability*. ***Macromolecules*** 1994, **273**, 825-831.

[72] MacDonald RT, McCarthy SP, Gross RA. *Enzymatic Degradability of Poly lactide Effects of Chain Stereochemistry and Material Crystallinity*. ***Macromolecules*** 1996, **2923**, 7356-7361.

[73] Li S, McCarthy S. *Influence of Crystallinity and Stereochemistry on the Enzymatic Degradation of Poly lactides*. ***Macromolecules*** 1999, **3213**, 4454-4456.

[74] Kikkawa Y, Abe H, Iwata T, Inoue Y, Doi Y. *Crystallization, Stability, and Enzymatic Degradation of Polyl -lactide Thin Film.* ***Biomacromolecules*** 2002, **32**, 350-356.

[75] Azevedo HS, Gama FM, Reis RL. *In vitro assessment of the enzymatic degradation of several starch based biomaterials*. ***Biomacromolecules*** 2003, **46**, 1703-1712.

[76] Duarte, Ana Rita C., Jo˜ao F. Mano, and Rui L. Reis. *Enzymatic degradation of 3D scaffolds of starch-poly-ε-caprolactone prepared by supercritical fluid technology.* ***Pol. Deg. Sta.*** 2010, **95**, 102110-102117.

[77] Ganesh M, Dave RN, L'Amoreaux W, Gross RA. *Embedded Enzymatic Biomaterial Degradation*. ***Macromolecules*** 2009, **4218**, 6836-6899.

[78] Ganesh M, Gross RA. *Embedded enzymatic biomaterial degradation Flow conditions & relative humidity.* ***Polymer*** 2012, **5316**, 3454-3461.

[79] Sharma, R., Chisti, Y., Banerjee, U.C. *Production, purification, characterization, and applications of lipases.* ***Biotech. Adv.*** 2001, **19**, 627 – 662.

[80] Chauhan, M., Garlapati, V.K. *Modelling and optimization studies on a novel lipase production by Staphylococcus arlette through submerged fermentation.* ***Appl. Biochem. Biotechnol.*** 2013, **171**, 1429-1443.

[81] Cherif, S., Mnif, S., Hadrich, F., Abdelkafi, S., Sayadi, S. *A newly high alkaline lipase an ideal choice for application in detergent formulations.* ***Lipids. Health. Dis***. 2010, **10**, 221.

[82] Weerasooriya, M.K.B., Kumarasinghe, A.A.N. *Isolation of alkaline lipase from rubber seed — Partial purification, characterization and its potential applications as a detergent additive.* ***Indian. J Chem. Techn.*** 2012, **19**, 244-249.

[83] Dalmaso, G.Z.L., Ferreira, D., Vermelho, A.B. *Marine Extremophiles A source of hydrolases for biotechnological applications.* ***Mar. Drugs*** 2015, **13**, 1925-1965.

[84] Caballeroa, V., Bautistaa, F.M., Campeloa, J.M., Lunaa, D., Marinas, J.M., Romeroa, A.A., Hidalgo, J.M., Luque, R., Macario, M., Giordano, G. *Sustainable*

preparation of a novel glycerol-free biofuel by using pig pancreatic lipase partial 1,3-regiospecific alcoholysis of sunflower oil. ***Process Biochem.*** 2009, **44**, 334-342.

[85] Korman, T.P., Sahachartsiri, B., Charbonneau, D.M., Huang, G.L., Beauregard, M., Bowie, J.U. *Dieselzymes development of a stable and methanol tolerant lipase for biodiesel production by directed evolution.* ***Biotechnol. Biofuels*** 2013, **6**, 70.

[86] Yoo, H.Y., Simkhada, J.R., Cho, S.S., Park, D.H., Kim, S.W., Seong, C.N., Yoo, J.C. *High-Level expression of pro-form lipase from Rhizopus oryzae in Pichia pastoris and Its Purification and Characterization.* ***Bioresour Technol.*** 2011, **102**, 6104-6111.

[87] Garlapati, V.K., Banerjee, R. *Solvent free synthesis of flavor esters through immobilized lipase mediated transesterification*. ***Enzyme Res.*** 2013, **2013**, 1-6.

[88] Selvam, K., Vishnupriya, B., Maanvizhi, M. *Enzymatic synthesis of fragrance ester by lipase from marine Actinomycetes for textile industry.* ***Int J Eng Adv Technol.*** 2013, **3**, 91-96.

[89] Padilha, G.S., de Barros M., Alegrea, R.M., Tambourgi, E.B. *Production of ethyl valerate from Burkholderia cepacia lipase immobilized in alginate.* ***Chem Eng Trans.*** 2013, **32**, 1063-1068.

[90] Macedo, G.A., Lozano, M.M.S., Pastore, G.M. *Enzymatic synthesis of short chain citronellyl esters by a new lipase from Rhizopus sp.* ***Electron. J Biotechn.*** 2003, **6**, 72-75.

[91] Kynclova, E., Hartig. A., Schalkhammer, T. *Oligonucleotide labeled lipase as a new sensitive hybridization probe and its use in bioassays and biosensors*. ***J Mol Recognit.*** 1995, **8**, 139–145.

[92] Imamura, S., Takahashi, M., Misaki, H., Matsuura, K. *Method and reagent containing lipases for enzymatic determination of triglycerides* **West Germany Patent**. 1989, **3**, 912, 226.

[93] Fukumoto, J., Iwai, M. Tenjisaka, Y. Studies on lipase. I. *Purification and crystallisation of lipase secreted by Aspergillus niger* ***J Gen Appl Microbiol.*** 1963, **9**, 353-361.

[94] Turki, S., Mrabet, G., Jabloun, Z., Destain, J., Thonart, P., Kallel, H. *A highly stable Yarrowia lipolytica lipase formulation for the treatment of pancreatic exocrine insufficiency*. ***Biotechnol Appl. Biochem.*** 2010, **57**, 139-149.

[95] Berrobi, C., Manoussos, G., Oreal, S.A. *Cosmetic, Pharmaceutical preparations containing lipase, hyalyuronidase and/or Thiomucase enzymes.* **West Germany Patent**, 1940, **1,** 847-856.

[96] Yang, F., Weber, T.W., Gainer, J.L., Carta, G. *Synthesis of lovastatin with immobilized Candida rugosa lipase in organic solvents Effects of reaction conditions on initial rates*. ***Biotechnol Bioeng.*** 1997, **56**, 671-680.

[97] Matsumae, H., Furui, M., Shibatani. T. *Lipase-catalyzed asymmetric hydrolysis of 3-phenylglycidic acid ester, the key intermediate in the synthesis of diltiazem hydrochloride*. ***J Ferment Bioeng.*** 1993, **75**, 93–98.

[98] Salis., Bhattacharyya, M.S., Monduzzi, M., Solinas, V. *Role of the support surface on the loading and the activity of Pseudomonas fluorescens lipase used for biodiesel synthesis.* ***J. Mol Catal B Enzym.*** 2009, **57**, 262–269.

[99] Iravani S, Korbekandi H, Mirmohammadi SV, Zolfaghari B. *Synthesis of silver nanoparticles Chemical, physical and biological methods.* ***Res Pharm Sci.*** 2014, **96**, 385-406.

[100] Ahmad A, Mukherjee P, Mandal D, Senapati S, Khan MI,Kumar R, Sastry M. *Enzyme mediated extracellular synthesis of CdS nanoparticles by the fungus, Fusarium oxysporum.* ***J. Am Chem Soc.*** 2002, **12441**, 12108-09.

[101] Anil Kumar S, Abyaneh MK, Gosavi SW, Kulkarni SK, Pasricha R, Ahmad A, Khan MI. *Nitrate reductase-mediated synthesis of silver nanoparticles from $AgNO_3$.* ***Biotechnol Lett.*** 2007, **293**, 439-45.

[102] Brayner R, Barberousse H, Hemadi M, Djedjat C,Y´epr´emian C, Coradin T, Livage J, Fi´evet F, and Cout´eA. *Cyanobacteria as Bioreactors for the Synthesis of Au, Ag, Pd, and Pt Nanoparticles via an Enzyme-Mediated Route*. ***J Nanosci Nanotechnol.*** 2007, **78**, 2696-708.

[103] Rai M, Yadav A, Gade A. *Silver nanoparticles as a new generation of antimicrobials.* ***Biotechnol Adv*** 2009, **271**, 76-83.

[104] Mishra A, Sardar M. *Alpha-Amylase Mediated Synthesis of Silver Nanoparticles.* ***Sci Adv Mater*** 2012, **41,** 143-46.

[105] Dur´an N, Marcato PD, Alves OL, Souzagihde, Esposito E. *Mechanistic aspects of biosynthesis of silver nanoparticles by several Fusarium oxysporum strains*. ***J Nanobiotechnology*** 2005, **31**, 1-7.

[106] Gaikwad S, *Green Synthesis of Silver Nanoparticles Using Aspergillus niger and Its Efficacy Against Human Pathogens*. ***Braz J Microbiol.*** 2014, **454**, 1654-1658.

[107] Kim JS, Kuk E, Yu KN, Kim J-H, Park SJ, Lee HJ, Kim SH, Park YK, Park YH, Hwang CY, Kim YK, Lee YS, Jeong DH, Cho MH. *Antimicrobial effects of silver nanoparticles*. ***Nanomedicine*** 2007, **31**, 95-101.

[108] Shahverdi AR, Minaeian S, Shahverdi HR, Jamalifar H, Nohi A-A. *Rapid synthesis of silver nanoparticles using culture supernatants of Enterobacteria A novel biological approach.* ***Process Biochem*** 2007, **425,** 919-923.

[109] Govender Y, Riddin TL, GerickeM, Whiteley CG. *On the enzymatic formation of platinum nanoparticles.* ***J Nanoparticle Res*** 2009, **121**, 261-271.

[110] Ghosh P, Han G, De M, Kim CK, Rotello VM. *Gold nanoparticles in delivery applications*. ***Adv Drug Deliv Rev*** 2008, **60**, 111307-111315.

[111] Narayanan KB, Sakthivel N. *Facile green synthesis of gold nanostructures by NADPH-dependent enzyme from the extract of Sclerotium rolfsii*. ***Colloids Surfaces A Physicochem Eng Asp*** 2011, **3801-3**, 156-161.

[112] Rangnekar A, Sarma TK, Singh AK, Deka J, Ramesh A, Chattopadhyay A. *Retention of enzymatic activity of alpha amylase in the reductive synthesis of gold nanoparticles*. ***Langmuir.*** 2007, **23**, 5700-5706.

[113] Ku SA, Abyaneh MK, Gosavi SW, Kulkarni SK, Ahmad A, Khan MI. *Sulfite reductase-mediated synthesis of gold nanoparticles capped with phytochelatin*. ***Biotechnol Appl Biochem*** 2007, **474**, 191-195.

[114] He S, Guo Z, Zhang Y, Zhang S, Wang J, Gu N. *Biosynthesis of gold nanoparticles using the bacteria Rhodopseudomonas capsulata. **Mater Lett*** 2007, **6118,** 3984-3987.

[115] Kisailus D, Choi JH, Weaver JC, Yang W, Morse DE. *Enzymatic Synthesis and Nanostructural Control of Gallium Oxide at Low Temperature*. ***Adv Mater*** 2005, **173**, 314-318

[116] Gupta R, Gupta N, Rathi P, *Bacterial lipases an overview of production, purification and biochemical properties.*, ***Appl. Microbiol. Biotechnol.*** 2004, **64**, 763–781.

[117] Reid G, Jass J, Sebulsky MT, McCormick JK, *Potential Uses of Probiotics in Clinical Practice*, ***Clin. Microbiol. Rev.*** 2003, **16**, 658–672.

[118] McKay LL, Baldwin KA, *Applications for biotechnology present and future improvements in lactic acid bacteria.*, ***FEMS Microbiol. Rev***. 1990, **7**, 3–14.

[119] Tokiwa Y, Calabia BP, Ugwu CU, S. Aiba, *Biodegradability of plastics*., ***Int. J. Mol. Sci.*** 2009, **10**, 3722–42.

[120] Hasan F, Shah AA, Hameed A, *Industrial applications of microbial lipases*, ***Enzyme Microb. Technol.*** 2006, **39,** 235–251.

[121] Banerjee A, Chatterjee K, Madras G, *Enzymatic degradation of polymers a brief review*, ***Mater. Sci. Technol.*** 2014, **30**, 567–573.

[122] Song JH, Murphy RJ, Narayan R, Davies GBH, *Biodegradable and compostable alternatives to conventional plastics.*, ***Philos. Trans. R. Soc. Lond. B. Biol. Sci***. 2009, **364**, 2127–39.

[123] Kweon H, Yoo MK, Park IK *et. al., A novel degradable polycaprolactone networks for tissue engineering*, ***Biomaterials.*** 2003, **24**, 801–808.

[124] Schneider T *et. al., Viability, Adhesion and Differentiated Phenotype of Articular Chondrocytes on Degradable Polymers and Electro-Spun Structures Thereof*, ***Macromol. Symp.*** 2011, **309**, 28–39.

[125] Kyrikou I, Briassoulis D, *Biodegradation of Agricultural Plastic Films A Critical Review*, ***J. Polym. Environ.*** 2007, **5**, 227–227.

[126] Nair LS, Laurencin CT, *Biodegradable polymers as biomaterials*, ***Prog. Polym. Sci.*** 2007, **32**, 762–798.

[127] Martins AM *et. al., The role of lipase and alpha-amylase in the degradation of starch/polyepsilon-caprolactone fiber meshes and the osteogenic differentiation of cultured marrow stromal cells.*, ***Tissue Eng. Part A.*** 2009, **15**, 295–305.

[128] Goldberg D, *A review of the biodegradability and utility of polyϵ-caprolactone*, ***J. Environ. Polym. Degrad.*** 1995, **15**, 61–67.

[129] Plackett DV *et. al., Characterization ofl-polylactide andl-polylactide–polycaprolactone co-polymer films for use in cheese-packaging applications*, ***Packag. Technol. Sci.*** 2006, **19,** 1–24.

[130] Miao Z M *et. al., Degradation and drug release property of star polyϵ-caprolactones with dendritic cores.*, ***J. Biomed. Mater. Res. B. Appl. Biomater***. 2007, **81**, 40–9.

[131] Mochizuki M, Hirami M, *Structural Effects on the Biodegradation of Aliphatic Polyesters*, **Polym. Adv. Technol**. 1997, **8**, 203–209.

[132] Shah AA *et. al., Degradation of polyε-caprolactone by a thermophilic bacterium Ralstonia sp. strain MRL-TL isolated from hot spring*, ***Int. Biodeterior. Biodegradation***. 2015, **98**, 35–42.

[133] Wischke C *et. al., A Blend of Polyε-caprolactone and Poly[ε-caprolactone-co-glycolide] with Remarkable Mechanical Features and Wide Applicability as Biomaterial*, ***Macromol. Symp.*** 309-310 2011, **309**, 59–67.

[134] Hoshino A, Isono Y, *Degradation of aliphatic polyester films by commercially*

available lipases with special reference to rapid and complete degradation of polyL-lactide film by lipase PL derived from Alcaligenes sp., ***Biodegradation.*** 2002, **13**, 141–7.

[135] Zeng J *et. al., Enzymatic degradation of polyL-lactide and polyepsilon-caprolactone electrospun fibers.*, ***Macromol. Biosci***. 2004, **4**, 1118–25.

[136] Pastorino L *et. al., Lipase-catalyzed degradation of polyε-caprolactone*, ***Enzyme Microb. Technol.*** 2004, **35**, 321–326.

[137] Benedict CV *et. al., Fungal degradation of polycaprolactones*, ***J. Appl. Polym. Sci.*** 1983, **28**, 327–334.

[138] Gan Z, Liang Q, Zhang J, Jing X, *Enzymatic degradation of polyε-caprolactone film in phosphate buffer solution containing lipases*, ***Polym. Degrad. Stab***. 1997, **56,** 209–213.

[139] Kulkarni A *et. al., Enzymatic Chain Scission Kinetics of Polyε-caprolactone* ***Monolayers.*** 2007,**24,** 12202-12207.

[140] Murphy CA *et. al., Fusarium polycaprolactone depolymerase is cutinase., Appl. Environ. Microbiol.* 1996, **62,** 456–60.

[141] Ramyasree US, Dutta JR, *The effect of process parameters in enhancement of lipase production by co-culture of lactic acid bacteria and their mutagenesis study.* ***Biocatal. Agric. Biotechnol***. 2013, **4**, 393–398.

[142] Pera L, Romero C, Baigori M, *Catalytic properties of lipase extracts from Aspergillus niger*, ***Food Technol***. 2006,**44**, 242-247 .

[143] Maia M. de M.D. *et. al., Production of extracellular lipase by the phytopathogenic fungus Fusarium solani FS1*, **Rev. Microbiol.** 1999, **3**, 304–309.

[144] Mario Lebendiker TD, *Purification of Proteins Fused to Maltose-Binding Protein - Springer*, ***Methods Mol. Biol.*** 2010, **681**, 281–293.

[145] Tang ZG *et. al., Surface properties and biocompatibility of solvent-cast poly[-caprolactone] films.*, ***Biomaterials***. 2004, **25**, 4741–8.

[146] Bosworth LA, *Physicochemical characterisation of degrading polycaprolactone scaffolds*, ***Polym. Degrad. Stab***. 2010, **95**, 2269–2276.

[147] Cho K, Lee J, Xing P, *Enzymatic degradation of blends of polyϵ-caprolactone and polystyrene-co-acrylonitrile by Pseudomonas lipase*, ***J. Appl. Polym. Sci.*** 2002, **83**, 868–879.

[148] Eldsäter C *et. al., The biodegradation of amorphous and crystalline regions in film-blown polyϵ-caprolactone*, ***Polymer Guildf***. 2000, **41**, 1297–1304.

[149] Lijian L *et. al., Selective Enzymatic Degradations of Polyl-lactide and Polyε-caprolactone Blend Films*, ***Biomacromolecules,*** 2000, **1**, 350-359.

[150] Nair, L. S.; Laurencin, C. T. Biodegradable Polymers as Biomaterials. ***Prog. Polym. Sci.*** 2007, ***32*** **(8),** 762–798.

[151] Ulery, B. D.; Nair, L. S.; Laurencin, C. T. Biomedical Applications of Biodegradable Polymers. ***J. Polym. Sci. B. Polym. Phys.*** 2011, ***49*** **(12),** 832–864.

[152] Zheng, Y.; Yanful, E. K.; Bassi, A. S. A Review of Plastic Waste Biodegradation. ***Crit. Rev. Biotechnol***. 2005, ***25*** **(4),** 243–250.

[153] Mülhaupt, R. Green Polymer Chemistry and Bio-Based Plastics: Dreams and Reality. ***Macromol. Chem. Phys***. 2013, ***214*** **(2),** 159–174.

[154] Zaikov, G. E.; Lomakin, S. M. Ecological Issue of Polymer Flame Retardancy. ***J. Appl. Polym. Sci***. 2002, ***86*** **(10),** 2449–2462.

[155] Royer, S.-J.; Ferrón, S.; Wilson, S. T.; Karl, D. M. Production of Methane and Ethylene from Plastic in the Environment. ***PLoS One*** 2018, ***13*** **(8),** e0200574.

[156] Shimao, M. Biodegradation of Plastics. ***Curr. Opin. Biotechnol***. 2001, ***12*** **(3),** 242–247.

[158] Cerniglia, C. E. Biodegradation of Polycyclic Aromatic Hydrocarbons. ***Curr. Opin. Biotechnol***. 1993, ***4*** **(3),** 331–338.

[159] Bhardwaj, H.; Gupta, R.; Tiwari, A. Communities of Microbial Enzymes Associated with Biodegradation of Plastics. ***J. Polym. Environ***. 2013, ***21*** **(2),** 575–579.

[160] Suzuki, M.; Tachibana, Y.; Oba, K.; Takizawa, R.; Kasuya, K. Microbial degradation of poly(ε-caprolactone) in a coastal environment. ***Polym. Degrad. Stab***. 2018, **149,** 1-8.

[161] Miao, Z.-M.; Cheng, S.-X.; Zhang, X.-Z.; Wang, Q.-R.; Zhuo, R.-X. Degradation and Drug Release Property of Star Poly(Epsilon-Caprolactone)s with Dendritic Cores. ***J. Biomed. Mater. Res. B. Appl. Biomater***. 2007, ***81*** **(1),** 40–49.

[162] Labet, M.; Thielemans, W. Synthesis of Polycaprolactone: A Review. ***Chem. Soc. Rev***. 2009, ***38* (12),** 3484–3504.

[163] Yeniad, B.; Naik, H.; Heise, A. Lipases in Polymer Chemistry. ***Adv. Biochem. Eng. Biotechnol***. 2011, ***125*,** 69–95.

[164] Uppada, S. R.; Akula, M.; Bhattacharya, A.; Dutta, J. R. Immobilized Lipase from *Lactobacillus Plantarum* in Meat Degradation and Synthesis of Flavor Esters. ***J. Genet. Eng. Biotechnol***. 2017, ***15* (2),** 331–334.

[165] Kobayashi, S.; Uyama, H.; Takamoto, T. Lipase-Catalyzed Degradation of Polyesters in Organic Solvents. A New Methodology of Polymer Recycling Using Enzyme as Catalyst. ***Biomacromolecules*** 2000, ***1* (1),** 3–5.

[166] Dash, T. K.; Konkimalla, V. B. Poly-ϵ-Caprolactone Based Formulations for Drug Delivery and Tissue Engineering: A Review. ***J. Control. Release*** 2012, ***158* (1),** 15–33.

[167] Ganesh, M.; Dave, R. N.; L'Amoreaux, W.; Gross, R. A. Embedded Enzymatic Biomaterial Degradation. ***Macromolecules*** 2009, ***42* (18),** 6836–6839.

[168] Ganesh, M.; Gross, R. A. Embedded Enzymatic Biomaterial Degradation: Flow Conditions & Relative Humidity. ***Polymer (Guildf).*** 2012, ***53* (16),** 3454–3461.

[169] Khan, I.; Ray Dutta, J.; Ganesan, R. Lactobacillus Sps. Lipase Mediated Poly (ε-Caprolactone) Degradation. ***Int. J. Biol. Macromol***. 2017, ***95***, 126–131.

[170] Ganesh, M.; Nachman, J.; Mao, Z.; Lyons, A.; Rafailovich, M.; Gross, R. Patterned enzymatic degradation of poly (ε-caprolactone) by high-affinity microcontact printing and polymer pen lithography. ***Biomacromolecules*** 2013, **14,** 2470-2476.

[171] Mao, Z.; Ganesh, M.; Bucaro, M.; Smolianski, I.; Gross, R.A.; Lyons, A.M., High throughput, high resolution enzymatic lithography process: Effect of crystallite size, moisture, and enzyme concentration. ***Biomacromolecules*** 2014, ***15*,** 4627-4636.

[172] Y. Yan, S.C. Warren, P. Fuller, B.A. Grzybowski, *Chemoelectronic circuits based on metal nanoparticles, **Nat. Nanotechnol.*** 2016, **11**, 603–608.

[173] Y.-C. Yeh, B. Creran, V.M. Rotello, *Gold nanoparticles preparation, properties, and applications in bionanotechnology, **Nanoscale***. 2012, **4,** 1871–1880.

[174] M.-C.D. and, D. Astruc, *Gold Nanoparticles Assembly, Supramolecular Chemistry, Quantum-Size-Related Properties, and Applications toward Biology, Catalysis, and Nanotechnology, 2003. **Chem. Rev.,*** 2004, **104**, 293–346.

[175] H. Duan, D. Wang, Y. Li, *Green chemistry for nanoparticle synthesis*, ***Chem. Soc. Rev.*** 2015, **44**, 5778–5792.

[176] P. Murawala, A. Tirmale, A. Shiras, B.L.V. Prasad, *In situ synthesized BSA capped gold nanoparticles Effective carrier of anticancer drug Methotrexate to MCF-7 breast cancer cells**, Mater. Sci. Eng. C.*** 2014, **34**, 158–167.

[177] D. Joseph, N. Tyagi, C. Geckeler, K. E Geckeler, *Protein-coated pH-responsive gold nanoparticles Microwave-assisted synthesis and surface charge-dependent anticancer activity.*, ***Beilstein J. Nanotechnol.*** 2014, **5,** 1452–1462.

[178] S.A. Khan, A. Ahmad, *Enzyme mediated synthesis of water-dispersible, naturally protein capped, monodispersed gold nanoparticles, their characterization and mechanistic aspects, **RSC Adv.*** 2014, **4**, 7729–7734.

[179] Chanana M *et. al., Insulin-Coated Gold Nanoparticles A Plasmonic Device for Studying Metal-Protein Interactions, **Small***. 2011, **7**, 2650–2660.

[180] Navin Jain, Aprit Bhargava, Jitendra Panwar, *Enhanced photocatalytic degradation of methylene blue using biologically synthesized "protein-capped" ZnO nanoparticles*, ***Chem. Eng. J.*** 2014, **243**, 549–555.

[181] R. Sanghi, P. Verma, S. Puri, *Enzymatic Formation of Gold Nanoparticles Using Phanerochaete Chrysosporium, **Adv. Chem. Eng. Sci***. 2011, **1**, 154–162.

[182] Hye-Young Park, Mark J. Schadt, Lingyan Wang, I-Im Stephanie Lim, Peter N. Njoki, Soo Hong Kim, et al., *Fabrication of Magnetic Core@Shell Fe Oxide@Au Nanoparticles for Interfacial Bioactivity and Bio-separation, 2007*. ***Langmuir***, 2007, **23,** 9050–9056

[183] B. Devika Chithrani and Arezou A. Ghazani, Warren C. W. Chan, *Determining the Size and Shape Dependence of Gold Nanoparticle Uptake into Mammalian Cells*, ***Nano Lett***., 2006, **6**, 662-668

[184] I. Khan, J.R. Dutta, R. Ganesan, *Enzymes' action on materials Recent trends,* ***J. Cell. Biotechnol.*** 2016, **1,** 131–144.

[185] M.S. Al-Harbi, B.A. El-Deeb, N. Mostafa, S.A.M. Amer, *Extracellular Biosynthesis of AgNPs by the Bacterium & Its Toxic Effect on Some Aspects of Animal Physiology,* ***Adv. Nanoparticles***. 2014, **3,** 83–91.

[186] Y. Yu, S.Y. New, J. Xie, X. Su, Y.N. Tan, Y. Lu, et al., *Protein-based fluorescent metal nanoclusters for small molecular drug screening*, ***Chem. Commun***. 2014, **50,** 13805–13808.

[187] S. Anil Kumar, M.K. Abyaneh, S.W. Gosavi, S.K. Kulkarni, R. Pasricha, A. Ahmad, et al., *Nitrate reductase-mediated synthesis of silver nanoparticles from AgNO3.*, ***Biotechnol. Lett***. 2007, **29,** 439–445.

[188] A. Rangnekar, T.K. Sarma, A.K. Singh, J. Deka, A. Ramesh, A. Chattopadhyay, *Retention of enzymatic activity of alpha-amylase in the reductive synthesis of gold nanoparticles.*, ***Langmuir.*** 2007, **23,** 5700–5706.

[189] J. Virkutyte, R.S. Varma, V. Kumar, S.K. Yadav, J.A. Dahl, B.L.S. Maddux, et al., *Green synthesis of metal nanoparticles Biodegradable polymers and enzymes in stabilization and surface functionalization*, ***Chem. Sci.*** 2011, **2,** 837–846.

[190] N. Goswami, R. Saha, S.K. Pal, *Protein-assisted synthesis route of metal*

nanoparticles exploration of key chemistry of the biomolecule, ***J. Nanoparticle Res.*** 2011, **13,** 5485–5495.

[191] J. Kimling, M. Maier, B. Okenve, V. Kotaidis, and H. Ballot, A. Plech, *Turkevich Method for Gold Nanoparticle Synthesis Revisited*, ***J. Phys. Chem. B***, , 2006, **110,** 15700–15707.

[192] E. Park, M.R. Quinn, G. Schuller-Levis, *Taurine chloramine attenuates the hydrolytic activity of matrix metalloproteinase-9 in LPS-activated murine peritoneal macrophages.*, ***Adv. Exp. Med. Biol***. 2000, **483,** 389–398.

[193] L. Rastogi, A.J. Kora, A. J., *Highly stable, protein capped gold nanoparticles as effective drug delivery vehicles for amino-glycosidic antibiotics*, ***Mater. Sci. Eng. C.*** 2012, **32,** 1571–1577.

[194] Tao Yang, Zhuang Li, Li Wang, and Cunlan Guo, Y. Sun, *Synthesis, Characterization, and Self-Assembly of Protein Lysozyme Monolayer-Stabilized Gold Nanoparticles*, ***Langmuir,*** 2007, **23,** 10533–10538.

[195] S. Ramyasree, J.R. Dutta, *The effect of process parameters in enhancement of lipase production by co-culture of lactic acid bacteria and their mutagenesis study*, ***Biocatal. Agric. Biotechnol.*** 2013, **4,** 393–398.

[196] I. Khan, J. Ray Dutta, R. Ganesan, *Lactobacillus sps. lipase mediated poly ε-caprolactone degradation*, ***Int. J. Biol. Macromol.*** 2017, **95,** 126–131.

[197] SitaRamyasree Uppadaa, Mahesh Akula. Anupam Bhattacharya, Jayati Ray Dutta

Immobilized lipase from Lactobacillus plantarum in meat degradation and synthesis of flavor esters, ***J. Genet. Eng. Biotechnol.*** 2017, **15,** 331–334.

[198] Mazumder JA, Ahmad R, Sardar M. *Reusable magnetic nanobiocatalyst for synthesis of silver and gold nanoparticles*, ***Int. J. Biol. Macromol.*** 2016, **93,** 66–74.

[199] Z.-H. Wang, G. Jin, *Covalent immobilization of proteins for the biosensor based on imaging ellipsometry, **J. Immunol. Methods.*** 2004, **285,** 237–243.

[200] M.R. Dewi, G. Laufersky, T. Nann, *Selective assembly of Au-Fe3O4 nanoparticle hetero-dimers., **Mikrochim. Acta***. 2015, **182,** 2293–2298.

[201] K. Kuroda, T. Ishida, M. Haruta, *Reduction of 4-nitrophenol to 4-aminophenol over Au nanoparticles deposited on PMMA, **J. Mol. Catal. A Chem.*** 2009, **298,** 7–11.

[202] Zhichuan Xu, and Yanglong Hou, S. Sun, *Magnetic Core/Shell Fe3O4/Au and Fe3O4/Au/Ag Nanoparticles with Tunable Plasmonic Properties**, J. Am. Chem. Soc.,*** 2007, **129** 8698–8699

[203] Y.S. Seo, E.-Y. Ahn, J. Park, T.Y. Kim, J.E. Hong, K. Kim, et al., *Catalytic reduction of 4-nitrophenol with gold nanoparticles synthesized by caffeic acid., **Nanoscale Res. Lett***. 2017, **12,** 7-18.

[204] Zhang Q, Xie J, Yu Y, Yang J, Lee JY. *Tuning the Crystallinity of Au Nanoparticles. **Small***, 2010, **6**, 523–527.

[205] M. Boudart, *Turnover Rates in Heterogeneous Catalysis, **Chem. Rev.*** 1995, **95,** 661–666.

[206] Yeh Y-C, Creran B, Rotello VM. *Gold nanoparticles preparation, properties, and applications in bionanotechnology. **Nanoscale*** . 2012, **4**, 61871–1880.

[207] Pranjali Yadava, Surya Prakash Singh, Aravind Kumar Rengan, Asif khan Shanavas, Rohit Srivastava. *Gold laced bio-macromolecules for theranostic application. **Int J Biol Macromol.*** 2018, **110**, 39-53.

[208] Ghosh P, Han G, De M, Kim CK, Rotello VM. *Gold nanoparticles in delivery applications. **Adv Drug Deliv Rev*** . 2008, **60**, 111307–1315.

[209] Sau TK, Murphy CJ. *Room Temperature, High-Yield Synthesis of Multiple Shapes of Gold Nanoparticles in Aqueous Solution. **J. Am. Chem. Soc.***, 2004, **126** 8648–8649

[210] Rastogi L, Kora AJ, J. A. *Highly stable, protein capped gold nanoparticles as effective drug delivery vehicles for amino-glycosidic antibiotics*. ***Mater Sci Eng C.*** 2012, **326,** 1571–1577.

[211] Cai W, Gao T, Hong H, Sun J. *Applications of gold nanoparticles in cancer nanotechnology*. ***Nanotechnol Sci Appl***. 2008, **19** 117–32.

[212] Yigit M V, Medarova Z. *In vivo and ex vivo applications of gold nanoparticles for biomedical SERS imaging*. ***Am J Nucl Med Mol Imaging.*** 2012, **22**, 232–241.

[213] Rengan AK, Bukhari AB, Pradhan A, Malhotra R, Banerjee R, Srivastava R, *et al., In Vivo Analysis of Biodegradable Liposome Gold Nanoparticles as Efficient Agents for Photothermal Therapy of Cancer*. ***Nano Lett.*** 2015, **15** 842–848.

[214] Dobrovolskaia MA, Patri AK, Zheng J, Clogston JD, Ayub N, Aggarwal P, *et al., Interaction of colloidal gold nanoparticles with human blood effects on particle size and analysis of plasma protein binding profiles*. ***Nanomedicine Nanotechnology, Biol Med.*** 2009, **52** 106–117.

[215]. Casals E, Pfaller T, Duschl A, Oostingh GJ, Puntes V. *Time Evolution of the Nanoparticle Protein Corona.* ***ACS Nano.*** 2010, **47**, 3623–3632.

[216] Benetti F, Fedel M, Minati L, Speranza G, Migliaresi C. *Gold nanoparticles role of size and surface chemistry on blood protein adsorption.* ***J Nanoparticle Res.*** 2013, **156**, 1694-1696.

[217]. Goy-López S, Juárez J, Alatorre-Meda M, Casals E, Puntes VF, Taboada P, *et al., Physicochemical Characteristics of Protein–NP Bioconjugates The Role of Particle Curvature and Solution Conditions on Human Serum Albumin Conformation and Fibrillogenesis Inhibition.* ***Langmuir.*** 2012, **28,** 9113–9126.

[218] Khan S, Gupta A, Verma NC, Nandi CK. *Kinetics of protein adsorption on gold nanoparticle with variable protein structure and nanoparticle size*. ***J Chem Phys***. 2015,

143 4709-18

[219] Walkey CD, Olsen JB, Song F, Liu R, Guo H, Olsen DWH, *et al., Protein Corona Fingerprinting Predicts the Cellular Interaction of Gold and Silver Nanoparticles*. ***ACS Nano.*** 2014, **83** 2439–2455.

[220] Dobrovolskaia MA, Neun BW, Man S, Ye X, Hansen M, Patri AK, *et al,. Protein corona composition does not accurately predict hematocompatibility of colloidal gold nanoparticles.* ***Nanomedicine Nanotechnology, Biol Med.*** 2014, **10** 1453–1463.

[221] Ajdari N, Vyas C, Bogan SL, Lwaleed BA, Cousins BG. *Gold nanoparticle interactions in human blood a model evaluation*. ***Nanomedicine Nanotechnology, Biol Med***. 2017, **13** 1531–1542.

[222] Szymusiak M, Donovan AJ, Smith SA, Ransom R, Shen H, Kalkowski J, *et al., Colloidal Confinement of Polyphosphate on Gold Nanoparticles Robustly Activates the Contact Pathway of Blood Coagulation*. ***Bioconjug Chem.*** 2016, **27** 102–109.

[223] Zhao Y, Tian Y, Cui Y, Liu W, Ma W, Jiang X. *Small Molecule-Capped Gold Nanoparticles as Potent Antibacterial Agents That Target Gram-Negative Bacteria.* ***J Am Chem Soc.*** 2010, **132,** 12349–12356.

[224] Ehmann HMA, Breitwieser D, Winter S, Gspan C, Koraimann G, Maver U, *et al., Gold nanoparticles in the engineering of antibacterial and anticoagulant surfaces.* ***Carbohydr Polym.*** 2015, **117**, 34–42.

[225] Sanfins E, Augustsson C, Dahlbäck B, Linse S, Cedervall T. *Size-Dependent Effects of Nanoparticles on Enzymes in the Blood Coagulation Cascade*. ***Nano Lett.*** 2014, **14**, 4736–4744.

[226] Aggarwal P, Hall JB, McLeland CB, Dobrovolskaia MA, McNeil SE. *Nanoparticle interaction with plasma proteins as it relates to particle biodistribution, biocompatibility and therapeutic efficacy*. ***Adv Drug Deliv Rev***. 2009, **61**, 428–437.

[227] Park MS, Martini WZ, Dubick MA, Salinas J, Butenas S, Kheirabadi BS, *et al., Thromboelastography as a Better Indicator of Hypercoagulable State After Injury Than Prothrombin Time or Activated Partial Thromboplastin Time.* ***J Trauma Inj Infect Crit Care***. 2009, **672** 266–276.

[228] Braune S, Sperling C, Maitz MF, Steinseifer U, Clauser J, Hiebl B, Krajewski S, Wendel HP, Jung F. *Evaluation of platelet adhesion and activation on polymers Round-robin study to assess inter-center variability.* ***Colloids Surf B Biointerfaces.*** 2017,**15** 8416-422.

[229] Dhurat R, Sukesh M. *Principles and Methods of Preparation of Platelet-Rich Plasma A Review and Author's Perspective.* ***J Cutan Aesthet Surg***. 2014, **74** 189–197.

[230] Szponder T, Wessely-Szponder J, Smolira A. *Evaluation of Platelet-Rich Plasma and Neutrophil Antimicrobial Extract as Two Autologous Blood-Derived Agents.* ***Tissue Eng Regen Med.*** 2017, **143**, 287–296.

[231] Braune S, Basu S, Kratz K, Johansson JB, ReinthalerM, Lendlein A, Jung F. *Strategy for the hemocompatibility testing of microparticles.* ***Clin Hemorheol Microcirc.*** 2016, **64** 3345-53.

[232] Khan I, Ray Dutta J, Ganesan R. *Lactobacillus sps. lipase mediated poly ε-caprolactone degradation.* ***Int J Biol Macromol.*** 2017, **95**, 126–131.

[233] Ramyasree S, Dutta JR. *The effect of process parameters in enhancement of lipase production by co-culture of lactic acid bacteria and their mutagenesis study.* ***Biocatal Agric Biotechnol.*** 2013, **42** 393–398.

[234] Khan I, Dutta JR, Ganesan R. *Enzymes' action on materials Recent trends.* ***J Cell Biotechnol.*** 2016, **1** 131–144.

[235] J. Kimling, M. Maier, B. Okenve, V. Kotaidis, H. Ballot and, Plech, A. *Turkevich Method for Gold Nanoparticle Synthesis Revisited.* ***J. Phys. Chem. B***, 2006, **110**, 15700–

15707.

[236] Radomski A, Jurasz P, Alonso-Escolano D, Drews M, Morandi M, Malinski T, *et al., Nanoparticle-induced platelet aggregation and vascular thrombosis.* ***Br J Pharmacol.*** 2005, **146** 882–893.

[237] Chen G, Ni N, Zhou J, *et al., Fibrinogen clot induced by gold-nanoparticle in vitro.* ***J Nanosci Nanotechnol.*** 2011, **111,** 74-81.

[238] Dobrovolskaia MA, Patri AK, Zheng J, *et al., Interaction of colloidal gold nanoparticles with human blood Effects on particle size and analysis of plasma protein binding profiles*. ***Nanomedicine***. 2009, **52,** 106-17.

[239] Deb S, Patra HK, Lahiri P, Dasgupta AK, Chakrabarti K, Chaudhuri U. *Multistability in platelets and their response to gold nanoparticles.* ***Nanomedicine.*** 2011,**74** 376-84.

[240] Nel AE,Madler L,Velegol D, *et al., Understanding biophysicochemical interactions at the nano-bio interface*. ***NatMater.*** 2009,**87** 543-57.

[241] Sperling C, Fischer M, Maitz MF, Werner C. *Blood coagulation on biomaterials requires the combination of distinct activation processes.* ***Biomaterials.*** 2009, **30,** 74447-56.

[242] Lacerda SHDP, Park JJ, Meuse C, Pristinski D, Becker ML, Karim A, *et al., Interaction of Gold Nanoparticles with Common Human Blood Proteins*. ***ACS Nano***. 2010, **4**, 365–379.

[243] Li W-R, Xie X-B, Shi Q-S, Zeng H-Y, OU-Yang Y-S, Chen Y-B. *Antibacterial activity and mechanism of silver nanoparticles on Escherichia coli.* ***Appl Microbiol Biotechnol.*** 2010, **85,** 1115–2

[244] Bush K. *The coming of age of antibiotics: discovery and therapeutic value.* ***Ann N Y Acad Sci .*** *2010,* **1213,** 1–4.

[245] Kardos N, Demain AL. *Penicillin: the medicine with the greatest impact on therapeutic outcomes.* **Appl Microbiol Biotechnol**. 2011, **92,** 677–87.

[246] Sandegren L. *Selection of antibiotic resistance at very low antibiotic concentrations. Ups* ***J Med Sci*** **.** 2014, **119,** 103–7.

[247] Carter D, Charlett A, Conti S, Robotham J V, Johnson AP, Livermore DM, et al. A *Risk Assessment of Antibiotic Pan-Drug-Resistance in the UK: Bayesian Analysis of an Expert Elicitation Study*. ***Antibiot***. 2017, **6**, 9-20.

[248] Mao B-H, Chen Z-Y, Wang Y-J, Yan S-J. *Silver nanoparticles have lethal and sublethal adverse effects on development and longevity by inducing ROS-mediated stress responses.* **Sci Rep.** 2018, **8,** 2445.

[249] Westerband EI, Hicks AL. *Life cycle impact of nanosilver polymer-food storage containers as a case study informed by literature review.* ***Environ Sci Nano.*** 2018, **5,** 933–45.

[250] Hajipour MJ, Fromm KM, Akbar Ashkarran A, Jimenez de Aberasturi D, Larramendi IR de, Rojo T, *et al. Antibacterial properties of nanoparticles.* ***Trends Biotechnol***. 2012, **30,** 499–511.

[251] Tolaymat TM, El Badawy AM, Genaidy A, Scheckel KG, Luxton TP, Suidan M. *An evidence-based environmental perspective of manufactured silver nanoparticle in syntheses and applications: A systematic review and critical appraisal of peer-reviewed scientific papers.* ***Sci Total Environ***. 2010, **408,** 999–1006.

[252] Ajitha B, Kumar Reddy YA, Reddy PS, Jeon H-J, Ahn CW, Prikulis J, *et al. Role of capping agents in controlling silver nanoparticles size, antibacterial activity and potential application as optical hydrogen peroxide sensor.* ***RSC Adv.*** 2016, **6**, 36171–9.

[253] Mohan S, Oluwafemi OS, Songca SP, Jayachandran VP, Rouxel D, Joubert O, et al. *Synthesis, antibacterial, cytotoxicity and sensing properties of starch-capped silver*

nanoparticles. ***J Mol Li***q. 2016; **213,** 75–81.

[254] Chen J, Wang J, Zhang X, Jin Y. *Microwave-assisted green synthesis of silver nanoparticles by carboxymethyl cellulose sodium and silver nitrate.* ***Mater Chem Phys .*** 2008, **108,** 421–4.

[255] Kora AJ, Manjusha R, Arunachalam J. *Superior bactericidal activity of SDS capped silver nanoparticles: Synthesis and characterization.* ***Mater Sci Eng C*** . 2009, **29**, 2104–9.

[256] Gebregeorgis A, Bhan C, Wilson O, Raghavan D. Characterization of Silver/Bovine Serum Albumin (Ag/BSA) nanoparticles structure: Morphological, compositional, and interaction studies. ***J Colloid Interface Sci*** . 2013, **389**, 31–41.

[257] Gopinath V, Priyadarshini S, Meera Priyadharsshini N, Pandian K, Velusamy P. *Biogenic synthesis of antibacterial silver chloride nanoparticles using leaf extracts of Cissus quadrangularis Linn*. ***Mater Lett.*** 2013, **91**, 224–7.

[258] Matsumoto H, Koyama Y, Tanioka A. *Interaction of proteins with weak amphoteric charged membrane surfaces: effect of pH*. ***J Colloid Interface Sci.*** 2003, **264**, 82–8.

[259] Sanghi R, Verma P. *Biomimetic synthesis and characterisation of protein capped silver nanoparticles.* ***Bioresour Technol***. 2009, **100,** 501–4.

[260] Drake PL, Hazelwood KJ. *Exposure-Related Health Effects of Silver and Silver Compounds:* ***A Review. Ann Occup Hyg.*** 2005, **49**, 575–85.

[261] Bilberg K, Hovgaard MB, Besenbacher F, Baatrup E. *In Vivo Toxicity of Silver Nanoparticles and Silver Ions in Zebrafish (Danio rerio).* ***J Toxicol***. 2012, 293784. doi: 10.1155/2012/293784

[262] Barker LK, Giska JR, Radniecki TS, Semprini L. *Effects of short- and long-term exposure of silver nanoparticles and silver ions to Nitrosomonas europaea biofilms and*

planktonic cells. Chemosphere. ***Pergamon***; 2018, **206**, 606–14.

[263] Khan I, Vishwakarma SK, Khan AA, Ramakrishnan G, Dutta JR. *In vitro hemocompatability evaluation of gold nanoparticles capped with Lactobacillus plantarum derived lipase1*. ***Clin Hemorheol Microcirc*** . 2018, **69,** 197–205.

[264] Khan I, Nagarjuna R, Ray Dutta J, Ganesan R. *Towards single crystalline, highly monodisperse and catalytically active gold nanoparticles capped with probiotic Lactobacillus plantarum derived lipase.* ***Appl Nanosci .*** 2018, 1-9.

[265] Khan I, Ray Dutta J, Ganesan R. *Lactobacillus sps. lipase mediated poly (ε-caprolactone) degradation.* ***Int J Biol Macromol.*** 2017, **95**, 126–31.

[266] Song KC, Lee SM, Park TS, Lee BS. *Preparation of colloidal silver nanoparticles by chemical reduction method*. ***Korean J Chem Eng,*** 2009, **26,** 153–5.

[267] Boudebbouze S, Coleman AW, Tauran Y, Mkaouar H, Perret F, Garnier A, *et al., Discriminatory antibacterial effects of calix[n]arene capped silver nanoparticles with regard to Gram positive and Gram negative bacteria*. ***Chem Commun.*** 2013, **49**,7150-8

[268] Prabhu S, Poulose EK. *Silver nanoparticles: mechanism of antimicrobial action, synthesis, medical applications, and toxicity effects.* ***Int Nano Lett.*** 2012, **2,** 32-40.

[269] Kim JS, Kuk E, Yu KN, Kim J-H, Park SJ, Lee HJ, *et al. Antimicrobial effects of silver nanoparticles.* ***Nanomedicine,*** 2007, **3,** 95–101.

[270] Sondi I, Salopek-Sondi B. *Silver nanoparticles as antimicrobial agent: a case study on E. coli as a model for Gram-negative bacteria.* ***J Colloid Interface Sci***. 2004; **275,** 177–82.

[271] Reidy B, Haase A, Luch A, Dawson K, Lynch I. *Mechanisms of Silver Nanoparticle Release, Transformation and Toxicity: A Critical Review of Current Knowledge and Recommendations for Future Studies and Applications*. ***Materials***. 2013, **6,** 2295–350.

[272] Niemeyer CM. *Nanoparticles, Proteins, and Nucleic Acids: Biotechnology Meets Materials Science.* ***Angew Chemie Int Ed.*** 2001, **40,** 4128–58.

[273] Ibrahim HMM. *Green synthesis and characterization of silver nanoparticles using banana peel extract and their antimicrobial activity against representative microorganisms.* ***J Radiat Res Appl Sci***. 2015, **8,** 265–75.

[274] Samberg ME, Orndorff PE, Monteiro-Riviere NA. *Antibacterial efficacy of silver nanoparticles of different sizes, surface conditions and synthesis methods.* ***Nanotoxicology***, 2011, **5,** 244–53.

[275] Kora AJ, Arunachalam J. *Assessment of antibacterial activity of silver nanoparticles on Pseudomonas aeruginosa and its mechanism of action*. ***World J Microbiol Biotechnol*** . 2011, **27,**1209–16.

[276] Martínez-Castañón GA, Niño-Martínez N, Martínez-Gutierrez F, Martínez-Mendoza JR, Ruiz F. *Synthesis and antibacterial activity of silver nanoparticles with different sizes.* ***J Nanoparticle Res***, 2008, **10,** 1343–48.

[277] Krishnan R, Arumugam V, Vasaviah SK. *The MIC and MBC of Silver Nanoparticles against Enterococcus faecalis - A Facultative Anaerobe*. ***J Nanomed Nanotechnol***. 2015, **6,** DOI: 10.4172/2157-7439.1000285

[278] Agnihotri S, Mukherji S, Mukherji S. *Size-controlled silver nanoparticles synthesized over the range 5–100 nm using the same protocol and their antibacterial efficacy.* **RSC Adv.** 2014, **4,** 3974–83.

[279] Lok C-N, Ho C-M, Chen R, He Q-Y, Yu W-Y, Sun H, *et al. Silver nanoparticles: partial oxidation and antibacterial activities*. ***J Biol Inorg Chem***. 2007, **12,** 527–34.

[280] Li P, Li J, Wu C, Wu Q, Li J. *Synergistic antibacterial effects of β-lactam antibiotic combined with silver nanoparticles.* **Nanotechnology.** 2005, **16,** 1912–17.

[281] Zhou Y, Kong Y, Kundu S, Cirillo JD, Liang H. *Antibacterial activities of gold*

and silver nanoparticles against Escherichia coli and bacillus Calmette-Guérin. ***J Nanobiotechnology***. 2012, **10**, 19. https://doi.org/10.1186/1477-3155-10-19

[282] Supraja N, Prasad TNVK V., Krishna TG, David E. *Synthesis, characterization, and evaluation of the antimicrobial efficacy of Boswellia ovalifoliolata stem bark-extract-mediated zinc oxide nanoparticles*. ***Appl Nanosci.*** 20166, **4,** 581–90.

[283] Senthamilselvi S, Kumar P, Prabha AL, Govindaraju M. *Green Simplistic Biosynthesis of Anti-Bacterial Silver Nanoparticles Using Annona Squamosa Leaf Extract.* ***Nano Biomed Eng.*** 2013, **5**, 102-106.

[284] Martínez-Abad A, Lagarón JM, Ocio MJ. *Antimicrobial beeswax coated polylactide films with silver control release capacity.* ***Int J Food Microbiol.*** 2014, **174**, 39–46.

[285] Eby DM, Schaeublin NM, Farrington KE, Hussain SM, Johnson GR. *Lysozyme catalyzes the formation of antimicrobial silver nanoparticles.* ***ACS* Nan**o. 2009, ***3,*** 984–94.

[286] Nam S, Park B, Condon BD. *Water-based binary polyol process for the controllable synthesis of silver nanoparticles inhibiting human and foodborne pathogenic bacteria*. ***RSC Adv***. 2018, **8**, 1937–47.

[287] Thiyagarajan K, Bharti VK, Tyagi S, Tyagi PK, Ahuja A, Kumar K, *et al. Synthesis of non-toxic, biocompatible, and colloidal stable silver nanoparticle using egg-white protein as capping and reducing agents for sustainable antibacterial application.* ***RSC Adv.*** 2018, **8,** 213–29.

[288] Saha S, Gupta B, Gupta K, Chaudhuri MG. *Production of putrescine-capped stable silver nanoparticle: its characterization and antibacterial activity against multidrug-resistant bacterial strains.* ***Appl Nanosci.*** 2016, **6,** 1137–47.

[289] Agnihotri S, Mukherji S, Mukherji S. *Size-controlled silver nanoparticles*

synthesized over the range 5–100 nm using the same protocol and their antibacterial efficacy. ***RSC Adv.*** 2014, **4,** 3974–83.

[290] Lu H, Yu L, Liu Q, Du J. *Ultrafine silver nanoparticles with excellent antibacterial efficacy prepared by a handover of vesicle templating to micelle stabilization*. ***Polym Chem***. 2013, **4,** 3448-58.

[291] Ashraful AM, Masjuki HH, Kalam MA, Rizwanul Fattah IM, Imtenan S, Shahir SA, *Production and comparison of fuel properties, engine performance, and emission characteristics of biodiesel from various non-edible vegetable oils A review.* ***Energy Convers Manag*** 2014,**80,** 202–28.

[292] Singh SP, Singh D. *Biodiesel production through the use of different sources and characterization of oils and their esters as the substitute of diesel A review.* ***Renew Sustain Energy Rev*** 2010, **14,** 200–16.

[293] Barnwal BK, Sharma MP. *Prospects of biodiesel production from vegetable oils in India.* ***Renew Sustain Energy Rev*** 2005, **93,** 63–78.

[294] Gui MM, Lee KT, Bhatia S. *Feasibility of edible oil vs. non-edible oil vs. waste edible oil as biodiesel feedstock.* ***Energy,*** 2008, **33,** 1646–53.

[295] Granda CB, Zhu L, Holtzapple MT. *Sustainable liquid biofuels and their environmental impact.* ***Environ Prog.*** 2007,**262,** 33–50.

[296] Yilmaz N, Vigil FM, Benalil K, Davis SM, Calva A. *Effect of biodiesel–butanol fuel blends on emissions and performance characteristics of a diesel engine*. ***Fuel***, 2014,**13,** 546–50.

[297] Rakopoulos DC, Rakopoulos CD, Giakoumis EG. *Impact of properties of vegetable oil, bio-diesel, ethanol and n-butanol on the combustion and emissions of turbocharged HDDI diesel engine operating under steady and transient conditions.* ***Fuel,*** 2015,**15,** 61–119.

[298] Verma P, Sharma MP. *Review of process parameters for biodiesel production from different feedstocks*. ***Renew Sustain Energy Rev.*** 2016,**62,** 1063–71.

[299] Zhao X, Qi F, Yuan C, Du W, Liu D. *Lipase-catalyzed process for biodiesel production Enzyme immobilization, process simulation and optimization.* ***Renew Sustain Energy Rev.*** 2015,**44,** 182–97.

[300] Amini Z, Ong HC, Harrison MD, Kusumo F, Mazaheri H, Ilham Z. *Biodiesel production by lipase-catalyzed transesterification of Ocimum basilicum L. sweet basil seed oil*. ***Energy Convers Manag.*** 2017,**13,** 282–90.

[301] Mardhiah HH, Ong HC, Masjuki HH, Lim S, Lee HV. *A review on latest developments and future prospects of heterogeneous catalyst in biodiesel production from non-edible oils*. ***Renew Sustain Energy Rev.*** 2017,**6** 71225–36.

[302] Gurunathan B, Ravi A. *Process optimization and kinetics of biodiesel production from neem oil using copper doped zinc oxide heterogeneous nanocatalyst*. ***Bioresour Technol.*** 2015,**19,** 424–8.

[303] Roschat W, Siritanon T, Kaewpuang T, Yoosuk B, Promarak V. *Economical and green biodiesel production process using river snail shells-derived heterogeneous catalyst and co-solvent method.* ***Bioresour Technol.*** 2016,**209,** 343–50.

[304] Dai Y-M, Wu J-S, Chen C-C, Chen K-T. *Evaluating the optimum operating parameters on transesterification reaction for biodiesel production over a LiAlO2 catalyst*. ***Chem Eng J.*** 2015,**28,** 70–6.

[305] Chuah LF, Yusup S, Abd Aziz AR, Bokhari A, Klemeš JJ, Abdullah MZ. *Intensification of biodiesel synthesis from waste cooking oil Palm Olein in a Hydrodynamic Cavitation Reactor Effect of operating parameters on methyl ester conversion.* ***Chem Eng Process Process Intensif***. 2015,**95,** 235–40.

[306] Guldhe A, Singh P, Ansari FA, Singh B, Bux F. *Biodiesel synthesis from*

microalgal lipids using tungstated zirconia as a heterogeneous acid catalyst and its comparison with homogeneous acid and enzyme catalysts. ***Fuel,*** 2017,**18,** 7180–8.

[307] Sani YM, Daud WMAW, Abdul Aziz AR. *Activity of solid acid catalysts for biodiesel production A critical review*. ***Appl Catal A Gen.*** 2014, **4,** 70140–61.

[308] Aransiola EF, Ojumu TV, Oyekola OO, Madzimbamuto TF, Ikhu-Omoregbe DIO. *A review of current technology for biodiesel production State of the art.* ***Biomass Bioenergy,*** 2014,**6,** 1276–97.

[309] Mangesh G. Kulkarni, and Ajay K. Dalai., AK. *Waste Cooking Oil An Economical Source for Biodiesel,* ***Ind. Eng. Chem. Res***., 2006, **45,** 2901–2913.

[310] Awasthi MK, Selvam A, Chan MT, Wong JWC. *Bio-degradation of oily food waste employing thermophilic bacterial strains.* ***Bioresour Technol.*** 2018,**24,** 8141–7.

[311] César A da S, Werderits DE, de Oliveira Saraiva GL, Guabiroba RC da S. *The potential of waste cooking oil as supply for the Brazilian biodiesel chain.* ***Renew Sustain Energy Rev.*** 2017,**72,** 246–53.

[312] Ramyasree S, Dutta JR. *The effect of process parameters in enhancement of lipase production by co-culture of lactic acid bacteria and their mutagenesis study.* ***Biocatal Agric Biotechnol***. 2013,**43,** 93–8.

[313] Imanparast S, Hamedi J, Faramarzi MA. *Enzymatic esterification of acylglycerols rich in omega-3 from flaxseed oil by an immobilized solvent-tolerant lipase from Actinomadura sediminis UTMC 2870 isolated from oil-contaminated soil*. ***Food Chem.*** 2018, **24,** 5934–42.

[314] Knothe G. *Avocado and olive oil methyl esters.* ***Biomass Bioenergy,*** 2013, **58,** 143–8.

[315] Sanchez F, Vasudevan PT. *Enzyme Catalyzed Production of Biodiesel From Olive Oil*. ***Appl Biochem Biotechnol*** 2006, **13,** 51–14.

[316] Li YX, Dong BX, Li YX, Dong BX. *Optimization of Lipase-Catalyzed Transesterification of Cotton Seed Oil for Biodiesel Production Using Response Surface Methodology.* ***Brazilian Arch Biol Technol.*** 2016, **59,** e16150357.

[317] Istiningrum RB, Aprianto T, Pamungkas FLU. *Effect of reaction temperature on biodiesel production from waste cooking oil using lipase as biocatalyst.* ***AIP Conf. Proc***., vol. 1911, AIP Publishing LLC , 2017, p. 20031.

[318] Ghaly AE, Dave D, Brooks MS, Budge S, Ghaly AE, Dave D, et al. *Production of Biodiesel by Enzymatic Transesterification Review*. ***Am J Biochem Biotechnol.*** 2010, **6,** 54–76.

[319] Nie K, Xie F, Wang F, Tan T. *Lipase catalyzed methanolysis to produce biodiesel Optimization of the biodiesel production.* ***J Mol Catal B Enzym***. 2006,**43,** 142–7.

[320] Dorado M., Ballesteros E, Arnal J., Gómez J, López F. *Exhaust emissions from a Diesel engine fueled with transesterified waste olive oil.* ***Fuel*** 2003, **82,** 1311–5.

[321] Stavarache C, Vinatoru M, Nishimura R, Maeda Y. *Fatty acids methyl esters from vegetable oil by means of ultrasonic energy.* ***Ultrason Sonochem.*** 2005, **12,** 367–72.

[322] Meher LC, Vidya Sagar D, Naik SN. *Technical aspects of biodiesel production by transesterification—a review*. ***Renew Sustain Energy Rev.*** 2006, **10,** 248–68.

[323] Leung DYC, Guo Y. *Transesterification of neat and used frying oil Optimization for biodiesel production.* ***Fuel Process Technol.*** 2006, **87,** 883–90.

[324] Erbeldinger M, Ni X, Halling PJ. *Enzymatic synthesis with mainly undissolved substrates at very high concentrations.* ***Enzyme Microb Technol,*** 1998, **23,** 141–8.

[325] Musa IA. *The effects of alcohol to oil molar ratios and the type of alcohol on biodiesel production using transesterification process.* ***Egypt J Pet.*** 2016, **25,** 21–31.

Biography of Student

Mr. Imran Khan obtained his Master's degree (M.Sc) in Biotechnology from Pondicherry University, Pondicherry, India in 2011 and started his research as a research fellow in the Department of Biological Sciences at BITS Pilani, Hyderabad Campus, India in 2013. He is well versed in various microbial and protein expression techniques. He has good number of publications and awards to his credit and has presented his work in several national and international conferences. Currently, his career interests are focus on the development of genetically based diagnostic kits based on hybridization applications of nano-technology.

Publications:

1. Enzyme Embedded Degradation of Poly(ε-caprolactone) using Lipase Derived from Probiotic Lactobacillus plantarum, Acs Omega, (Accepted for Publication, January 2019)

2. Extracellular probiotic lipase capped silver nanoparticles as highly efficient broad spectrum antimicrobial agents, Imran Khan, Nivetha S, Ravikiran Nagarjuna, Jayati Ray Dutta and R. Ganesan, RSC Adv., 2018, 8, 31358-31365

3. Towards single crystalline, highly monodisperse and catalytically active gold nanoparticles capped with probiotic Lactobacillus plantarum derived lipase, Imran Khan, Ravikiran Nagarjuna, Jayati Ray Dutta and R. Ganesan, Applied Nanoscience, Springer, 2018, pp 1-9.

4. In vitro hemocompatability evaluation of gold nanoparticles capped with Lactobacillus plantarum derived lipase. I Khan, SK Vishwakarma, AA Khan, G Ramakrishnan, JR Dutta, Clinical Hemorheology and Microcirculation, Clinical Hemorheology and Microcirculation, vol. 69, no. 1-2, pp. 197-205, 2018

5. Imran Khan, Jayati Ray Dutta and Ramakrishnan Ganesan, Lactobacillus sps. Lipase mediated poly (ε-caprolactone) degradation, International Journal of Biological Macromolecules, Elsevier, 95, 2017, pp. 126-131.

6. Imran Khan, Jayati Ray Dutta and Ramakrishnan Ganesan, Enzymes's action on materials: Recent trends, accepted in Journal of Cellular Biotechnology, 1, 2016, pp. 131-144. IOS Press.

7. K Harini, Imran Khan, Nishank reddy, Effect of alcohol on adipose tissue: a review on ethanol mediated adipose tissue injury, Adipocyte, 2014, 1.

8. Kema VH, Khan I, Kapur S, Mandal P. Evaluating the effect of diallyl sulfide on regulation of inflammatory mRNA expression in 3T3L1 adipocytes and RAW 264.7

macrophages during ethanol treatment. Drug Chem Toxicol 2018:1–12. doi:10.1080/01480545.2017.1405969.

9. Kema VH, Khan I, Jamal R, Vishwakarma SK, Lakki Reddy C, Parwani K, et al. Protective Effects of Diallyl Sulfide Against Ethanol-Induced Injury in Rat Adipose Tissue and Primary Human Adipocytes. Alcohol Clin Exp Res 2017;41:1078–92. doi:10.1111/acer.13398

Conference Proceedings:

1. Imran Khan, Sandeep K. Viswakarma, A. A. Khan, R. Ganesan and Jayati Ray Dutta, Lactobacillus sps. lipase capped gold nanoparticles hemocompatability studies, 4th Biennial Conference of PAi and International Symposium on Probiotic Therapy: Translating to Health and Clinical Practice (PAi-2018), AIIMS, Delhi, 2018, Feb 16-17, India, Page no.84.

2. Nivetha Sivasankaran, Imran Khan, Raj Maguluri, Ravikiran Nagarjuna, R. Ganesan and Jayati Ray Dutta, Evaluation of antimicrobial activity of Lactobacillus sps. lipase capped silver nanoparticle, National Symposium on "Emerging Environmental Challenges: An Engineering Approach (EEC-2018)" February 16, 2018 at BITS-Pilani, Hyderabad Campus.

3. Imran Khan, Ravikiran Nagarjuna, Almas Shamaila, Ramakrishnan Ganesan and Jayati Ray Dutta, "Highly monodisperse gold nanoparticles capped with probiotic Lactobacillus plantarum derived lipase" in National Symposium on Convergence of Chemistry and Materials, BITS-Pilani, Hyderabad, 2017, Dec, 21-22, India.

4. Imran Khan, Ravikiran Nagarjuna, Ramakrishnan Ganesan and Jayati Ray Dutta, Lactobacillus sps. Lipase capped Gold nanoparticles cytotoxic evaluation, International Conference on Nanotechnology: Ideas, Innovations and Initiatives (ICN:3I-2017), IIT Roorkee, Uttarakhand, India, Page No, 581.

Manuscript under review:

1. Biodiesel synthesis from waste olive oil employing lipase isolated from probiotic *Lactobacillus plantarum* and *Lactobacillus brevis*, Imran Khan[1], Ramakrishnan Ganesan[2] and Jayati Ray Dutta[1*]

Biography of Supervisor

Dr. Jayati Ray Dutta, Associate Professor of Biological Sciences Department, has been with Birla Institute of Technology and Science, Pilani, Hyderabad Campus, India since 2008.She obtained her Master's degree from Calcutta University and Ph.D. from Indian Institute of Technology (IIT, Kharagpur, India in 2004. She also served as DST FAST TRACK Young Scientist in IIT, Kharagpur, India till July, 2008.

Dr. Ray Dutta's research focus is on Environmental Biotechnology, Microbial Enzymology and their biotechnological applications. Beginning her professional career in 2000, Dr. Ray Dutta has almost 18 years of academic and industry experience in the field of Microbial Biotechnology. She has published over 38 research papers with good citations in reputed international journals and conferences. She has been member of academic societies and associations including European Federation of Biotechnology and Probiotic Association of India. She has been editorial board member and reviewer for many International Journals. Currently, her group is engaged in the development of industrially important enzymes like lipases and proteases which are natural biocatalysts from different microbial sources for commercial purposes. She has successfully completed research projects and ongoing projects sponsored by DST, DBT and UGC, India.

Biography of Co-Supervisor

Dr. G Ramakrishnan, Associate Professor of Chemistry department, has been with Birla Institute of Technology and Science, Pilani, Hyderabad Campus, India since 2012.He obtained his Master's degree from Anna University and Ph.D. from Korea Advanced Institute of Science and Technology (KAIST 2006). He also served as scientific employee at Helmholtz-Zentrum Geesthacht (HZG), Teltow, Germany and as a Scientist, Institute of Materials Research and Engineering (IMRE), Singapore during 2010-2012.

Dr. Ramakrishnan's research focus is on Material Characterization, Nanomaterials, Thin Films and Nanotechnology, Polymers, Material Characteristics, Nanomaterials Synthesis, Thin Film Deposition, Nanostructured Materials. Beginning his professional career in 2006, Dr. Ramakrishnan has almost 11 years of academic and industry experience in the field of Materials Chemistry. He has published over 44 research papers with good citations in reputed international journals and conferences. He has been editorial board member and reviewer for many International Journals. Currently, his group is engaged in the development of industrially important materials based on precious metals. He has successfully completed various Institute research projects and projects sponsored by DST, India.